Measurement of substructure-dependent jet suppression in Pb+Pb collisions at 5.02 TeV with the ATLAS detector

G. Aad *et al.*[*]
(ATLAS Collaboration)

(Received 22 November 2022; accepted 25 January 2023; published 12 May 2023)

The ATLAS detector at the Large Hadron Collider has been used to measure jet substructure modification and suppression in Pb+Pb collisions at a nucleon–nucleon center-of-mass energy $\sqrt{s_{NN}} = 5.02$ TeV in comparison with proton–proton (pp) collisions at $\sqrt{s} = 5.02$ TeV. The Pb+Pb data, collected in 2018, have an integrated luminosity of 1.72 nb^{-1}, while the pp data, collected in 2017, have an integrated luminosity of 260 pb^{-1}. Jets used in this analysis are clustered using the anti-k_t algorithm with a radius parameter $R = 0.4$. The jet constituents, defined by both tracking and calorimeter information, are used to determine the angular scale r_g of the first hard splitting inside the jet by reclustering them using the Cambridge–Aachen algorithm and employing the soft-drop grooming technique. The nuclear modification factor, R_{AA}, used to characterize jet suppression in Pb+Pb collisions, is presented differentially in r_g, jet transverse momentum, and in intervals of collision centrality. The R_{AA} value is observed to depend significantly on jet r_g. Jets produced with the largest measured r_g are found to be twice as suppressed as those with the smallest r_g in central Pb+Pb collisions. The R_{AA} values do not exhibit a strong variation with jet p_T in any of the r_g intervals. The r_g and p_T dependence of jet R_{AA} is qualitatively consistent with a picture of jet quenching arising from coherence and provides the most direct evidence in support of this approach.

DOI: 10.1103/PhysRevC.107.054909

I. INTRODUCTION

In ultrarelativistic heavy-ion collisions a hot and dense state of matter known as a quark-gluon plasma (QGP) is produced. The temperatures attained in the fireball are such that quarks and gluons are no longer confined within their parent hadrons [1,2]. Producing a QGP in the laboratory provides unique opportunities to study quantum chromodynamics (QCD). Experimental results from the Relativistic Heavy Ion Collider (RHIC) and the Large Hadron Collider (LHC) comparing proton–proton (pp) and heavy-ion collisions have led to the conclusion that the QGP expands hydrodynamically. The remarkably small viscosity needed to describe the data suggests that this matter exhibits strong-coupling behavior at large distance scales [3]. In contrast, at short distance scales the interactions among quarks and gluons are expected to become weaker because QCD exhibits asymptotic freedom. It is not fully understood how such hydrodynamic behavior arises from the interactions among elementary quarks and gluons [4]. To address this challenge, the dynamics of the QGP must be characterized over a range of length scales.

Jets are highly collimated sprays of particles resulting from the point-like, hard scattering of quarks and gluons, collectively referred to as partons. Jets are produced at the earliest stages of a high-energy heavy-ion collision and become attenuated while passing through the plasma, a phenomenon known as jet quenching [5,6]. The energy loss suffered by a jet and the modification of its radiation pattern provide information about the plasma's microscopic structure. Scattered partons in the vacuum, studied using pp collisions, experience a cascade of radiative processes and thus the modification of the jet evolution process in the QGP is inherently a multiscale problem.

Techniques that enable the identification of the hardest splitting in the parton shower of a jet, and more generally the substructure of the jet and its overall radiation pattern, have been developed [7,8]. In theoretical calculations the soft-drop grooming procedure [9], a generalization of the modified mass-drop tagger [8], shows less sensitivity to the effects of initial-state radiation, multiparton interactions, and nonperturbative contributions to substructure observables. Since these effects typically contribute large uncertainties, their mitigation allows more rigorous comparisons with experimental data [10,11]. The potential of such techniques to characterize jet substructure in heavy-ion collisions has also been recognized [12–14], and a first series of measurements have been performed indicating a mild modification of jet-substructure variables in Pb+Pb collisions relative to pp results [15–19]. However these initial studies have not yet elucidated the relationship between the observed modifications and the energy loss of the jet.

Measurements of jet quenching in heavy-ion collisions performed at RHIC and the LHC [20,21] typically fall into one of two categories: quantifying the total energy loss or studying the modification of the jet's radiation pattern. The

[*]Full author list given at the end of the article.

Published by the American Physical Society under the terms of the Creative Commons Attribution 4.0 International license. Further distribution of this work must maintain attribution to the author(s) and the published article's title, journal citation, and DOI.

 ©2023 CERN, for the ATLAS Collaboration

rate of jets produced in central heavy-ion collisions at a given jet transverse momentum, $p_{\mathrm{T}}^{\mathrm{jet}}$, is observed to be approximately a factor of two lower than in pp collisions [22–26]. Additionally, back-to-back dijet and photon/Z–jet pairs are observed to have poorer p_{T} balance in Pb+Pb collisions than in pp collisions [27–30]. These measurements provide information about the total jet energy loss and its parametric dependence on the in-medium path length and flavor of the initiating parton. They also constrain how energy loss may fluctuate on a jet-by-jet basis. Another class of measurements which studies the fragmentation properties of quenched jets, typically through the particle-momentum distributions within jets [31–35], is less sensitive to the energy loss but can directly assess how the radiation pattern is modified. This class includes the current heavy-ion jet-substructure measurements [15–18,36] because the distributions of substructure quantities are normalized per jet. Currently missing from the experimental program are analyses that correlate a jet's energy loss with its radiation pattern.

A common theoretical framework for describing jet quenching is the coherence picture in which interference effects, crucial for determining the structure of the vacuum parton shower [37], become disrupted by the medium, resulting in energy loss in the form of additional radiation [38]. Recent studies have also shown the emergence of a critical angle in the first hard splitting of a jet, above which the jet loses energy incoherently, i.e. as multiple color entities [39–43]. This approach leads to the expectation that a wide jet with two prongs, each of which may act as a separate emitter of radiation, will lose more energy than a narrow jet which acts as a single source of radiation. More generally, jets with different substructure are expected to experience different amounts of energy loss according to the degree to which the medium resolves the jet and induces decoherence of its radiation pattern [12].

This paper describes a measurement of jet suppression, a measure of the energy loss, as a function of the observed substructure of the jet. The measurements are based on $1.72\,\mathrm{nb}^{-1}$ of Pb+Pb collision data collected in 2018 and $260\,\mathrm{pb}^{-1}$ of pp collision data collected in 2017, both at $\sqrt{s_{NN}} = 5.02$ TeV. The jets are reconstructed from energy deposits in the ATLAS calorimeters with the anti-k_t algorithm with a radius parameter of $R = 0.4$ [44] and by applying a subtraction procedure that removes the underlying event contribution to the jet kinematics on an event-by-event basis [22]. The soft-drop grooming procedure is applied with parameters $\beta = 0$ and $z_{\mathrm{cut}} = 0.2$ to jet constituents formed from charged-particle tracks and calorimeter energy deposits. The substructure is quantified through r_{g}, the angle subtended by the subjets chosen using the soft-drop procedure to tag the first hard splitting of a jet. Jets which fail the soft-drop requirement are considered as single-prong jets and assigned $r_{\mathrm{g}} = 0$. The per-event jet yields as a function of $p_{\mathrm{T}}^{\mathrm{jet}}$ and r_{g} are measured in four centrality intervals, which characterize the overlap of the colliding nuclei in Pb+Pb collisions. The analogous differential cross-sections are measured in pp collisions, and the suppression is quantified through the nuclear modification factor, R_{AA}. The cross-sections, yields, and R_{AA} are reported for jets with $p_{\mathrm{T}}^{\mathrm{jet}} > 158\,\mathrm{GeV}$ and $0 \leqslant r_{\mathrm{g}} < 0.4$. The measured cross-sections and yields are unfolded to a particle-level phase space.

II. ATLAS DETECTOR

The ATLAS detector [45] at the LHC is a multipurpose particle detector with a forward–backward symmetric cylindrical geometry and a near-4π coverage in solid angle.[1] It consists of an inner tracking detector surrounded by a thin superconducting solenoid, electromagnetic and hadron calorimeters, and a muon spectrometer. The inner-detector system is immersed in a 2 T axial magnetic field and provides charged-particle tracking within $|\eta| < 2.5$. The high-granularity silicon pixel detector covers the vertex region and typically provides four measurements per track, with the first hit typically being in the insertable B-layer installed before Run 2 [46,47]. It is followed by the silicon microstrip tracker (SCT) which usually provides eight measurements per track. These silicon detectors are complemented by the transition radiation tracker, a drift-tube-based detector, which surrounds the SCT and has coverage up to $|\eta| = 2.0$.

The calorimeter system covers the pseudorapidity range $|\eta| < 4.9$. Within the region $|\eta| < 3.2$, electromagnetic calorimetry is provided by barrel and endcap high-granularity lead/liquid-argon (LAr) calorimeters, with an additional thin LAr presampler covering $|\eta| < 1.8$ to correct for energy loss in material upstream of the calorimeters. Hadronic calorimetry is provided by the steel/scintillator-tile calorimeter, segmented into three barrel structures within $|\eta| < 1.7$, and two copper/LAr hadronic endcap calorimeters. The solid angle coverage is completed with copper/LAr and tungsten/LAr calorimeter modules (FCal), covering the forward regions of $3.1 < |\eta| < 4.9$. The zero-degree calorimeters (ZDC) consist of layers of alternating quartz rods and tungsten plates and are located symmetrically at $z = \pm 140$ m and cover $|\eta| \geqslant 8.3$. In Pb+Pb collisions, the ZDCs primarily measure "spectator" neutrons: neutrons that do not interact hadronically when the incident nuclei collide.

Events of interest are selected for recording and offline analysis by the first-level (L1) trigger system implemented in custom hardware, followed by selections made by algorithms implemented in software in the high-level trigger [48].

An extensive software suite [49] is used in data simulation, in reconstruction and analysis of real and simulated events, in detector operations, and in the trigger and data acquisition systems of the experiment. The events used in this analysis

[1] ATLAS uses a right-handed coordinate system with its origin at the nominal interaction point (IP) in the center of the detector and the z axis along the beam pipe. The x-axis points from the IP to the center of the LHC ring, and the y-axis points upward. Cylindrical coordinates (r, ϕ) are used in the transverse plane, ϕ being the azimuthal angle around the z-axis. The pseudorapidity is defined in terms of the polar angle θ as $\eta = -\ln\tan(\theta/2)$. The rapidity is defined as $y = 0.5\ln[(E + p_z)/(E - p_z)]$ where E and p_z are the energy and z component of the momentum along the beam direction, respectively. Angular distance is measured in units of $\Delta R \equiv \sqrt{(\Delta\eta)^2 + (\Delta\phi)^2}$.

TABLE I. The $\langle T_{AA}\rangle$ values and uncertainties for the centrality selections used in this measurement.

Centrality selection	$\langle T_{AA}\rangle \pm \delta\langle T_{AA}\rangle [1/mb]$	$\delta\langle T_{AA}\rangle/\langle T_{AA}\rangle [\%]$
0–10%	23.21 ± 0.06	0.26
10–30%	11.57 ± 0.12	1.04
30–50%	3.92 ± 0.11	2.73
50–80%	0.73 ± 0.04	5.67

were selected by a jet trigger [48]. The L1 trigger identified jet candidates by applying a sliding-window algorithm and selecting events passing a p_T threshold of 30 GeV. These events were then passed to the high-level jet trigger, which uses a jet reconstruction and background subtraction procedure similar to that used in the offline analysis and requires a minimum p_T^{jet} of 100 GeV for anti-k_t $R = 0.4$ jets. The jet trigger was fully efficient for the p_T^{jet} range considered in this measurement.

III. DATA SAMPLES AND EVENT SELECTION

The data used in this analysis are taken from the 2018 Pb+Pb and 2017 pp runs, both at $\sqrt{s_{NN}} = 5.02$ TeV. The average number of collisions per bunch-crossing (pileup) was 0.003 in the Pb+Pb data and ranges from 1.4 to 4.4 in the pp data depending on the data-taking run. Events from both the Pb+Pb and pp collisions were collected using the jet triggers with the same p_T threshold as described above. The events are required to have been collected during stable beam conditions, and to satisfy detector and data-quality requirements [50]. Both the pp and Pb+Pb events are required to have at least one reconstructed primary vertex, and the Pb+Pb events are also required to satisfy nominal offline minimum-bias Pb+Pb collision criteria, identical to those used in Ref. [51]. This additional requirement, based on a combination of the total transverse energy E_T measured in the FCal, denoted by ΣE_T^{FCal}, and the total energy deposited in the ZDC identifies and rejects 0.2% of the selected events as pile-up events.

The degree of geometric overlap of the colliding Pb nuclei is characterized by "event centrality," and each collision event is assigned to a centrality interval. The procedure used to experimentally define centrality intervals in this paper follows that used in other measurements of Pb+Pb collisions performed by the ATLAS Collaboration [28]. The distribution of the total transverse energy deposited in the FCal is divided into successive quantiles of the total inelastic cross-section for Pb+Pb collisions, with the highest ΣE_T^{FCal} events corresponding, on average, to the events with the largest geometric overlap between the colliding nuclei. The centrality intervals used are: 0–10% (highest ΣE_T^{FCal}), 10–30%, 30–50%, and 50–80%. A Glauber model analysis of the ΣE_T^{FCal} distribution is used to evaluate the mean nuclear thickness function, $\langle T_{AA}\rangle$, for different centrality intervals [52,53]. The $\langle T_{AA}\rangle$ values and uncertainties, which are discussed in Ref. [54], are listed in Table I for each centrality selection considered in this measurement.

The Monte Carlo (MC) simulations used in this analysis are multijet events modeled with the PYTHIA 8 [55] MC generator with leading-order matrix elements for dijet production which were matched to the parton shower. The A14 set of tuned parameters [56] and the NNPDF23LO parton distribution functions [57] were used. The events generated by PYTHIA 8 were passed through a GEANT4-based simulation [58,59] of the ATLAS detector and its response. By reproducing the detector conditions in the data-taking run, this allows the simulations to account for underlying-event (UE) effects in the jet reconstruction. For Pb+Pb collisions, the simulated dijet events were overlaid with minimum-bias Pb+Pb data, and this "overlay" sample was reweighted on an event-by-event basis to obtain the same centrality distribution as in the jet-triggered Pb+Pb data sample. The simulated events are digitized and reconstructed in the same way as data events.

IV. ANALYSIS PROCEDURE

A. Jet reconstruction

The jet reconstruction procedures follow those used by the ATLAS Collaboration for previous jet measurements in Pb+Pb collisions [24,60]. Jets are reconstructed using the anti-k_t algorithm [44] implemented in the FastJet software package [61]. In both pp and Pb+Pb collisions, jets with $R = 0.4$ are formed by clustering calorimeter towers with $\Delta\eta \times \Delta\phi = 0.1 \times \pi/32$ in the pseudorapidity range $|\eta| < 4.9$ over the full azimuthal range. The energies in the towers are obtained by summing the energies of calorimeter cells at the electromagnetic energy scale [62] within the tower boundaries. The UE contribution to each tower is subtracted on an event-by-event basis by estimating the average local energy density, $\rho(\eta, \phi)$. This estimate is obtained by measuring the average energy in calorimeter towers as a function of η and including the azimuthal modulation due to harmonic flow characterized by the second-, third-, and fourth-order flow coefficients [63]. The ϕ-dependent background subtraction is performed only for jet reconstruction in Pb+Pb events, as the event activity is observed to be aziumthally symmetric in minimum-bias pp data [64]. An iterative procedure is applied to prevent the jets from biasing the determination of ρ [60]. Following the UE subtraction, new estimates of ρ are obtained by excluding the contributions coming from towers within jets from the average energy density and flow parametrization. Additionally, the UE is also corrected for η- and ϕ-dependent nonuniformities in the detector response to soft particles by applying correction factors derived in minimum-bias Pb+Pb data. In pp collisions, the same background subtraction procedure is used, but without the nonuniformity correction and no harmonic modulation of the UE.

Following the UE subtraction, η- and p_T-dependent multiplicative calibration factors derived in MC simulations are applied to the jet four-momentum vector to account for the noncompensating hadronic response of the calorimeter [65]. An additional correction based on in situ studies of jets recoiling against photons, Z bosons, and jets in other regions of the calorimeter is applied to account for known differences between data and the MC sample used to derive the calibration [28]. This calibration is followed by a cross-calibration which relates the jet energy scale (JES) of jets reconstructed using

the procedure outlined in this section to the JES in 13 TeV pp collisions [65]. The performance of the jet reconstruction in pp and Pb+Pb collisions has been studied in detail as described in Ref. [24]. The jet transverse momentum, denoted by $p_{\mathrm{T}}^{\mathrm{jet}}$, is defined as the calibrated p_{T} of $R = 0.4$ jets formed from calorimeter towers. Calibrations are applied to the p_{T} of the jet and not individually to the constituent calorimeter towers in this procedure. Fully calibrated jets having $p_{\mathrm{T}}^{\mathrm{jet}} > 158\,\mathrm{GeV}$ and $|y| < 2.1$ are used in this measurement. The $p_{\mathrm{T}}^{\mathrm{jet}}$ binning was designed to match previous jet measurements by ATLAS [22–24] and have uniformly spaced bins on the logarithmic scale. MC-truth jets are defined in simulated events at particle level by applying the anti-k_t algorithm with $R = 0.4$ to stable particles with a proper lifetime greater than 30 ps in the generator's event record, but excluding muons and neutrinos, which do not leave significant energy deposits in the calorimeter.

B. Jet constituents

The granularity of the ATLAS calorimeter towers, which are used as constituents in the initial jet reconstruction, is too coarse to resolve collimated prongs within a jet that have small opening angles comparable to the expected resolving power of the QGP [41,42]. In order to improve the angular and energy resolution of the jet constituents, new constituents are defined by combining the superior angular resolution of the tracker with calorimeter information. These objects, referred to as track-calo-clusters (TCCs), are built using the energies of topological cell clusters (topoclusters) [66] and the spatial coordinates of charged-particle tracks [67]. TCCs were used in previous ATLAS studies to improve the resolution of jet-substructure variables used in W/Z–boson tagging [68]. They were also used in combination with particle-flow [69] objects to optimize jet reconstruction in pp collisions [70]. In this measurement, TCCs are reconstructed in a manner similar to that in Ref. [67] but with some adjustments to account for the UE in Pb+Pb collisions as detailed below.

Topo-clusters, used to define the energy scale of the TCCs, are built from calorimeter cells using a noise-suppression algorithm [66] and have been used extensively in jet-substructure measurements in pp collisions [10,11]. In Pb+Pb collisions, a ϕ-modulated background subtraction, similar to the UE subtraction procedure employed for jet reconstruction (Sec. IV A), is applied to the calorimeter cells before using them to build topoclusters. Charged-particle tracks are reconstructed from hits in the inner detector using standard optimization algorithms for Pb+Pb collisions as detailed in Refs. [71,72]. Reconstructed tracks used as seeds in the TCC reconstruction are required to have $p_{\mathrm{T}} > 3\,\mathrm{GeV}$ and to also meet several criteria designed to select primary charged particles [31]. Tracks in an event are extrapolated to the calorimeter and are matched to one or more topoclusters, depending on the topocluster size and the track extrapolation uncertainty.

Following the track and topocluster matching, the procedure to determine TCC four-momentum vectors is described briefly below and is detailed further in Ref. [67]. For an isolated match between a track from the selected primary vertex and a topocluster, the topocluster energy and the track direction are used to form a single TCC. In the case of topoclusters which do not match any tracks, the topocluster's four-momentum vector is directly used to create a TCC. Conversely, instances where tracks are not matched to any topoclusters, observed to occur in less than 1% of the cases, are treated analogously by creating a TCC using the track's four-momentum vector. In cases where multiple tracks are matched to one or more topoclusters, the TCC algorithm is designed to create exactly one TCC object per track originating from the primary vertex. Such multiple matches are handled by using the track's angular coordinates, while splitting the topocluster energy between the corresponding TCC objects to account for energy sharing between the different matches.

The topocluster energy sharing procedure for tracks matched to clusters makes use of three general concepts and is detailed in Ref. [67]. First, each cluster matched to the seed track should contribute to the resulting TCC object in proportion to its share of the total p_{T} of all matched clusters. Second, if a cluster is matched to multiple TCC objects, its contribution to a given TCC should be proportional to the share of the seed track of the total p_{T} of all tracks matched to the cluster. Third, the proportion of topocluster energy assigned to each of those tracks should itself be weighted by that cluster's share of the total energy of all clusters matching the track. The 3 GeV p_{T} threshold for charged tracks in the TCC reconstruction is optimized to prevent low-p_{T} UE tracks from sharing the energy of high-p_{T} topoclusters.

All TCCs having $p_{\mathrm{T}} > 4\,\mathrm{GeV}$ are used in this measurement. Jets considered in this measurement with $p_{\mathrm{T}}^{\mathrm{jet}} > 158\,\mathrm{GeV}$ and $|y| < 2.1$ have an average of 6–7 associated TCCs above the 4 GeV threshold in pp and Pb+Pb collisions. TCCs built by matching tracks to topoclusters account for ≈77% of the total number of TCCs within a jet in pp collisions. Due to the lower tracking efficiency in Pb+Pb compared to pp collisions, the fraction of TCCs within a jet built by matching tracks to topoclusters drops to ≈59% in central Pb+Pb collisions. The remaining TCCs are mostly cases where topoclusters are not matched to any tracks.

C. Jet grooming and r_{g}

Jet grooming algorithms are used to isolate the prongs of a jet that correspond to a hard splitting in the evolution of the parton shower by systematically removing the contributions of soft wide-angle radiation. The soft-drop grooming procedure [9], a generalization of the modified mass-drop tagger [8] is employed in this measurement to distinguish perturbative radiation from soft, mostly nonperturbative, components of the jet [15–17,36]. The angular distance r_{g} between the subjets that tag the first hard splitting of a jet is measured in this analysis.

The procedure starts with reclustering the constituents of a jet using the Cambridge–Aachen (C/A) algorithm [73,74] to form a clustering tree with a purely angle-ordered structure. In this measurement, jets are initially reconstructed from calorimeter towers with the anti-k_t algorithm as described in Sec. IV A, and the calorimeter's response is well-defined [60]. Calorimeter-tower jets satisfying the kinematic thresholds listed in Sec. IV A are selected to be reclustered using the

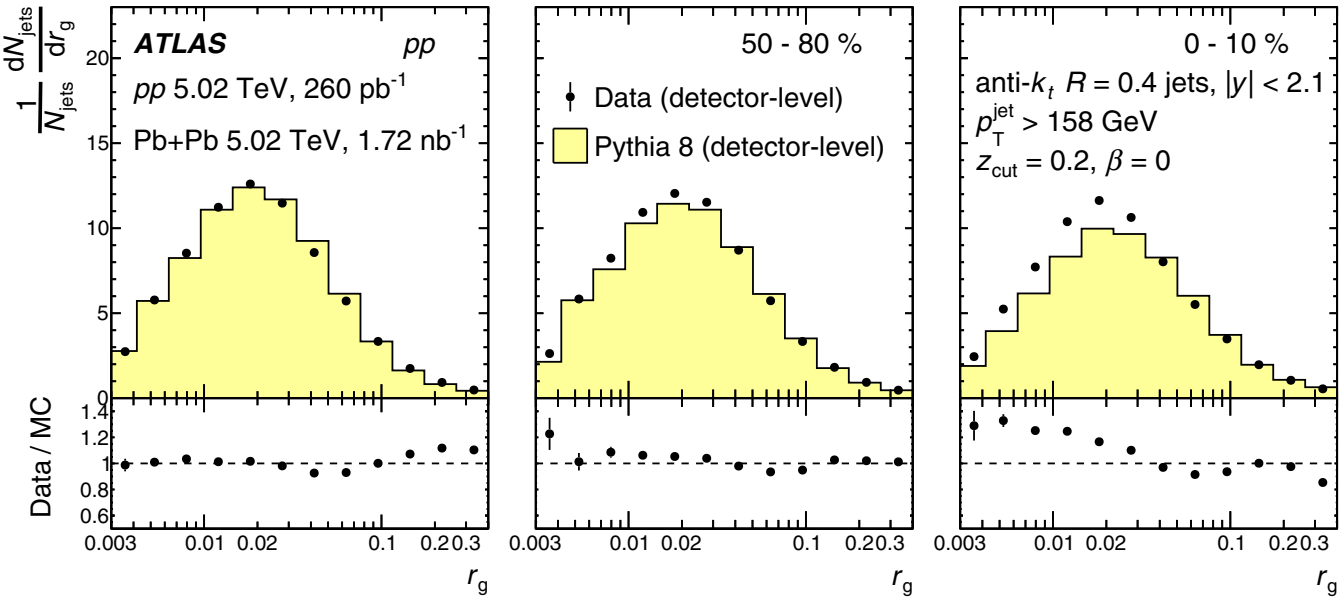

FIG. 1. Top: Self-normalized r_g distributions measured using detector-level TCCs from pp data at $\sqrt{s} = 5.02$ TeV (left) and Pb+Pb data at $\sqrt{s_{NN}} = 5.02$ TeV (second and third panels) for different centrality intervals, compared with the detector-level distributions predicted by the PYTHIA 8 generator. The error bars represent statistical uncertainties. Bottom: Data-to-MC ratios of r_g distributions at detector level. The legend applies to all the panels.

TCCs associated with the jet. TCCs having p_T above 4 GeV and within $\Delta R < 0.4$ of a reconstructed jet's axis are utilized in the jet reclustering process of the soft-drop procedure. The 4 GeV p_T threshold for the TCCs, applied only at the detector level, is used to further reduce the influence of the UE on the measurement of r_g. When reclustering MC-truth particle-level jets, all stable charged and neutral particles within the jets are used in the soft-drop reclustering procedure. The C/A algorithm clusters the nearest constituents first, working outward toward the wider-angle constituents, independent of their p_T. The C/A reclustered jet is then recursively declustered into two "subjets" and it is determined whether the subjets sj_1 and sj_2 with transverse momenta $p_T^{sj_1}$ and $p_T^{sj_2}$ satisfy the soft-drop condition:

$$\frac{\min\left(p_T^{sj_1}, p_T^{sj_2}\right)}{p_T^{sj_1} + p_T^{sj_2}} > z_{\rm cut}\left(\frac{\Delta R_{12}}{R}\right)^{\beta}, \tag{1}$$

where $z_{\rm cut}$ and β are algorithm parameters, R is the radius parameter value used to cluster the jets ($R = 0.4$), and $\Delta R_{12} = \sqrt{(\Delta y_{12})^2 + (\Delta\phi_{12})^2}$ is the distance in y–ϕ between the subjets, where y is the rapidity. If the soft-drop condition in Eq. (1) is not satisfied, then the subjet with the smaller p_T is dropped and the procedure is iterated on the remaining subjets. If the soft-drop condition is satisfied at any point, then the algorithm terminates and r_g is set to the ΔR_{12} value between the subjets sj_1 and sj_2.

If the condition described in Eq. (1) cannot be satisfied, then $r_g = 0$ is assigned to the jet to indicate that the soft-drop procedure cannot find two subjets that satisfy Eq. (1). Jets with $r_g = 0$ are primarily those with a single TCC object or MC-truth particle carrying a significant fraction of the jet energy. For all $z_{\rm cut} > 0$ and $\beta > 0$, the procedure is infrared- and collinear-safe, while it is infrared-safe when $\beta = 0$ [9]. The soft-drop parameter values $z_{\rm cut} = 0.2$ and $\beta = 0$, corresponding to an angle-independent grooming setting, are used for the results shown. These values are chosen to maximize the efficiency of selecting the two hardest prongs of the jet against the competing effect of jets failing the soft-drop grooming with a high $z_{\rm cut}$ value [75]. At the particle level, less than 4% of the jets fail the soft-drop condition when using $z_{\rm cut} = 0.2$ and $\beta = 0$, thereby minimizing a possible bias from looking at different populations of jets in pp and Pb+Pb collisions. The r_g value of a jet measured using $z_{\rm cut} = 0.2$ and $\beta = 0$ is also observed to be insensitive to lowering the 4 GeV threshold for the TCCs.

Distributions of r_g measured using detector-level TCCs from pp and Pb+Pb data are shown in Fig. 1, and are compared with the detector-level distributions from the PYTHIA 8 MC events. The detector-level r_g distributions measured using TCCs show good agreement between data and MC events in pp and peripheral Pb+Pb collisions. The r_g distribution differences between data and simulation for central Pb+Pb collisions can plausibly be attributed to effects from jet quenching, not modeled in simulation, and are discussed in detail in Sec. VI. No systematic uncertainties are shown in Fig. 1 because it is only intended to demonstrate the performance of TCCs in measuring r_g.

D. Unfolding

The jet yields are unfolded in both jet $p_T^{\rm jet}$ and r_g to the particle level in order to account for nonuniformities in detector performance and bin migration due to the finite resolution in jet energy, TCC energy, and TCC position, including migration in and out of the measurement phase space. The measurement phase space in this analysis corresponds to $p_T^{\rm jet} > 158$ GeV, $|y| < 2.1$, and $0 < r_g < 0.4$ for the jets.

At the particle level, the soft-drop procedure is applied to MC-truth jets using all stable charged and neutral particles within the jet as constituents. Utilizing the RooUnfold package [76], the yields of groomed jets are unfolded using a two-dimensional iterative Bayesian unfolding algorithm [77] simultaneously in $p_{\mathrm{T}}^{\mathrm{jet}}$ and r_{g}, while the inclusive jet yields are unfolded using a one-dimensional unfolding in $p_{\mathrm{T}}^{\mathrm{jet}}$. The migration matrices are reweighted simultaneously in MC-truth $p_{\mathrm{T}}^{\mathrm{jet}}$ and r_{g} by the ratios of the corresponding distributions in data to those in the reconstructed MC sample, separately for pp collisions and each centrality interval in Pb+Pb collisions. The reweighting factors are smoothed as a function of r_{g} and $p_{\mathrm{T}}^{\mathrm{jet}}$, and their effect on bin values of the migration matrices is typically less than 25%. The uncertainty from the reweighting procedure is estimated by unfolding with and without the reweighting factors and is detailed in Sec. V. The effects of inefficiencies and misidentified jets in the measurement are accounted for in the analysis by applying an efficiency correction and subtraction procedure, respectively, through the unfolding procedure. In the iterative Bayesian unfolding method implemented in RooUnfold, the inefficiencies are handled by applying a multiplicative factor to each MC-truth bin of the migration matrix. The inefficiencies in this measurement arise mainly from jets migrating out of the measurement phase space at the detector level because of energy resolution effects and from jets that fail the soft-drop grooming procedure. MC-truth jets having significantly lower p_{T} than 158 GeV (the $p_{\mathrm{T}}^{\mathrm{jet}}$ threshold) that migrate into the measurement phase space at the detector level are treated as misidentified jets. The rate of such misidentified jets is observed to be negligible in this measurement, and are accounted for by treating them as an additive background. The effect of jets reconstructed entirely from overlapping UE particles in this measurement is insignificant.

The migration matrices used in the unfolding procedure are binned uniformly on a logarithmic scale and have 13 bins along r_{g} from 0 to 0.4 and 16 bins along $p_{\mathrm{T}}^{\mathrm{jet}}$ from 158 GeV to 1 TeV. Additionally, in the MC-truth phase space, $p_{\mathrm{T}}^{\mathrm{jet}}$ has one overflow bin and six underflow bins down to 80 GeV for a smooth inefficiency correction, and r_{g} has one overflow and one underflow bin in the migration matrix. There is no significant migration between centrality intervals in this measurement. A separate migration matrix is generated for each centrality interval in Pb+Pb collisions, using the PYTHIA 8 sample overlaid with minimum-bias Pb+Pb data and for pp collisions, using the PYTHIA 8 sample. The number of iterations in the unfolding procedure is optimized independently for different centrality intervals to balance minimizing any bias from the unfolding against fluctuations in MC samples. The optimal number of iterations ranges from four to six depending on the centrality interval. The remnant unfolding bias evaluated in MC samples is better than 1%.

The differential jet cross-section in pp collisions is defined as

$$\frac{d^2\sigma_{\mathrm{jet}}}{dp_{\mathrm{T}}^{\mathrm{jet}}dr_{\mathrm{g}}} = \frac{1}{L_{\mathrm{int}}}\frac{N_{\mathrm{jets}}}{\Delta p_{\mathrm{T}}^{\mathrm{jet}}\Delta r_{\mathrm{g}}},$$

where N_{jets} is the unfolded jet yield, $\Delta p_{\mathrm{T}}^{\mathrm{jet}}$ and Δr_{g} are the widths of the $p_{\mathrm{T}}^{\mathrm{jet}}$ and r_{g} bins, respectively, and L_{int} is the integrated luminosity.

The jet yield per minimum-bias event jet yield in Pb+Pb collisions, referred to as the per-event yield for simplicity, is defined as

$$\frac{1}{N_{\mathrm{evt}}^{\mathrm{cent}}}\frac{d^2N_{\mathrm{jet}}^{\mathrm{cent}}}{dp_{\mathrm{T}}^{\mathrm{jet}}dr_{\mathrm{g}}} = \frac{1}{N_{\mathrm{evt}}^{\mathrm{cent}}}\frac{N_{\mathrm{jets}}^{\mathrm{cent}}}{\Delta p_{\mathrm{T}}^{\mathrm{jet}}\Delta r_{\mathrm{g}}},$$

where $N_{\mathrm{jet}}^{\mathrm{cent}}$ is the unfolded jet yield in Pb+Pb collisions within intervals of $p_{\mathrm{T}}^{\mathrm{jet}}$ and r_{g} for a given centrality (denoted by the superscript "cent"), and $N_{\mathrm{evt}}^{\mathrm{cent}}$ is the number of minimum-bias events in the centrality interval.

Modification of the jet yield in Pb+Pb collisions in a given centrality interval relative to the jet yield in pp collisions is quantified using the nuclear modification factor, R_{AA}, defined as

$$R_{AA}\left(p_{\mathrm{T}}^{\mathrm{jet}}, r_{\mathrm{g}}\right) = \frac{1}{N_{\mathrm{evt}}^{\mathrm{cent}}}\frac{1}{\langle T_{\mathrm{AA}}\rangle}\frac{d^2N_{\mathrm{jet}}^{\mathrm{cent}}}{dp_{\mathrm{T}}^{\mathrm{jet}}dr_{\mathrm{g}}}\Bigg/\frac{d^2\sigma_{\mathrm{jet}}}{dp_{\mathrm{T}}^{\mathrm{jet}}dr_{\mathrm{g}}}, \quad (2)$$

where $\langle T_{\mathrm{AA}}\rangle$ is the mean nuclear thickness function, presented in Table I. At a given $p_{\mathrm{T}}^{\mathrm{jet}}$, r_{g}, and centrality interval, $R_{AA} < 1$ indicates a suppression of jet production in Pb+Pb collisions relative to that in pp collisions.

V. SYSTEMATIC UNCERTAINTIES

Several sources of systematic uncertainty are considered for this analysis. The systematic uncertainties in the jet cross-sections in pp collisions and per-event yields in Pb+Pb collisions arise from the jet energy scale and resolution, the constituent TCC energy scale and resolution, the unfolding procedure, integrated pp luminosity, and $\langle T_{\mathrm{AA}}\rangle$ (Pb+Pb only). The jet- and TCC-related uncertainties are evaluated in the analysis by modifying the migration matrix for each uncertainty contribution. The deviations from the nominal unfolded result for each variation are then combined in quadrature to calculate the total contribution.

The systematic uncertainty in the JES has three parts. The first (labeled "JES baseline" in Figs. 2–5) is a centrality-independent component that is determined from in situ studies of the calorimeter response to jets reconstructed with the procedure used in 13 TeV pp collisions [62,78], with an additional component which accounts for the relative energy-scale difference between the jet reconstruction procedures used in 13 TeV pp collisions and in this measurement [65]. The potential mismodeling of relative abundances of jets initiated by quarks and gluons in the MC events, and of the calorimetric response to quark and gluon jets, are accounted for by the second component (labeled "JES flavor" in Figs. 2–5). The third, centrality-dependent component (applicable in Pb+Pb collisions only and labeled "JES quenching" in Figs. 2–5) accounts for modifications of the parton shower due to quenching [31,35] resulting in a different detector response to jets in Pb+Pb collisions that is not modeled by the MC simulation. It is evaluated by the method used for data collected by ATLAS in 2011 and 2015 [65], which compares the jet p_{T} measured in the calorimeter with the sum of the p_{T} of charged

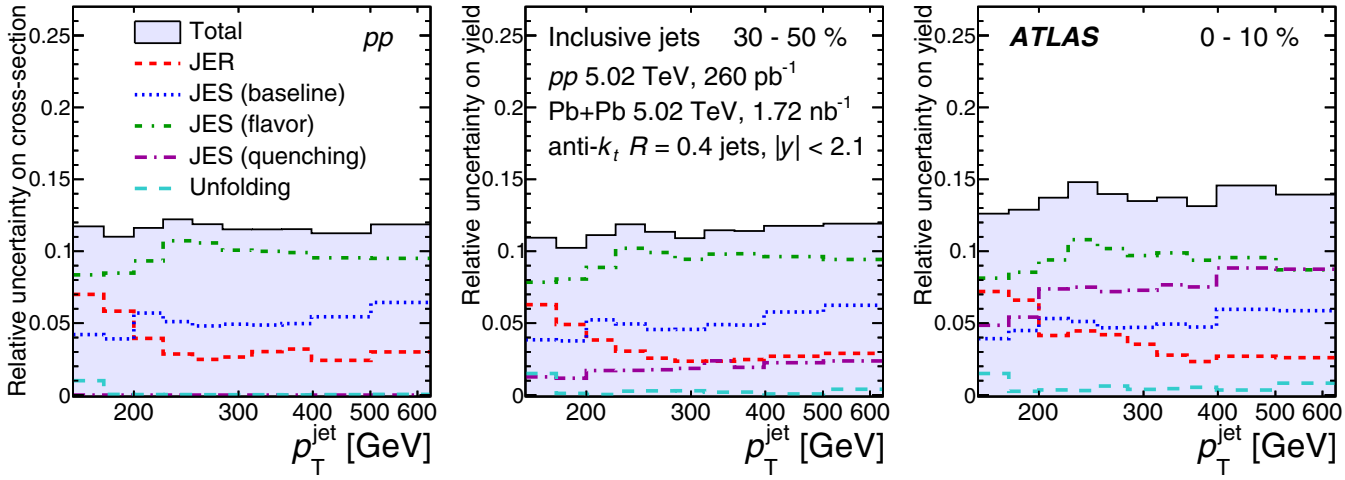

FIG. 2. The relative systematic uncertainties in inclusive $p_{\mathrm{T}}^{\mathrm{jet}}$ cross-sections in pp collisions at $\sqrt{s} = 5.02$ TeV (left) and in per-event jet yields in Pb+Pb collisions at $\sqrt{s_{NN}} = 5.02$ TeV for different event centralities (middle and right panels). The legend applies to all of the panels.

particles within the jet, in both the data and MC samples. The selected charged-particle tracks have $p_{\mathrm{T}} > 4$ GeV to exclude particles from the UE. The ratio of the sum of the charged-particle p_{T} to the $p_{\mathrm{T}}^{\mathrm{jet}}$ provides a data-driven estimate of the centrality-dependence of the JES. The centrality-dependent JES component, pertinent only to jets in Pb+Pb collisions, is the dominant source of uncertainty in the jet R_{AA} measurement, contributing to a relative uncertainty of ≈8% in central collisions.

The uncertainty due to the jet energy resolution (JER) is evaluated by applying a Gaussian smearing factor to the reconstructed $p_{\mathrm{T}}^{\mathrm{jet}}$ in the MC sample. The smearing factor is evaluated using an in situ technique in 13 TeV pp data that involves studies of dijet p_{T} balance [78,79]. Further, an uncertainty is included to account for differences between the tower-based jet reconstruction and the jet reconstruction used in 13 TeV pp data analyses, as well as differences between calibration procedures [65]. The jet energy scale and resolution are the dominant sources of uncertainty in measuring the jet cross-sections and R_{AA} in this analysis and contribute a maximum relative uncertainty of about 14% and 9%, respectively.

Although the TCC energies are not utilized in measuring $p_{\mathrm{T}}^{\mathrm{jet}}$, they are used in the measurement of r_{g} via the soft-drop procedure. The TCC energy response is primarily determined by the topocluster energy response. The uncertainties in the topocluster energy scale and resolution, measured using 13 TeV pp data [11], are applied directly to pp data. The cluster uncertainties from 13 TeV pp data [11] are scaled conservatively by a factor of two for Pb+Pb data to cover the uncertainty in the topocluster energy response in the dense Pb+Pb collision environment. The inefficiency of matching between tracks and topoclusters is driven by the angular resolution of the topoclusters, which is used to match these objects

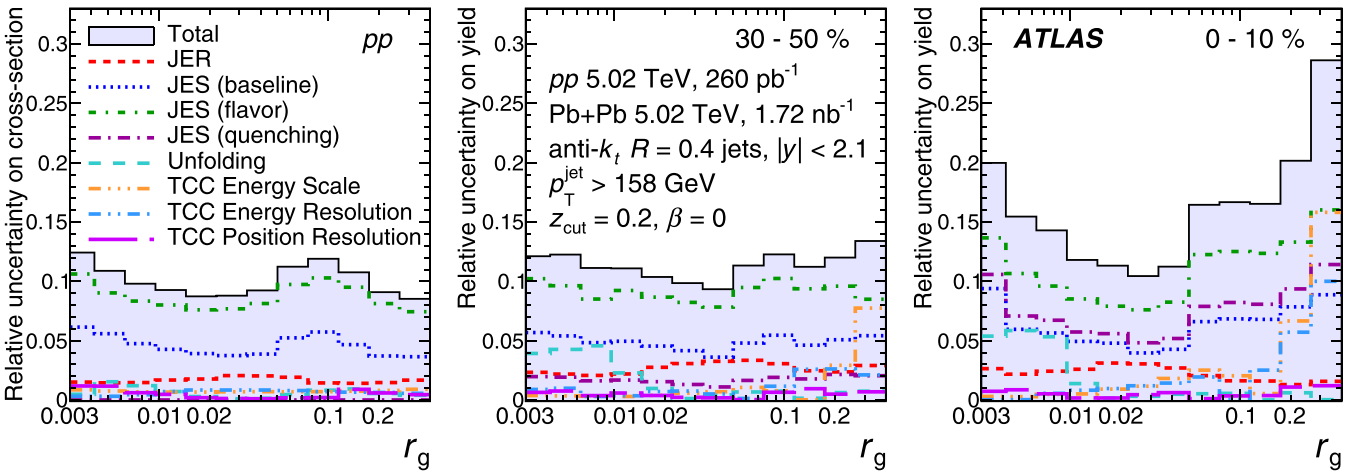

FIG. 3. The relative systematic uncertainties in inclusive r_{g} cross-sections in pp collisions at $\sqrt{s} = 5.02$ TeV (left) and in per-event jet yields in Pb+Pb collisions at $\sqrt{s_{NN}} = 5.02$ TeV for different event centralities (middle and right panels) shown for soft-drop parameters $z_{\mathrm{cut}} = 0.2$ and $\beta = 0$. The legend applies to all of the panels.

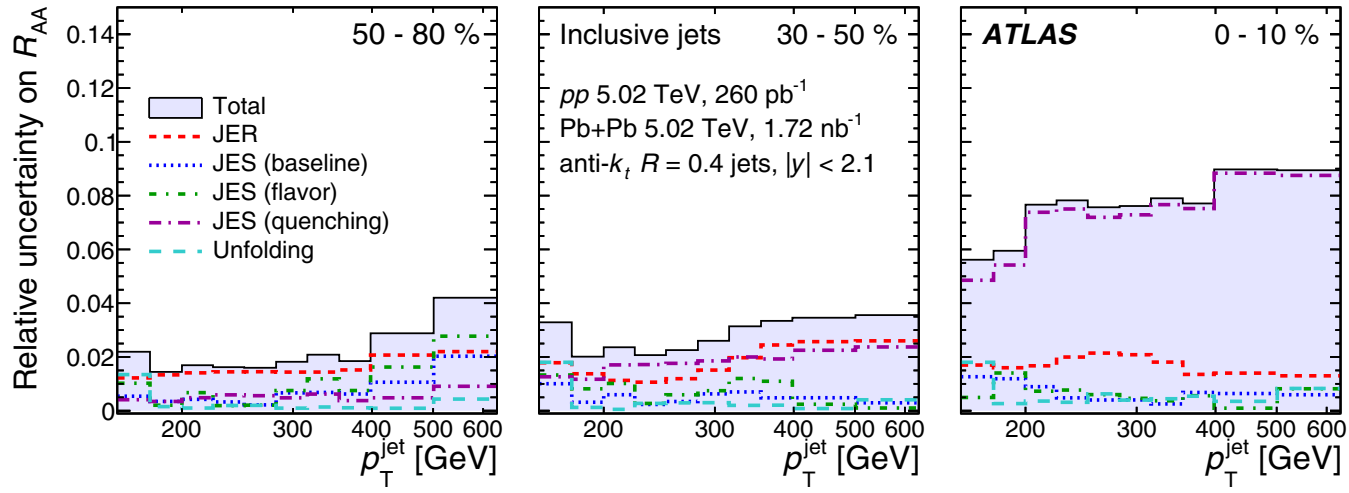

FIG. 4. The relative systematic uncertainties in the R_{AA} measurements as a function of p_T^{jet} in different centrality intervals of Pb+Pb collisions at $\sqrt{s_{NN}} = 5.02$ TeV. The legend applies to all of the panels.

in the TCC reconstruction. A random Gaussian smearing of 5-mrad is applied independently in η and ϕ, following previous ATLAS measurements [11,80], to account for potential mismodeling of topocluster positions and is observed to have a negligible effect on the resulting TCCs and the r_g distributions. TCCs are reconstructed using topoclusters with energies and positions varied according to their uncertainties in MC events and are used to unfold the data. The deviations from the nominal unfolded result, due to individual topocluster uncertainty sources, are combined in quadrature.

The effects of topocluster splitting and merging were studied in detail, following the method used in previous measurements [11]. The MC generator predictions precisely match each of the splitting and merging scenarios tested in data and thus no systematic uncertainty is assigned to these effects.

The angular coordinates (η, ϕ) of a TCC corresponding to a charged particle are determined by the track seeding the TCC object. Systematic variations of these coordinates are evaluated to account for tracking mismodeling in MC events. These differences are decomposed into two components: one from the uncertainty in the inner-detector material derived from studies in pp collisions [81], and the other from the modeling of pixel cluster merging inside dense environments [71,82], such as inside the core of high-energy jets and in central Pb+Pb collisions. These track uncertainties are propagated through the TCC reconstruction and are observed to have a negligible effect on the final r_g distributions.

In this measurement the TCC-related uncertainties typically have a more modest effect than jet-related uncertainties as only the angular distance between the subjets (r_g) is measured. They become significant, contributing a relative uncertainty of up to 15%, at large r_g (>0.3) in central Pb+Pb collisions as UE fluctuations in the outer region of the jet lead to poorer performance in identifying the hard subjets.

The differences between the unfolded results with and without the migration-matrix reweighting factors are assigned as systematic uncertainties arising from the unfolding

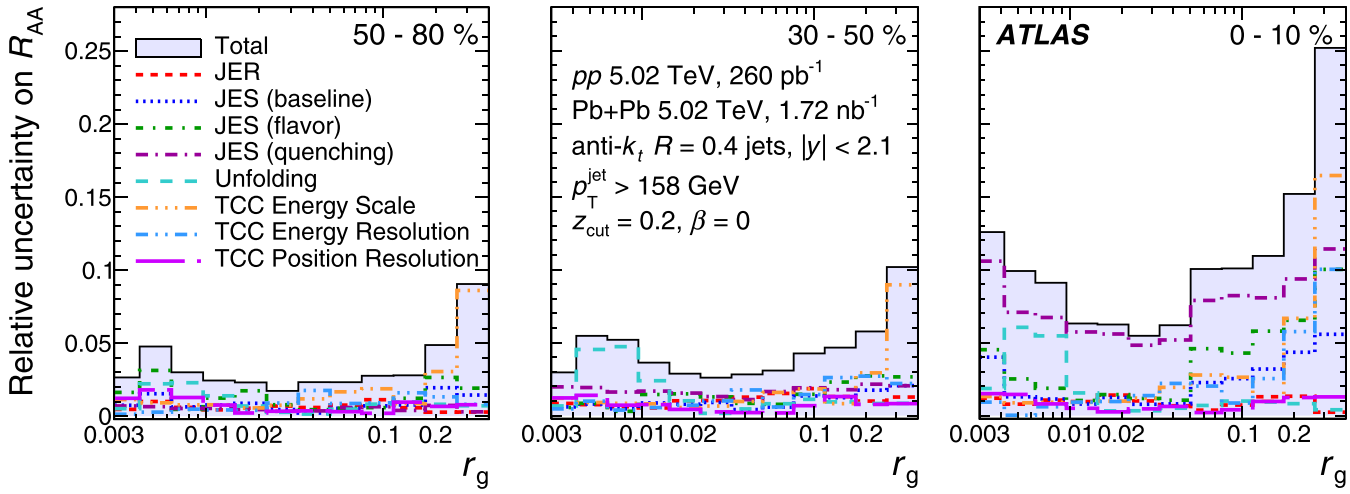

FIG. 5. The relative systematic uncertainties in the R_{AA} measurements as a function of r_g in different centrality intervals of Pb+Pb collisions at $\sqrt{s_{NN}} = 5.02$ TeV shown for soft-drop parameters $z_{cut} = 0.2$ and $\beta = 0$. The legend applies to all of the panels.

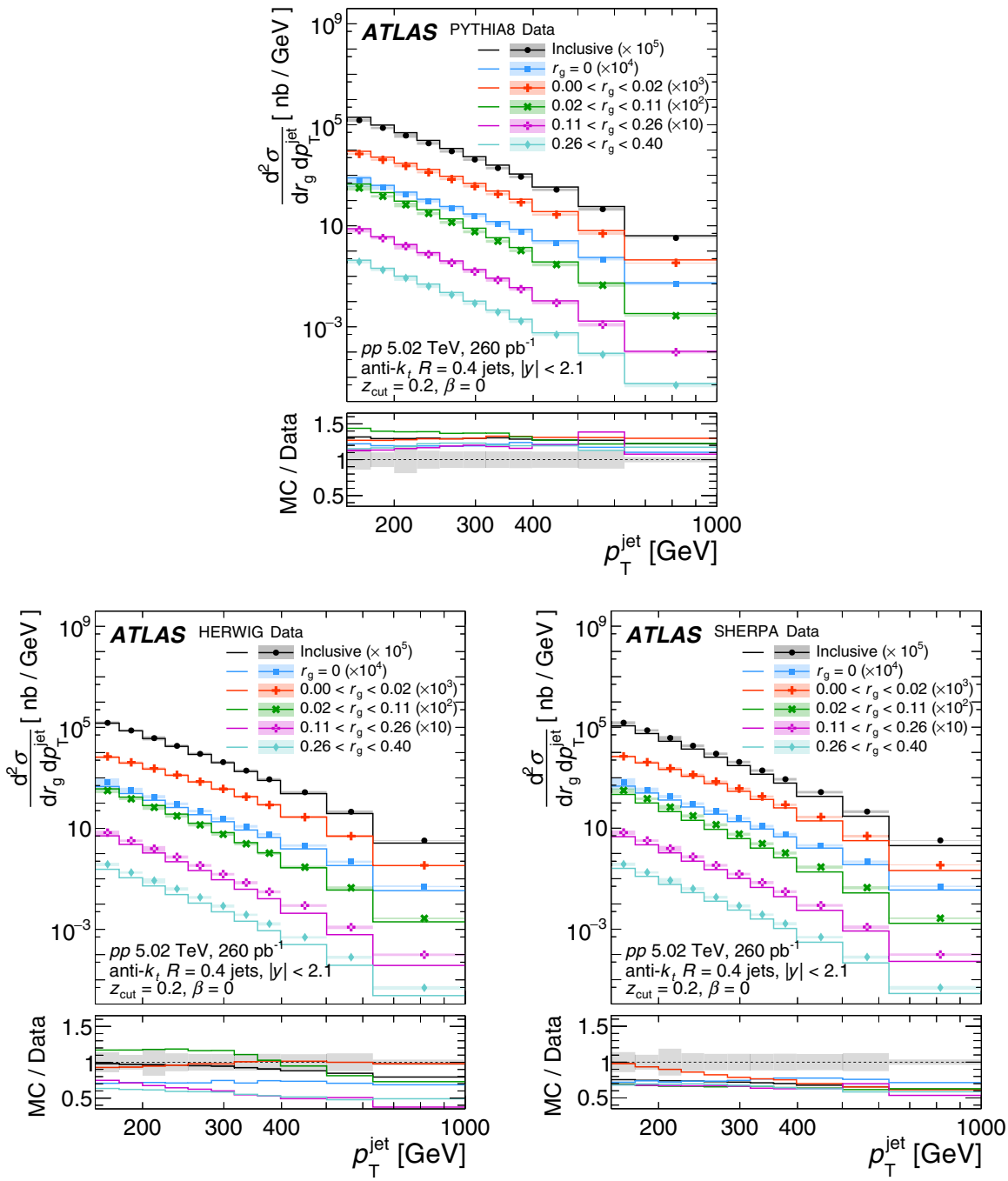

FIG. 6. Differential cross-section of jets passing the soft-drop grooming condition in different r_g intervals in pp collisions at $\sqrt{s} = 5.02$ TeV as a function of p_T^{jet}. Distributions for inclusive jets (no grooming) and for those jets that fail the soft-drop requirement ($r_g = 0$) are also shown. For visual clarity, the distributions are scaled by factors specified in the legend. The statistical uncertainties are smaller than the symbols, while shaded bars represent systematic uncertainties. Note that the highest p_T^{jet} bin does not contain the overflow and that the 1.6% luminosity uncertainty is not shown. The pp jet cross-sections are compared with predictions from three MC generators, PYTHIA 8 (top), HERWIG (bottom left), and SHERPA (bottom right). The ratios of jet cross-section predictions from different MC generators to the unfolded data are shown in the lower panels. The statistical uncertainties on the ratios are smaller than the line widths, while shaded bars in the lower panels represent systematic uncertainties in inclusive cross-section ratios.

procedure. The unfolding uncertainty is observed to have a smaller effect than other sources, contributing a relative uncertainty of <5% to the cross-section, yield, and R_{AA} results.

The statistical uncertainties in the unfolding due to the statistical uncertainties associated with the size of the accumulated dataset are evaluated using the pseudoexperiment technique with 500 separate stochastic variations of the input spectrum as described in Ref. [83]. The contributions from statistical fluctuations in the response matrix are similarly evaluated using the same number of stochastic variations. The

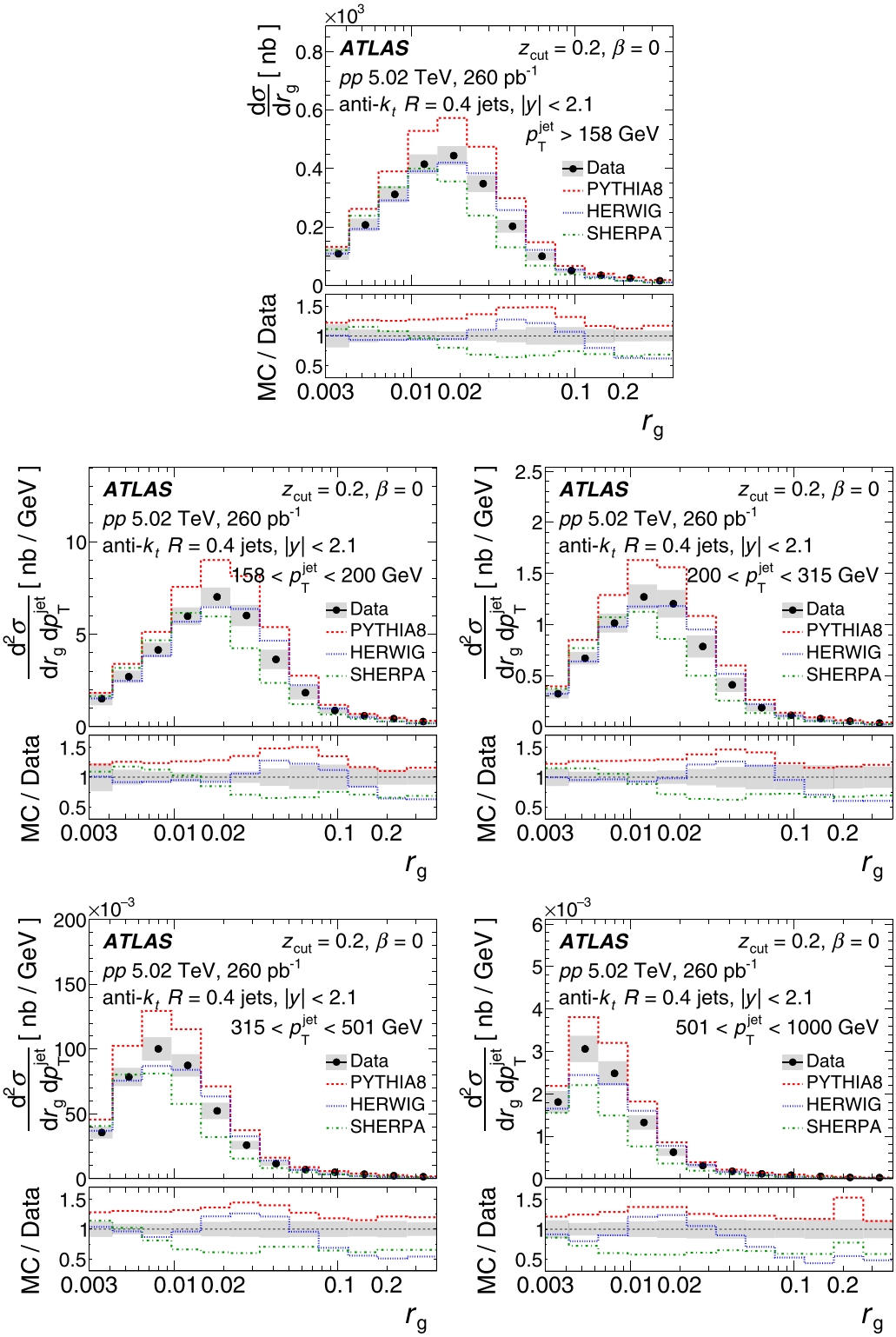

FIG. 7. Differential cross-section of jets passing the soft-drop grooming condition in pp collisions at $\sqrt{s} = 5.02$ TeV as a function of r_g is shown for different p_T^{jet} intervals and also for $p_T^{jet} > 158$ GeV. The error bars represent statistical uncertainties, and are smaller than the marker size here, while the shaded bars represent systematic uncertainties. The 1.6% uncertainty in the pp luminosity is not shown. The last bin does not contain the overflow. The ratios of jet cross-section predictions from different MC generators to the unfolded data are shown in the lower panels. The shaded bars in the lower panels represent systematic uncertainties in cross-section ratios.

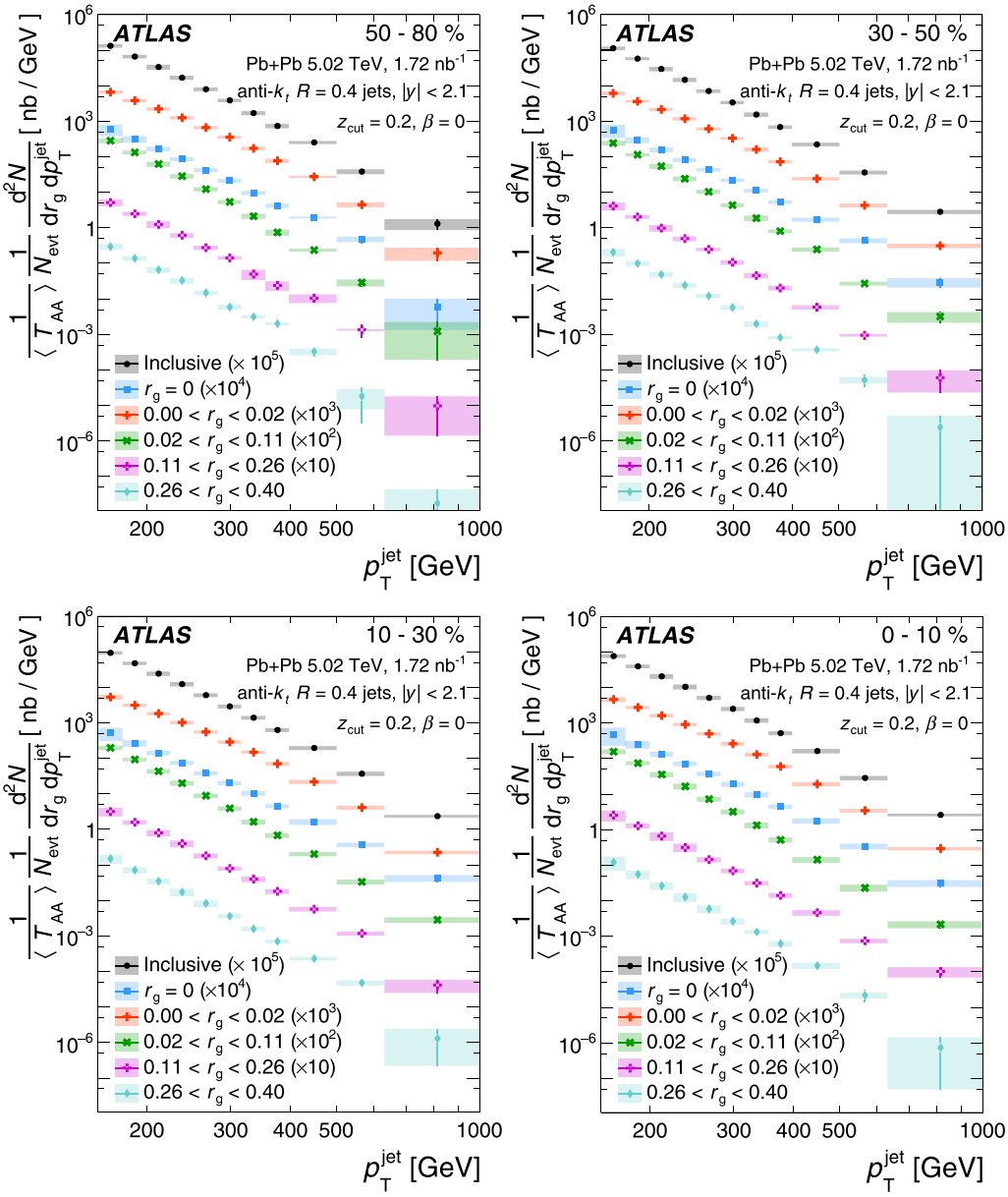

FIG. 8. The per-event inclusive jet yields in Pb+Pb collisions at $\sqrt{s_{NN}} = 5.02$ TeV normalized by $\langle T_{AA} \rangle$ as a function of p_T^{jet} in four centrality intervals. Distributions for inclusive jets (no grooming) and for those jets that fail the soft-drop requirement (denoted by $r_g = 0$) are also shown. For visual clarity, the distributions are scaled by factors specified in the legend. The last bin does not contain the overflow. The statistical uncertainties are indicated by the error bars while the systematic uncertainties are indicated by the shaded bars. The normalization uncertainties of $\langle T_{AA} \rangle$ for each centrality interval are not shown, but are listed in Table I.

two contributions to the statistical uncertainty are combined in quadrature and are observed to contribute <1% to the total systematic uncertainty in the results.

For the 2017 pp data, the LUCID-2 detector [84] was used for the primary luminosity measurement. The uncertainty in the integrated luminosity is estimated to be 1.6% using the methods described in Ref. [85]. For Pb+Pb collisions, the systematic uncertainty in the mean nuclear thickness function, $\langle T_{AA} \rangle$, is estimated by varying the MC Glauber model parameters as detailed in Ref. [63], and is listed in Table I.

A summary of the relative uncertainties in the unfolded inclusive jet cross-sections, yields, and nuclear modification factor are shown in Figs. 2–5. Figures 2 and 3 present a summary of the total and individual relative uncertainties in the jet cross-sections and per-event yields as a function of p_T^{jet} and r_g, respectively. The individual uncertainties are summed in quadrature to obtain the total uncertainty. The jet energy scale is the dominant source of uncertainty in the cross-sections and per-event jet yields except at large r_g in central Pb+Pb collisions, where the TCC energy-scale uncertainties have a comparable effect. A summary of the total and individual relative uncertainties in the R_{AA} is shown in Figs. 4 and 5 as a function of p_T^{jet} and r_g, respectively. The uncertainties which are common to pp and Pb+Pb collisions,

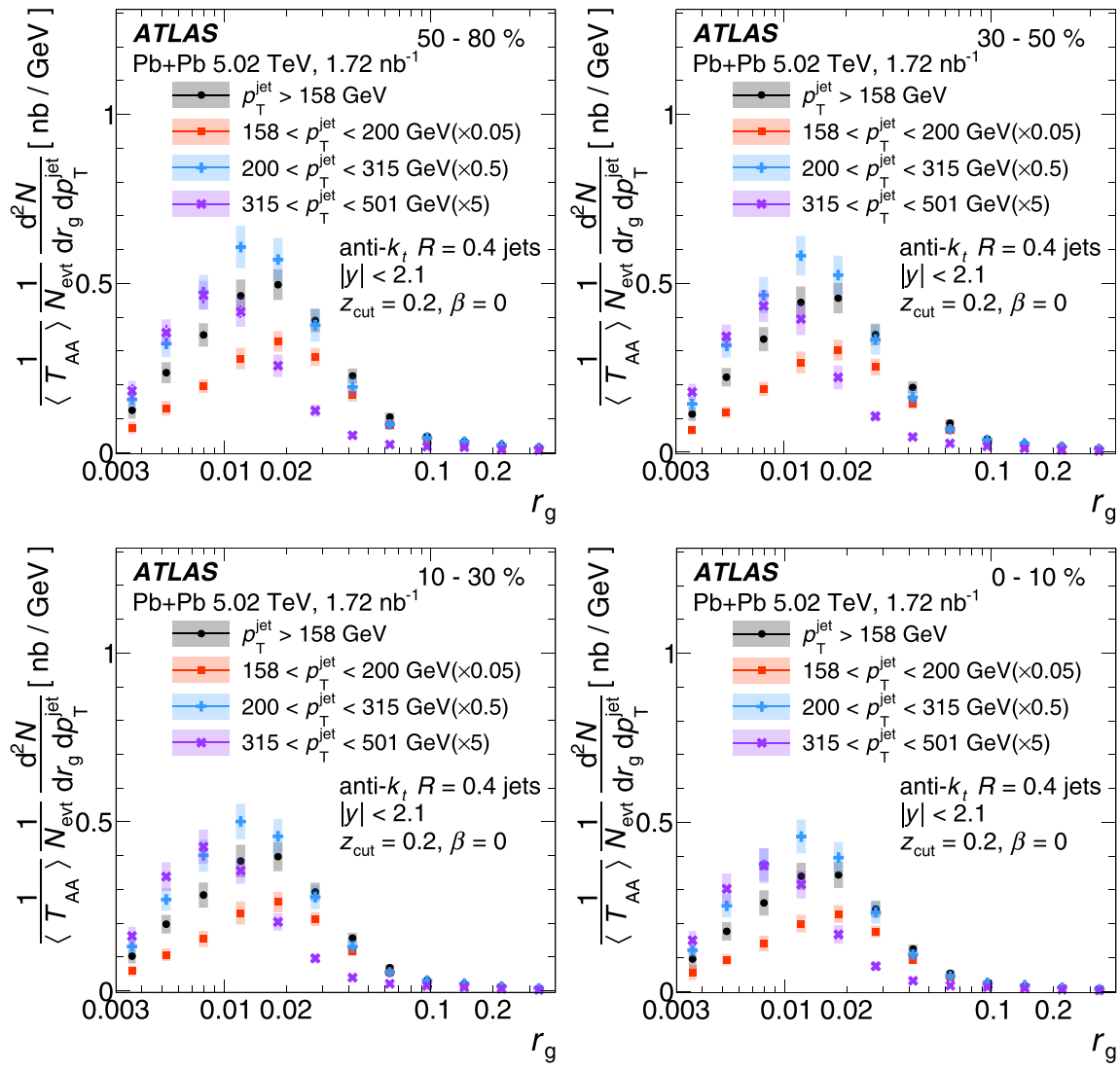

FIG. 9. The per-event jet yields in Pb+Pb collisions at $\sqrt{s_{NN}} = 5.02$ TeV normalized by $\langle T_{AA}\rangle$ as a function of soft-drop r_g in four centrality intervals and three p_T^{jet} intervals as well for $p_T^{jet} > 158$ GeV. The last bin does not contain the overflow. The statistical uncertainties are indicated by the error bars while the systematic uncertainties are indicated by the shaded bars. The normalization uncertainties of $\langle T_{AA}\rangle$ for each centrality interval are not shown, but are listed in Table I.

such as the centrality-independent JES and JER uncertainties, are treated as correlated when determining the uncertainty in R_{AA}. However, as the centrality-dependent component of the JES uncertainty (only for Pb+Pb collisions) does not cancel out in the cross-section ratios, it becomes the dominant source of uncertainty in the R_{AA} results.

VI. RESULTS

The unfolded differential jet cross-sections obtained from pp collision data are shown in Fig. 6 as a function of p_T^{jet} and r_g. The differential cross-sections are reported for four intervals in r_g, each scaled up by successive powers of 10. The cross-sections are also reported for jets that fail the soft-drop grooming condition. These are assigned a value of $r_g = 0$ in this analysis and they make up about 3.5% of the inclusive pp jet cross-section, and are also shown in Fig. 6.

Figure 7 shows the unfolded inclusive differential cross-section in pp collision data as a function of r_g. The differential cross-sections in r_g are also reported for four bins in p_T^{jet}. The distributions are observed to peak at lower values of r_g with increasing p_T^{jet}. Tighter collimation of jets with increasing p_T^{jet} is expected from the larger boost of the fragmenting parton and an increased quark-initiated jet fraction [67].

The jet differential cross-sections measured in pp data are compared with particle-level predictions from the PYTHIA 8, HERWIG, and SHERPA generators in Figs. 6 and 7. The HERWIG predictions are obtained from multijet events generated at next-to-leading order by HERWIG 7.1.3 [86] with the NNPDF3.0 PDF set [87] for the matrix element calculation.

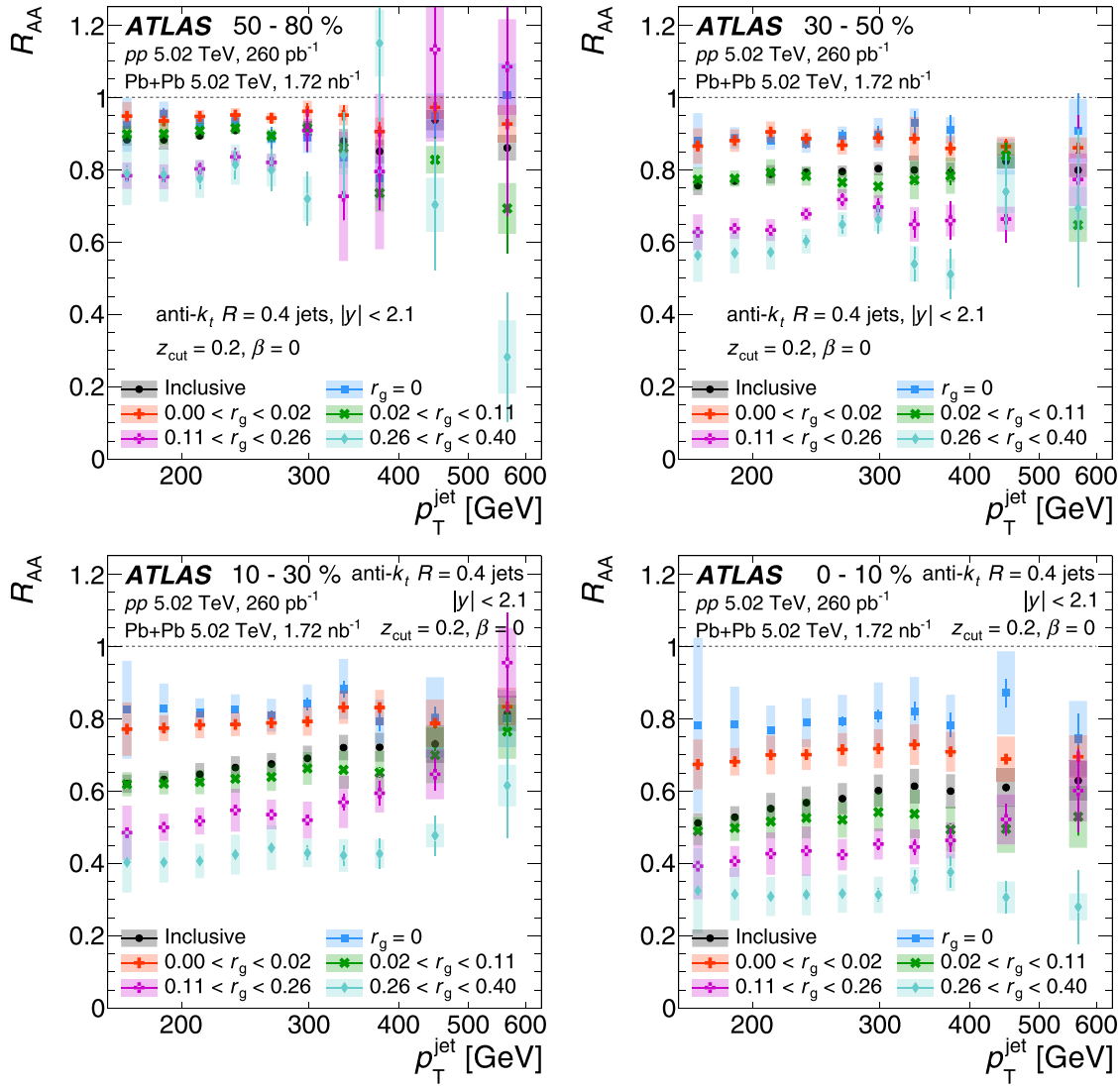

FIG. 10. Nuclear modification factor, R_{AA}, as a function of $p_{\mathrm{T}}^{\mathrm{jet}}$ for soft-drop groomed jets with $|y| < 2.1$ in four centrality intervals and four intervals of r_{g}. Groomed jet R_{AA} values are compared with R_{AA} values of jets without significant splitting identified by the soft-drop procedure ($r_{\mathrm{g}} = 0$) and jets without grooming (inclusive). The error bars represent statistical uncertainties while the shaded bars represent bin-wise correlated systematic uncertainties. The uncertainties in the pp luminosity (1.6%) and $\langle T_{\mathrm{AA}} \rangle$ are not included, but are listed in Table I.

The SHERPA predictions are from multijet events generated using SHERPA 2.2.5 [88]. The matrix element calculation was included for the $2 \to 2$ process at leading order, and the default SHERPA parton shower [89] based on Catani–Seymour dipole factorization was used for the showering with p_{T} ordering, using the CT14NNLO PDF set [90]. The PYTHIA 8 predictions overestimate the pp data jet cross-sections but describe the shape of the $p_{\mathrm{T}}^{\mathrm{jet}}$ and r_{g} distributions well, both inclusively and differentially in $p_{\mathrm{T}}^{\mathrm{jet}}$ and r_{g}. The HERWIG and SHERPA predictions underestimate the cross-sections but describe the shape of both the inclusive jet differential cross-section as a function of $p_{\mathrm{T}}^{\mathrm{jet}}$ and the differential cross-section in different r_{g} bins. The HERWIG generator predicts a slightly wider r_{g} distribution than seen in pp data across all $p_{\mathrm{T}}^{\mathrm{jet}}$ regions studied here. The SHERPA generator predicts a significantly narrower r_{g} distribution than seen in pp data at low $p_{\mathrm{T}}^{\mathrm{jet}}$ and underestimates the jet cross-sections at high $p_{\mathrm{T}}^{\mathrm{jet}}$. The trend of tighter collimation of jets with increasing $p_{\mathrm{T}}^{\mathrm{jet}}$ observed in pp data is reproduced by all three MC generators with varying levels of accuracy.

Figures 8 and 9 show the Pb+Pb per-event yields normalized by $\langle T_{\mathrm{AA}} \rangle$ for four centrality intervals as a function of $p_{\mathrm{T}}^{\mathrm{jet}}$ and r_{g}, respectively. The yields are also shown for jets that fail the soft-drop grooming condition (denoted by $r_{\mathrm{g}} = 0$) as a function of $p_{\mathrm{T}}^{\mathrm{jet}}$; they account for about 4–5.5% of the inclusive Pb+Pb jet yield. The per-event jet yields in Pb+Pb data normalized by $\langle T_{\mathrm{AA}} \rangle$ fall below the corresponding pp jet cross-sections for a given r_{g} or $p_{\mathrm{T}}^{\mathrm{jet}}$ interval, indicating jet suppression, and this difference increases for more central events and for increasing r_{g}. The r_{g} distributions are also observed to peak at lower values of r_{g} with increasing $p_{\mathrm{T}}^{\mathrm{jet}}$ in both pp collisions and all centrality intervals in Pb+Pb collisions. The

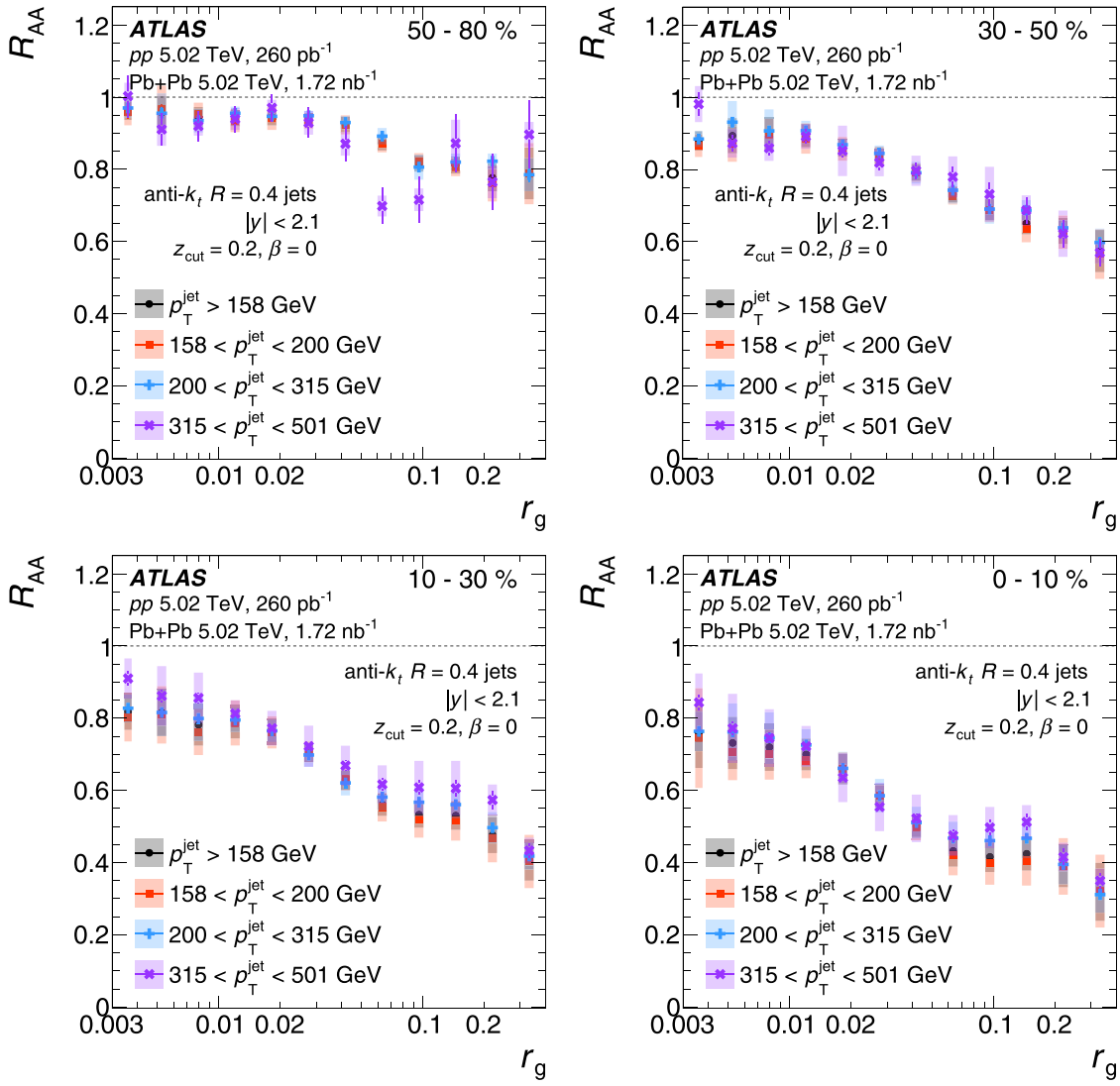

FIG. 11. Nuclear modification factor, R_{AA}, as a function of r_g for soft-drop groomed jets with $|y| < 2.1$ in four centrality intervals and three intervals of p_T^{jet}, in comparison with the p_T-inclusive results. The error bars represent statistical uncertainties while the shaded bars represent bin-wise correlated systematic uncertainties. The uncertainties in the pp luminosity (1.6%) and $\langle T_{AA} \rangle$ are not included, but are listed in Table I.

p_T^{jet} spectra are observed to have similar slopes in the different r_g regions for both pp and Pb+Pb collisions.

The nuclear modification factor R_{AA}, which quantifies the jet suppression in Pb+Pb collisions relative to pp collisions, is shown as a function of p_T^{jet} in Fig. 10 and as a function of r_g in Fig. 11 for four centrality intervals. The R_{AA} value for inclusive jets is observed to vary from ≈0.95 for jets in the 50–80% centrality interval to ≈0.55 for the most central collisions. The R_{AA} values for inclusive jets are also observed to have an upward slope with increasing p_T^{jet} and are consistent with the results measured for jets using 2015 Pb+Pb data with a lower integrated luminosity of 0.49 nb^{-1} [24].

The values of R_{AA} are observed to depend significantly on r_g, with a clear ordering with respect to the splitting angle. Jets that fail the soft-drop grooming procedure or have $r_g < 0.02$ are observed to be the least suppressed with an R_{AA} value of ≈0.75 in central Pb+Pb collisions. In contrast, jets with the widest splitting angle between their hardest subjets are observed to be suppressed with an R_{AA} value of ≈0.3. Notably, the difference in the R_{AA} values is largest between jets having r_g values below or above 0.02, supporting a coherence picture of jet quenching [41,42]. The R_{AA} values for jets in different r_g regions are observed to have a weaker dependence on p_T^{jet} in comparison with the R_{AA} behavior for the inclusive jets, especially in more central collisions. The increase in R_{AA} for inclusive jets as a function of p_T^{jet} may be explained as arising from tighter jet collimation with increasing p_T^{jet}. Jets with lower r_g values in Pb+Pb collisions are significantly less suppressed than jets with large r_g values and they also constitute a larger fraction of the inclusive jets with increasing p_T^{jet}, resulting in a rising trend for R_{AA} as a function of p_T^{jet}. As a function of r_g, R_{AA} decreases smoothly with increasing r_g

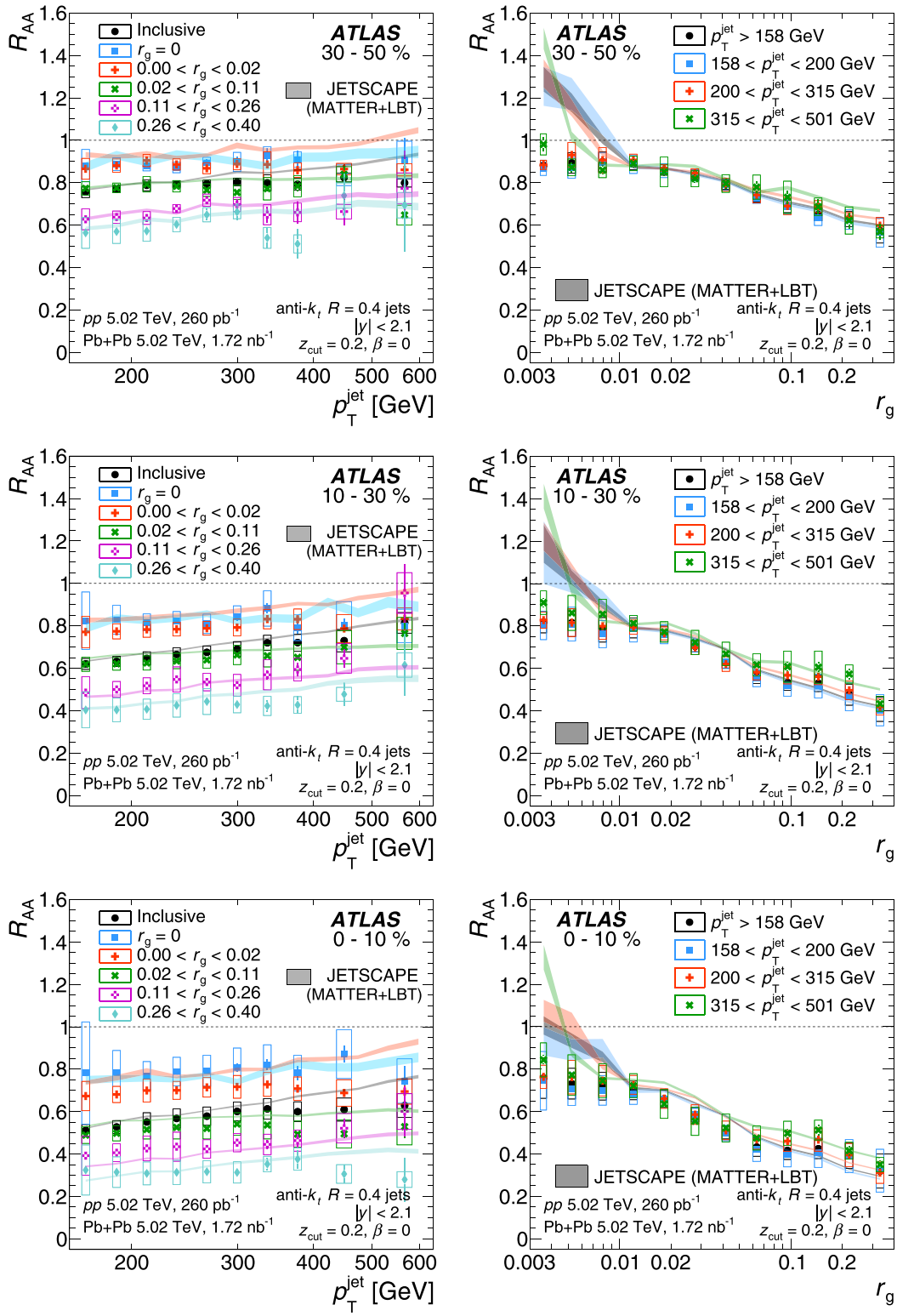

FIG. 12. Comparison of R_{AA} as a function of (left) p_T^{jet} for inclusive jets and for four intervals of r_g, (right) r_g for inclusive jets and for three intervals of p_T^{jet}, and in three centrality intervals of Pb+Pb events with predictions from the JETSCAPE framework [43,91]. The error bars and the open boxes around the data points represent the statistical and systematic uncertainties, respectively. The uncertainties in the *pp* luminosity (1.6%) and $\langle T_{AA} \rangle$ are not included, but are listed in Table I. The widths of the bands representing the JETSCAPE predictions indicate their statistical uncertainties.

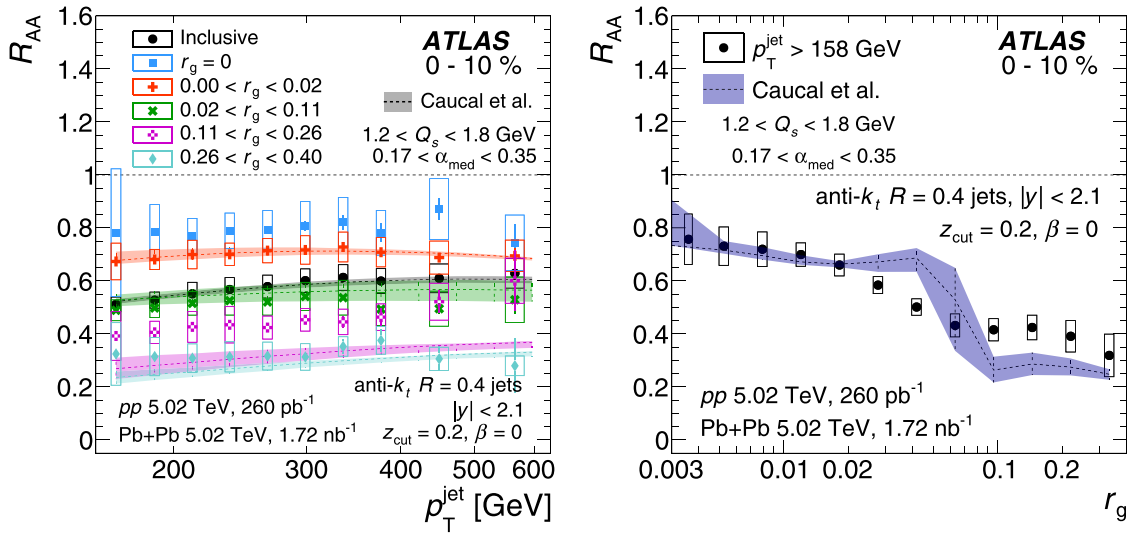

FIG. 13. Comparison of R_{AA} as a function of (left) p_T^{jet} for inclusive jets and for four intervals of r_g and (right) as a function of r_g for inclusive jets in 0–10% centrality Pb+Pb events with theoretical predictions from the pQCD framework of Caucal *et al.*, described in Refs. [41,42,92]. The error bars and the open boxes around the data points represent the statistical and systematic uncertainties, respectively. The uncertainties in the pp luminosity (1.6%) and $\langle T_{AA} \rangle$ are not included, but are listed in Table I. The shaded areas around the theoretical predictions represent the uncertainties arising from the variation of the transport coefficient ($\hat{q}$) and shower cutoff parameters.

(shown on logarithmic scale) in all centrality intervals and is again noted to not significantly depend on p_T^{jet} in the measured kinematic range.

The jet suppression measurements are compared with predictions from various theoretical models and frameworks including those from the JETSCAPE MC framework [43,91], Caucal *et al.* [41,42,92] and Ringer *et al.* [93]. JETSCAPE provides a multistage model of jet evolution by combining several jet-quenching formalisms applied in its range of validity in shower energy and virtuality. The JETSCAPE predictions combine jet energy-loss calculations from the MATTER [94] and LBT [95,96] models at high and low virtualities of the parton shower in the QGP medium, respectively. The parameters used in generating the predictions, including the transport coefficient ($\hat{q}$) and the virtuality at which to switch parton energy loss from MATTER to LBT (Q_{sw}), can be found in Ref. [43]. JETSCAPE also includes a virtuality-dependent onset of coherence effects in order to model the inability of the medium to resolve narrow splittings of highly virtual partons at earlier timescales. The model from Caucal *et al.* presents a perturbative QCD (pQCD) picture of jet quenching dictated by the factorization of medium-induced

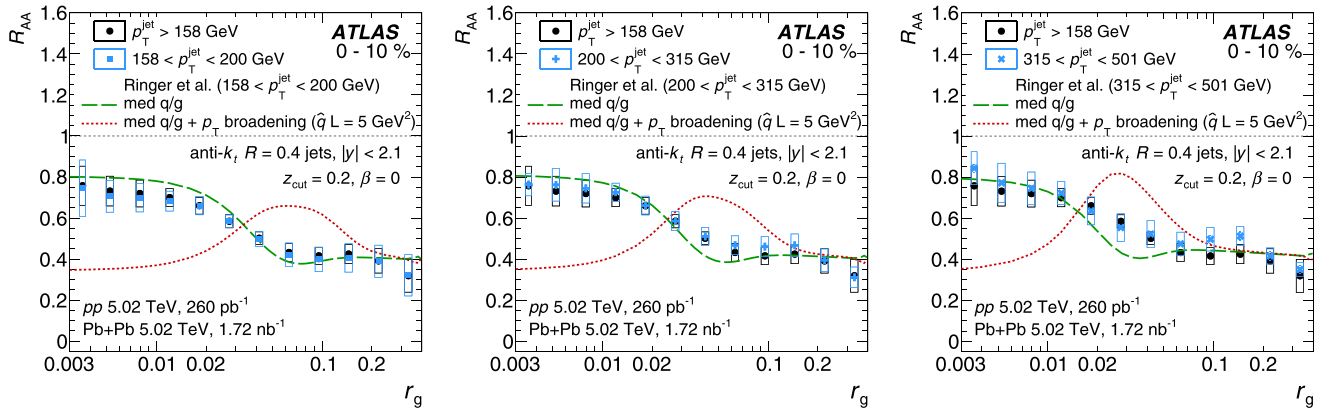

FIG. 14. Comparison of R_{AA} as a function of r_g for three intervals of p_T^{jet} in 0–10% centrality Pb+Pb events with theoretical predictions from Ringer *et al.* [93]. The error bars and the open boxes around the data points represent the statistical and systematic uncertainties, respectively. The uncertainties in the pp luminosity (1.6%) and $\langle T_{AA} \rangle$ are not included, but are listed in Table I. The green curve (med q/g) represents the quark and gluon differential energy loss setting. The red curve (med q/g + p_T broadening) adds transverse momentum broadening effects for all subjets in the medium.

parton branchings and vacuum-like emissions in a longitudinally expanding medium. An important aspect of this model is the onset of incoherent jet energy loss beyond a critical angle between the branches of the hardest jet splitting. It should be noted that the calculations from Caucal *et al.* are purely at the parton level and hadronization effects are not included. The analytic calculations for jet R_{AA} by Ringer *et al.* are based on medium-modified quark and gluon jet functions using a MC sampling approach. In conjunction with the quark and gluon differential jet energy loss, transverse momentum broadening is applied to all the subjets in this model, based on the transport coefficient parameter.

The jet R_{AA} results are compared with predictions from the above frameworks and models as a function of $p_{\mathrm{T}}^{\mathrm{jet}}$ and r_{g} in Figs. 12–14. Predictions from JETSCAPE (MATTER + LBT), shown in Fig. 12, are able to capture the trend of r_{g}-dependent jet suppression in three centrality intervals of Pb+Pb collisions. However, JETSCAPE overestimates the R_{AA} values for jets in the low r_{g} (<0.01) region, especially at higher $p_{\mathrm{T}}^{\mathrm{jet}}$. The R_{AA} predictions from the pQCD picture modeled by Caucal *et al.*, shown in Fig. 13, qualitatively describe the r_{g}-dependent suppression trend observed in the most central collisions. Compared to the data in Fig. 13, the parton-level pQCD model calculations predict a sharper drop in R_{AA} around the critical angle beyond which incoherent jet energy loss sets in. The quark versus gluon differential quenching effects modeled by Ringer *et al.*, labeled "med q/g" in Fig. 14, are able to describe the r_{g}-dependent jet suppression in three intervals of $p_{\mathrm{T}}^{\mathrm{jet}}$. Transverse momentum broadening effects are included in the model calculations by adding p_{T} kicks perpendicular to the direction of each subjet by sampling from a simple Gaussian distribution, whose width is determined using the transport coefficient parameter [93]. The combined model calculations with quark and gluon differential jet energy loss and transverse momentum broadening effects are labeled as "med q/g + p_{T} broadening" in Fig. 14. Adding p_{T}-broadening effects to the model results in a significant suppression of jets at lower r_{g} values and a peak in R_{AA} at mid-r_{g} values, neither of which are observed in data.

VII. CONCLUSION

Jet production in Pb+Pb and pp collisions, both at $\sqrt{s_{NN}} = 5.02$ TeV, is measured with the ATLAS detector at the LHC, using integrated luminosities of $1.72\,\mathrm{nb}^{-1}$ and $260\,\mathrm{pb}^{-1}$, respectively. The jets are reconstructed using the anti-k_t algorithm with $R = 0.4$ and groomed using the soft-drop procedure with parameters $z_{\mathrm{cut}} = 0.2$ and $\beta = 0$. The jet differential cross-sections and yields are presented as a function of $p_{\mathrm{T}}^{\mathrm{jet}}$ and r_{g}, the opening angle of the hardest splitting, and in intervals of collision centrality. Results unfolded to the particle level are presented for jets with $p_{\mathrm{T}}^{\mathrm{jet}} > 158$ GeV, $|y| < 2.1$, and $0 \leqslant r_{\mathrm{g}} < 0.4$.

The r_{g} distributions obtained in pp collisions are observed to peak at lower values of r_{g} with increasing $p_{\mathrm{T}}^{\mathrm{jet}}$, indicating that higher-momentum jets are more collimated. The differential cross-sections as a function of $p_{\mathrm{T}}^{\mathrm{jet}}$ and r_{g} are compared with results from MC event generators (PYTHIA 8, HERWIG, and SHERPA), with the PYTHIA 8 predictions best describing the shape of the $p_{\mathrm{T}}^{\mathrm{jet}}$ and r_{g} spectra seen in pp collisions.

The jet energy loss and the resulting suppression in Pb+Pb collisions is quantified by the nuclear modification factor, R_{AA}. The R_{AA} values are observed to depend primarily on the jet r_{g} value and the event centrality. In the most central collisions, the R_{AA} value ranges between $R_{AA} \approx 0.75$ for the most collimated jets ($r_{\mathrm{g}} < 0.02$) and $R_{AA} \approx 0.3$ for the widest jets ($0.26 < r_{\mathrm{g}} < 0.4$). The R_{AA} values are observed to decrease monotonically with increasing r_{g}, and do not depend strongly on $p_{\mathrm{T}}^{\mathrm{jet}}$ for a selected r_{g} range. Although the energy loss is not measured directly and must be inferred from the R_{AA} values and slope of the differential cross-sections as a function of $p_{\mathrm{T}}^{\mathrm{jet}}$, the $p_{\mathrm{T}}^{\mathrm{jet}}$-dependence is observed to be similar for different r_{g} ranges. These features together with the dependence of R_{AA} on r_{g} indicate that jets with larger opening angles lose more energy. Predictions from theoretical models of jet quenching are compared with the R_{AA} measurements presented here and are observed to describe the r_{g}-dependent jet suppression features with varying accuracy. The results presented here are qualitatively consistent with a picture of jet quenching dictated by coherence and provide the most direct evidence supporting this approach so far.

ACKNOWLEDGMENTS

We thank CERN for the very successful operation of the LHC, as well as the support staff from our institutions without whom ATLAS could not be operated efficiently. We acknowledge the support of ANPCyT, Argentina; YerPhI, Armenia; ARC, Australia; BMWFW and FWF, Austria; ANAS, Azerbaijan; CNPq and FAPESP, Brazil; NSERC, NRC and CFI, Canada; CERN; ANID, Chile; CAS, MOST and NSFC, China; Minciencias, Colombia; MEYS CR, Czech Republic; DNRF and DNSRC, Denmark; IN2P3-CNRS and CEA-DRF/IRFU, France; SRNSFG, Georgia; BMBF, HGF and MPG, Germany; GSRI, Greece; RGC and Hong Kong SAR, China; ISF and Benoziyo Center, Israel; INFN, Italy; MEXT and JSPS, Japan; CNRST, Morocco; NWO, Netherlands; RCN, Norway; MEiN, Poland; FCT, Portugal; MNE/IFA, Romania; MESTD, Serbia; MSSR, Slovakia; ARRS and MIZŠ, Slovenia; DSI/NRF, South Africa; MICINN, Spain; SRC and Wallenberg Foundation, Sweden; SERI, SNSF and Cantons of Bern and Geneva, Switzerland; MOST, Taiwan; TENMAK, Türkiye; STFC, United Kingdom; DOE and NSF, United States of America. In addition, individual groups and members have received support from BCKDF, CANARIE, Compute Canada and CRC, Canada; PRIMUS 21/SCI/017 and UNCE SCI/013, Czech Republic; COST, ERC, ERDF, Horizon 2020 and Marie Skłodowska-Curie Actions, European Union; Investissements d'Avenir Labex, Investissements d'Avenir Idex and ANR, France; DFG and AvH Foundation, Germany; Herakleitos, Thales and Aristeia programmes co-financed by EU-ESF and the Greek NSRF, Greece; BSF-NSF and MINERVA, Israel; Norwegian Financial Mechanism 2014–2021, Norway; NCN and NAWA, Poland; La Caixa Banking Foundation, CERCA Programme Generalitat de Catalunya and PROMETEO and GenT Programmes Generalitat Valenciana, Spain; Göran Gustafssons Stiftelse, Sweden;

The Royal Society and Leverhulme Trust, United Kingdom. The crucial computing support from all WLCG partners is acknowledged gratefully, in particular from CERN, the ATLAS Tier-1 facilities at TRIUMF (Canada), NDGF (Denmark, Norway, Sweden), CC-IN2P3 (France), KIT/GridKA (Germany), INFN-CNAF (Italy), NL-T1 (Netherlands), PIC (Spain), ASGC (Taiwan), RAL (UK) and BNL (USA), the Tier-2 facilities worldwide, and large non-WLCG resource providers. Major contributors of computing resources are listed in Ref. [97].

[1] STAR Collaboration, Experimental and theoretical challenges in the search for the quark gluon plasma: The STAR Collaboration's critical assessment of the evidence from RHIC collisions, Nucl. Phys. A **757**, 102 (2005).
[2] PHENIX Collaboration, Formation of dense partonic matter in relativistic nucleus-nucleus collisions at RHIC: Experimental evaluation by the PHENIX collaboration, Nucl. Phys. A **757**, 184 (2005).
[3] M. Gyulassy and L. McLerran, New forms of QCD matter discovered at RHIC, Nucl. Phys. A **750**, 30 (2005).
[4] W. Busza, K. Rajagopal, and W. van der Schee, Heavy ion collisions: The big picture, and the big questions, Ann. Rev. Nucl. Part. Sci. **68**, 339 (2018).
[5] M. Gyulassy and M. Plümer, Jet quenching in dense matter, Phys. Lett. B **243**, 432 (1990).
[6] J. D. Bjorken, Energy Loss of Energetic Partons in Quark-Gluon Plasma: Possible Extinction of High p(t) Jets in Hadron-Hadron Collisions, FERMILAB-PUB-82-059-THY (1982).
[7] D. Krohn, J. Thaler, and L.-T. Wang, Jet trimming, J. High Energy Phys. 02 (2010) 084.
[8] M. Dasgupta, A. Fregoso, S. Marzani, and G. P. Salam, Towards an understanding of jet substructure, J. High Energy Phys. 09 (2013) 029.
[9] A. J. Larkoski, S. Marzani, G. Soyez, and J. Thaler, Soft drop, J. High Energy Phys. 05 (2014) 146.
[10] ATLAS Collaboration, Measurement of the Soft-Drop Jet Mass in pp Collisions at $\sqrt{s} = 13$ TeV with the ATLAS Detector, Phys. Rev. Lett. **121**, 092001 (2018).
[11] ATLAS Collaboration, Measurement of soft-drop jet observables in pp collisions with the ATLAS detector at $\sqrt{s} = 13$ TeV, Phys. Rev. D **101**, 052007 (2020).
[12] Y. Mehtar-Tani and K. Tywoniuk, Groomed jets in heavy-ion collisions: Sensitivity to medium-induced bremsstrahlung, J. High Energy Phys. 04 (2017) 125.
[13] Y.-T. Chien and I. Vitev, Probing the Hardest Branching Within Jets in Heavy-Ion Collisions, Phys. Rev. Lett. **119**, 112301 (2017).
[14] H. A. Andrews *et al.*, Novel tools and observables for jet physics in heavy-ion collisions, J. Phys. G **47**, 065102 (2020).
[15] CMS Collaboration, Measurement of the Splitting Function in pp and PbPb Collisions at $\sqrt{s_{\rm NN}} = 5.02$ TeV, Phys. Rev. Lett. **120**, 142302 (2018).
[16] CMS Collaboration, Measurement of the groomed jet mass in PbPb and pp collisions at $\sqrt{s_{\rm NN}} = 5.02$ TeV, J. High Energy Phys. 10 (2018) 161.
[17] ALICE Collaboration, Exploration of jet substructure using iterative declustering in pp and Pb-Pb collisions at LHC energies, Phys. Lett. B **802**, 135227 (2020).
[18] ALICE Collaboration, Measurement of the Groomed Jet Radius and Momentum Splitting Fraction in pp and Pb − Pb Collisions at $\sqrt{s_{NN}} = 5.02$ TeV, Phys. Rev. Lett. **128**, 102001 (2022).
[19] STAR Collaboration, Differential measurements of jet substructure and partonic energy loss in Au+Au collisions at $\sqrt{S_{NN}} = 200$ GeV, Phys. Rev. C **105**, 044906 (2022).
[20] P. Foka and M. A. Janik, An overview of experimental results from ultra-relativistic heavy-ion collisions at the CERN LHC: Hard probes, Rev. Phys. **1**, 172 (2016).
[21] L. Cunqueiro and A. M. Sickles, Studying the QGP with Jets at the LHC and RHIC, Prog. Part. Nucl. Phys. **124**, 103940 (2022).
[22] ATLAS Collaboration, Measurement of the jet radius and transverse momentum dependence of inclusive jet suppression in lead–lead collisions at $\sqrt{s_{\rm NN}} = 2.76$ TeV with the ATLAS detector, Phys. Lett. B **719**, 220 (2013).
[23] ATLAS Collaboration, Measurements of the Nuclear Modification Factor for Jets in Pb+Pb Collisions at $\sqrt{s_{\rm NN}} = 2.76$TeV with the ATLAS Detector, Phys. Rev. Lett. **114**, 072302 (2015).
[24] ATLAS Collaboration, Measurement of the nuclear modification factor for inclusive jets in Pb+Pb collisions at $\sqrt{s_{\rm NN}} = 5.02$ TeV with the ATLAS detector, Phys. Lett. B **790**, 108 (2019).
[25] CMS Collaboration, Measurement of inclusive jet cross-sections in pp and PbPb collisions at $\sqrt{s_{\rm NN}} = 2.76$ TeV, Phys. Rev. C **96**, 015202 (2017).
[26] CMS Collaboration, First measurement of large area jet transverse momentum spectra in heavy-ion collisions, J. High Energy Phys. 05 (2021) 284.
[27] ATLAS Collaboration, Observation of a Centrality-Dependent Dijet Asymmetry in Lead–Lead Collisions at $\sqrt{s_{\rm NN}} = 2.76$ TeV with the ATLAS Detector at the LHC, Phys. Rev. Lett. **105**, 252303 (2010).
[28] ATLAS Collaboration, Measurement of photon-jet transverse momentum correlations in 5.02 TeV Pb+Pb and pp collisions with ATLAS, Phys. Lett. B **789**, 167 (2019).
[29] CMS Collaboration, In-medium modification of dijets in PbPb collisions at $\sqrt{s_{\rm NN}} = 5.02$ TeV, J. High Energy Phys. 05 (2021) 116.
[30] CMS Collaboration, Study of Jet Quenching with Z+Jet Correlations in PbPb and pp Collisions at $\sqrt{s_{\rm NN}} = 5.02$ TeV, Phys. Rev. Lett. **119**, 082301 (2017).
[31] ATLAS Collaboration, Measurement of jet fragmentation in Pb+Pb and pp collisions at $\sqrt{s_{\rm NN}} = 5.02$ TeV with the ATLAS detector, Phys. Rev. C **98**, 024908 (2018).
[32] ATLAS Collaboration, Comparison of Fragmentation Functions for Jets Dominated by Light Quarks and Gluons from pp and Pb+Pb Collisions in ATLAS, Phys. Rev. Lett. **123**, 042001 (2019).
[33] CMS Collaboration, Measurement of jet fragmentation in PbPb and pp collisions at $\sqrt{s_{\rm NN}} = 2.76$ TeV, Phys. Rev. C **90**, 024908 (2014).
[34] CMS Collaboration, Observation of Medium Induced Modifications of Jet Fragmentation in Pb-Pb Collisions at $\sqrt{s_{\rm NN}} = 5.02$ TeV Using Isolated Photon-Tagged Jets, Phys. Rev. Lett. **121**, 242301 (2018).
[35] CMS Collaboration, Jet properties in PbPb and pp collisions at $\sqrt{s_{\rm NN}} = 5.02$ TeV, J. High Energy Phys. 05 (2018) 006.

[36] STAR Collaboration, Measurement of groomed jet substructure observables in p+p collisions at $\sqrt{s} = 200$ GeV with STAR, Phys. Lett. B **811**, 135846 (2020).

[37] Yu. L. Dokshitzer, V. A. Khoze, S. I. Troyan, and A. H. Mueller, QCD coherence in high-energy reactions, Rev. Mod. Phys. **60**, 373 (1988).

[38] R. Baier, Yu. L. Dokshitzer, A. H. Mueller, S. Peigné, and D. Schiff, Radiative energy loss of high-energy quarks and gluons in a finite volume quark - gluon plasma, Nucl. Phys. B **483**, 291 (1997).

[39] J. Casalderrey-Solana, Y. Mehtar-Tani, C. A. Salgado, and K. Tywoniuk, New picture of jet quenching dictated by color coherence, Phys. Lett. B **725**, 357 (2013).

[40] G. Milhano, U. A. Wiedemann, and K. C. Zapp, Sensitivity of jet substructure to jet-induced medium response, Phys. Lett. B **779**, 409 (2018).

[41] P. Caucal, E. Iancu, and G. Soyez, Deciphering the z_g distribution in ultrarelativistic heavy ion collisions, J. High Energy Phys. 10 (2019) 273.

[42] P. Caucal, E. Iancu, and G. Soyez, Jet radiation in a longitudinally expanding medium, J. High Energy Phys. 04 (2021) 209.

[43] A. Kumar *et al.*, Inclusive jet and hadron suppression in a multistage approach, Phys. Rev. C **107**, 034911 (2023).

[44] M. Cacciari, G. P. Salam, and G. Soyez, The anti-k_t jet clustering algorithm, J. High Energy Phys. 04 (2008) 063.

[45] ATLAS Collaboration, The ATLAS experiment at the CERN Large Hadron Collider, J. Instrum. **3**, S08003 (2008).

[46] ATLAS Collaboration, ATLAS Insertable B-Layer Technical Design Report, ATLAS-TDR-19; CERN-LHCC-2010-013 (2010), https://cds.cern.ch/record/1291633, Addendum: ATLAS-TDR-19-ADD-1; CERN-LHCC-2012-009 (2012), https://cds.cern.ch/record/1451888.

[47] B. Abbott *et al.*, Production and integration of the ATLAS insertable B-layer, JINST **13**, T05008 (2018).

[48] ATLAS Collaboration, Performance of the ATLAS trigger system in 2015, Eur. Phys. J. C **77**, 317 (2017).

[49] ATLAS Collaboration, The ATLAS Collaboration Software and Firmware, ATL-SOFT-PUB-2021-001 (2021), https://cds.cern.ch/record/2767187.

[50] ATLAS Collaboration, ATLAS data quality operations and performance for 2015–2018 data-taking, JINST **15**, P04003 (2020).

[51] ATLAS Collaboration, Measurement of azimuthal anisotropy of muons from charm and bottom hadrons in Pb+Pb collisions at $\sqrt{s_{\rm NN}} = 5.02$ TeV with the ATLAS detector, Phys. Lett. B **807**, 135595 (2020).

[52] M. L. Miller, K. Reygers, S. J. Sanders, and P. Steinberg, Glauber modeling in high-energy nuclear collisions, Ann. Rev. Nucl. Part. Sci. **57**, 205 (2007).

[53] C. Loizides, J. Nagle, and P. Steinberg, Improved version of the PHOBOS Glauber Monte Carlo, SoftwareX **1-2**, 13 (2015).

[54] ATLAS Collaboration, Measurement of $W^{\pm}$ boson production in Pb+Pb collisions at $\sqrt{s_{\rm NN}} = 5.02$ TeV with the ATLAS detector, Eur. Phys. J. C **79**, 935 (2019).

[55] T. Sjöstrand *et al.*, An introduction to PYTHIA 8.2, Comput. Phys. Commun. **191**, 159 (2015).

[56] ATLAS Collaboration, ATLAS Pythia 8 tunes to 7 TeV data, ATL-PHYS-PUB-2014-021 (2014), https://cds.cern.ch/record/1966419.

[57] R. D. Ball *et al.*, Parton distributions with LHC data, Nucl. Phys. B **867**, 244 (2013).

[58] S. Agostinelli *et al.*, Geant4–a simulation toolkit, Nucl. Instrum. Meth. A **506**, 250 (2003).

[59] ATLAS Collaboration, The ATLAS Simulation Infrastructure, Eur. Phys. J. C **70**, 823 (2010).

[60] ATLAS Collaboration, Measurements of azimuthal anisotropies of jet production in Pb+Pb collisions at $\sqrt{s_{NN}} = 5.02$ TeV with the ATLAS detector, Phys. Rev. C **105**, 064903 (2022).

[61] M. Cacciari, G. P. Salam, and G. Soyez, FastJet user manual, Eur. Phys. J. C **72**, 1896 (2012).

[62] ATLAS Collaboration, Jet energy measurement with the ATLAS detector in proton–proton collisions at $\sqrt{s} = 7$ TeV, Eur. Phys. J. C **73**, 2304 (2013).

[63] ATLAS Collaboration, Measurement of the azimuthal anisotropy of charged particles produced in $\sqrt{s_{\rm NN}} = 5.02$ TeV Pb+Pb collisions with the ATLAS detector, Eur. Phys. J. C **78**, 997 (2018).

[64] ATLAS Collaboration, Observation of Long-Range Elliptic Azimuthal Anisotropies in $\sqrt{s} = 13$ and 2.76 TeV pp Collisions with the ATLAS Detector, Phys. Rev. Lett. **116**, 172301 (2016).

[65] ATLAS Collaboration, Jet energy scale and its uncertainty for jets reconstructed using the ATLAS heavy ion jet algorithm, ATLAS-CONF-2015-016 (2015), https://cds.cern.ch/record/2008677.

[66] ATLAS Collaboration, Topological cell clustering in the ATLAS calorimeters and its performance in LHC Run 1, Eur. Phys. J. C **77**, 490 (2017).

[67] ATLAS Collaboration, Improving jet substructure performance in ATLAS using Track-CaloClusters, ATL-PHYS-PUB-2017-015 (2017), https://cds.cern.ch/record/2275636.

[68] ATLAS Collaboration, A W/Z-boson tagger using Track-CaloCluster jets with ATLAS, ATL-PHYS-PUB-2020-008 (2020), https://cds.cern.ch/record/2718218.

[69] ATLAS Collaboration, Jet reconstruction and performance using particle flow with the ATLAS Detector, Eur. Phys. J. C **77**, 466 (2017).

[70] ATLAS Collaboration, Optimisation of large-radius jet reconstruction for the ATLAS detector in 13 TeV proton–proton collisions, Eur. Phys. J. C **81**, 334 (2020).

[71] ATLAS Collaboration, Performance of the ATLAS track reconstruction algorithms in dense environments in LHC Run 2, Eur. Phys. J. C **77**, 673 (2017).

[72] ATLAS Collaboration, Measurement of charged-particle spectra in Pb+Pb collisions at $\sqrt{s_{\rm NN}} = 2.76$ TeV with the ATLAS detector at the LHC, J. High Energy Phys. 09 (2015) 050.

[73] M. Wobisch and T. Wengler, Hadronization corrections to jet cross-sections in deep inelastic scattering, in *Proceedings of the Workshop on Monte Carlo Generators for HERA Physics (Plenary Starting Meeting)* (1998), p. 270.

[74] Yu. L. Dokshitzer, G. D. Leder, S. Moretti, and B. R. Webber, Better jet clustering algorithms, J. High Energy Phys. 08 (1997) 001.

[75] J. Mulligan and M. Ploskon, Identifying groomed jet splittings in heavy-ion collisions, Phys. Rev. C **102**, 044913 (2020).

[76] T. Adye, Unfolding algorithms and tests using RooUnfold, in *Proceedings of the Workshop on Statistical Issues Related to Discovery Claims in Search Experiments and Unfolding (PHYSTAT'11)* (CERN, Geneva, Switzerland, 2011), p. 313.

[77] G. D'Agostini, A multidimensional unfolding method based on Bayes' theorem, Nucl. Instrum. Meth. A **362**, 487 (1995).

[78] ATLAS Collaboration, Jet energy scale measurements and their systematic uncertainties in proton–proton collisions at $\sqrt{s} =$ 13 TeV with the ATLAS detector, Phys. Rev. D **96**, 072002 (2017).
[79] ATLAS Collaboration, Jet energy resolution in proton–proton collisions at $\sqrt{s} = 7$ TeV recorded in 2010 with the ATLAS detector, Eur. Phys. J. C **73**, 2306 (2013).
[80] ATLAS Collaboration, Measurements of jet vetoes and azimuthal decorrelations in dijet events produced in pp collisions at $\sqrt{s} = 7$ TeV using the ATLAS detector, Eur. Phys. J. C **74**, 3117 (2014).
[81] ATLAS Collaboration, Study of the material of the ATLAS inner detector for Run 2 of the LHC, JINST **12**, P12009 (2017).
[82] ATLAS Collaboration, Measurement of track reconstruction inefficiencies in the core of jets via pixel dE/dx with the ATLAS experiment using $\sqrt{s} =$ 13 TeV pp collision data, ATL-PHYS-PUB-2016-007 (2016), https://cds.cern.ch/record/2140460.
[83] ATLAS Collaboration, Evaluating statistical uncertainties and correlations using the bootstrap method, ATL-PHYS-PUB-2021-011 (2021), https://cds.cern.ch/record/2759945.
[84] G. Avoni *et al.*, The new LUCID-2 detector for luminosity measurement and monitoring in ATLAS, JINST **13**, P07017 (2018).
[85] ATLAS Collaboration, Luminosity determination in pp collisions at $\sqrt{s} = 13$ TeV using the ATLAS detector at the LHC, ATLAS-CONF-2019-021 (2019), https://cds.cern.ch/record/2677054.
[86] J. Bellm *et al.*, Herwig 7.1 Release Note, arXiv:1705.06919.
[87] R. D. Ball *et al.*, Parton distributions for the LHC run II, J. High Energy Phys. 04 (2015) 040.
[88] E. Bothmann *et al.*, Event generation with Sherpa 2.2, SciPost Phys. **7**, 034 (2019).
[89] S. Schumann and F. Krauss, A parton shower algorithm based on Catani–Seymour dipole factorisation, J. High Energy Phys. 03 (2008) 038.
[90] S. Dulat, T. J. Hou, J. Gao, M. Guzzi, J. Huston, P. Nadolsky, J. Pumplin, C. Schmidt, D. Stump, and C. P. Yuan, New parton distribution functions from a global analysis of quantum chromodynamics, Phys. Rev. D **93**, 033006 (2016).
[91] J. H. Putschke *et al.*, The JETSCAPE framework, arXiv:1903.07706.
[92] P. Caucal, E. Iancu, A. H. Mueller, and G. Soyez, Vacuumlike Jet Fragmentation in a Dense QCD Medium, Phys. Rev. Lett. **120**, 232001 (2018).
[93] F. Ringer, B.-W. Xiao, and F. Yuan, Can we observe jet P_T-broadening in heavy-ion collisions at the LHC? Phys. Lett. B **808**, 135634 (2020).
[94] A. Majumder, Incorporating space-time within medium-modified jet event generators, Phys. Rev. C **88**, 014909 (2013).
[95] Y. He, T. Luo, X.-N. Wang, and Y. Zhu, Linear Boltzmann transport for jet propagation in the quark-gluon plasma: Elastic processes and medium recoil, Phys. Rev. C **91**, 054908 (2015); **97**, 019902(E) (2018).
[96] S. Cao, T. Luo, G.-Y. Qin, and X.-N. Wang, Linearized Boltzmann transport model for jet propagation in the quark-gluon plasma: Heavy quark evolution, Phys. Rev. C **94**, 014909 (2016).
[97] ATLAS Collaboration, ATLAS Computing Acknowledgements, ATL-SOFT-PUB-2021-003 (2021), https://cds.cern.ch/record/2776662.

G. Aad,[101] B. Abbott,[119] D. C. Abbott,[102] K. Abeling,[55] S. H. Abidi,[29] A. Aboulhorma,[35e] H. Abramowicz,[150] H. Abreu,[149] Y. Abulaiti,[116] A. C. Abusleme Hoffman,[136a] B. S. Acharya,[68a,68b,a] B. Achkar,[55] L. Adam,[99] C. Adam Bourdarios,[4] L. Adamczyk,[84a] L. Adamek,[154] S. V. Addepalli,[26] J. Adelman,[114] A. Adiguzel,[21c] S. Adorni,[56] T. Adye,[133] A. A. Affolder,[135] Y. Afik,[36] M. N. Agaras,[13] J. Agarwala,[72a,72b] A. Aggarwal,[99] C. Agheorghiesei,[27c] J. A. Aguilar-Saavedra,[129f] A. Ahmad,[36] F. Ahmadov,[38,b] W. S. Ahmed,[103] S. Ahuja,[94] X. Ai,[48] G. Aielli,[75a,75b] I. Aizenberg,[167] M. Akbiyik,[99] T. P. A. Åkesson,[97] A. V. Akimov,[37] K. Al Khoury,[41] G. L. Alberghi,[23b] J. Albert,[163] P. Albicocco,[53] M.J. Alconada Verzini,[89] S. Alderweireldt,[52] M. Aleksa,[36] I. N. Aleksandrov,[38] C. Alexa,[27b] T. Alexopoulos,[10] A. Alfonsi,[113] F. Alfonsi,[23b] M. Alhroob,[119] B. Ali,[131] S. Ali,[147] M. Aliev,[37] G. Alimonti,[70a] C. Allaire,[36] B. M. M. Allbrooke,[145] P. P. Allport,[20] A. Aloisio,[71a,71b] F. Alonso,[89] C. Alpigiani,[137] E. Alunno Camelia,[75a,75b] M. Alvarez Estevez,[98] M. G. Alviggi,[71a,71b] Y. Amaral Coutinho,[81b] A. Ambler,[103] C. Amelung,[36] C. G. Ames,[108] D. Amidei,[105] S. P. Amor Dos Santos,[129a] S. Amoroso,[48] K. R. Amos,[161] C. S. Amrouche,[56] V. Ananiev,[124] C. Anastopoulos,[138] N. Andari,[134] T. Andeen,[11] J. K. Anders,[19] S. Y. Andrean,[47a,47b] A. Andreazza,[70a,70b] S. Angelidakis,[9] A. Angerami,[41,c] A. V. Anisenkov,[37] A. Annovi,[73a] C. Antel,[56] M. T. Anthony,[138] E. Antipov,[120] M. Antonelli,[53] D. J. A. Antrim,[17a,17b] F. Anulli,[74a] M. Aoki,[82] T. Aoki,[152] J. A. Aparisi Pozo,[161] M. A. Aparo,[145] L. Aperio Bella,[48] C. Appelt,[18] N. Aranzabal,[36] V. Araujo Ferraz,[81a] C. Arcangeletti,[53] A. T. H. Arce,[51] E. Arena,[91] J.-F. Arguin,[107] S. Argyropoulos,[54] J.-H. Arling,[48] A. J. Armbruster,[36] O. Arnaez,[154] H. Arnold,[113] Z. P. Arrubarrena Tame,[108] G. Artoni,[74a,74b] H. Asada,[110] K. Asai,[117] S. Asai,[152] N. A. Asbah,[61] E. M. Asimakopoulou,[159] J. Assahsah,[35d] K. Assamagan,[29] R. Astalos,[28a] R. J. Atkin,[33a,33b] M. Atkinson,[160] N. B. Atlay,[18] H. Atmani,[62b] P. A. Atmasiddha,[105] K. Augsten,[131] S. Auricchio,[71a,71b] A. D. Auriol,[20] V. A. Austrup,[169] G. Avner,[149] G. Avolio,[36] K. Axiotis,[56] M. K. Ayoub,[14c] G. Azuelos,[107,d] D. Babal,[28a] H. Bachacou,[134] K. Bachas,[151,e] A. Bachiu,[34] F. Backman,[47a,47b] A. Badea,[61] P. Bagnaia,[74a,74b] M. Bahmani,[18] A. J. Bailey,[161] V. R. Bailey,[160] J. T. Baines,[133] C. Bakalis,[10] O. K. Baker,[170] P. J. Bakker,[113] E. Bakos,[15] D. Bakshi Gupta,[8] S. Balaji,[146] R. Balasubramanian,[113] E. M. Baldin,[37] P. Balek,[132] E. Ballabene,[70a,70b] F. Balli,[134] L. M. Baltes,[63a] W. K. Balunas,[32] J. Balz,[99] E. Banas,[85] M. Bandieramonte,[128] A. Bandyopadhyay,[24] S. Bansal,[24] L. Barak,[150] E. L. Barberio,[104] D. Barberis,[57b,57a] M. Barbero,[101] G. Barbour,[95] K. N. Barends,[33a] T. Barillari,[109] M.-S. Barisits,[36] J. Barkeloo,[122] T. Barklow,[142] R. M. Barnett,[17a] P. Baron,[121]

D. A. Baron Moreno,[100] A. Baroncelli,[62a] G. Barone,[29] A. J. Barr,[125] L. Barranco Navarro,[47a,47b] F. Barreiro,[98] J. Barreiro Guimarães da Costa,[14a] U. Barron,[150] M. G. Barros Teixeira,[129a] S. Barsov,[37] F. Bartels,[63a] R. Bartoldus,[142] A. E. Barton,[90] P. Bartos,[28a] A. Basalaev,[48] A. Basan,[99] M. Baselga,[49] I. Bashta,[76a,76b] A. Bassalat,[66] M. J. Basso,[154] C. R. Basson,[100] R. L. Bates,[59] S. Batlamous,[35e] J. R. Batley,[32] B. Batool,[140] M. Battaglia,[135] M. Bauce,[74a,74b] P. Bauer,[24] A. Bayirli,[21a] J. B. Beacham,[51] T. Beau,[126] P. H. Beauchemin,[157] F. Becherer,[54] P. Bechtle,[24] H. P. Beck,[19,f] K. Becker,[165] C. Becot,[48] A. J. Beddall,[21d] V. A. Bednyakov,[38] C. P. Bee,[144] L. J. Beemster,[15] T. A. Beermann,[36] M. Begalli,[81d,81d] M. Begel,[29] A. Behera,[144] J. K. Behr,[48] C. Beirao Da Cruz E Silva,[36] J. F. Beirer,[55,36] F. Beisiegel,[24] M. Belfkir,[115a,115b] G. Bella,[150] L. Bellagamba,[23b] A. Bellerive,[34] P. Bellos,[20] K. Beloborodov,[37] K. Belotskiy,[37] N. L. Belyaev,[37] D. Benchekroun,[35a] F. Bendebba,[35a] Y. Benhammou,[150] D. P. Benjamin,[29] M. Benoit,[29] J. R. Bensinger,[26] S. Bentvelsen,[113] L. Beresford,[36] M. Beretta,[53] D. Berge,[18] E. Bergeaas Kuutmann,[159] N. Berger,[4] B. Bergmann,[131] J. Beringer,[17a] S. Berlendis,[7] G. Bernardi,[5] C. Bernius,[142] F. U. Bernlochner,[24] T. Berry,[94] P. Berta,[132] A. Berthold,[50] I. A. Bertram,[90] S. Bethke,[109] A. Betti,[74a,74b] A. J. Bevan,[93] M. Bhamjee,[33c] S. Bhatta,[144] D. S. Bhattacharya,[164] P. Bhattarai,[26] V. S. Bhopatkar,[6] R. Bi,[128] R. Bi,[29,g] R. M. Bianchi,[128] O. Biebel,[108] R. Bielski,[122] M. Biglietti,[76a] T. R. V. Billoud,[131] M. Bindi,[55] A. Bingul,[21b] C. Bini,[74a,74b] S. Biondi,[23b,23a] A. Biondini,[91] C. J. Birch-sykes,[100] G. A. Bird,[20,133] M. Birman,[167] T. Bisanz,[36] E. Bisceglie,[43b,43a] D. Biswas,[168,h] A. Bitadze,[100] K. Bjørke,[124] I. Bloch,[48] C. Blocker,[26] A. Blue,[59] U. Blumenschein,[93] J. Blumenthal,[99] G. J. Bobbink,[113] V. S. Bobrovnikov,[37] M. Boehler,[54] D. Bogavac,[36] A. G. Bogdanchikov,[37] C. Bohm,[47a] V. Boisvert,[94] P. Bokan,[48] T. Bold,[84a] M. Bomben,[5] M. Bona,[93] M. Boonekamp,[134] C. D. Booth,[94] A. G. Borbély,[59] H. M. Borecka-Bielska,[107] L. S. Borgna,[95] G. Borissov,[90] D. Bortoletto,[125] D. Boscherini,[23b] M. Bosman,[13] J. D. Bossio Sola,[36] K. Bouaouda,[35a] J. Boudreau,[128] E. V. Bouhova-Thacker,[90] D. Boumediene,[40] R. Bouquet,[5] A. Boveia,[118] J. Boyd,[36] D. Boye,[29] I. R. Boyko,[38] J. Bracinik,[20] N. Brahimi,[62d] G. Brandt,[169] O. Brandt,[32] F. Braren,[48] B. Brau,[102] J. E. Brau,[122] W. D. Breaden Madden,[59] K. Brendlinger,[48] R. Brener,[167] L. Brenner,[36] R. Brenner,[159] S. Bressler,[167] B. Brickwedde,[99] D. Britton,[59] D. Britzger,[109] I. Brock,[24] G. Brooijmans,[41] W. K. Brooks,[136f] E. Brost,[29] P. A. Bruckman de Renstrom,[85] B. Brüers,[48] D. Bruncko,[28b,i] A. Bruni,[23b] G. Bruni,[23b] M. Bruschi,[23b] N. Bruscino,[74a,74b] L. Bryngemark,[142] T. Buanes,[16] Q. Buat,[137] P. Buchholz,[140] A. G. Buckley,[59] I. A. Budagov,[38,i] M. K. Bugge,[124] O. Bulekov,[37] B. A. Bullard,[61] S. Burdin,[91] C. D. Burgard,[48] A. M. Burger,[40] B. Burghgrave,[8] J. T. P. Burr,[32] C. D. Burton,[11] J. C. Burzynski,[141] E. L. Busch,[41] V. Büscher,[99] P. J. Bussey,[59] J. M. Butler,[25] C. M. Buttar,[59] J. M. Butterworth,[95] W. Buttinger,[133] C. J. Buxo Vazquez,[106] A. R. Buzykaev,[37] G. Cabras,[23b] S. Cabrera Urbán,[161] D. Caforio,[58] H. Cai,[128] Y. Cai,[14a,14d] V. M. M. Cairo,[36] O. Cakir,[3a] N. Calace,[36] P. Calafiura,[17a] G. Calderini,[126] P. Calfayan,[67] G. Callea,[59] L. P. Caloba,[81b] D. Calvet,[40] S. Calvet,[40] T. P. Calvet,[101] M. Calvetti,[73a,73b] R. Camacho Toro,[126] S. Camarda,[36] D. Camarero Munoz,[98] P. Camarri,[75a,75b] M. T. Camerlingo,[76a,76b] D. Cameron,[124] C. Camincher,[163] M. Campanelli,[95] A. Camplani,[42] V. Canale,[71a,71b] A. Canesse,[103] M. Cano Bret,[79] J. Cantero,[161] Y. Cao,[160] F. Capocasa,[26] M. Capua,[43b,43a] A. Carbone,[70a,70b] R. Cardarelli,[75a] J. C. J. Cardenas,[8] F. Cardillo,[161] T. Carli,[36] G. Carlino,[71a] B. T. Carlson,[128,j] E. M. Carlson,[163,155a] L. Carminati,[70a,70b] M. Carnesale,[74a,74b] S. Caron,[112] E. Carquin,[136f] S. Carrá,[70a,70b] G. Carratta,[23b,23a] F. Carrio Argos,[33g] J. W. S. Carter,[154] T. M. Carter,[52] M. P. Casado,[13,k] A. F. Casha,[154] E. G. Castiglia,[170] F. L. Castillo,[63a] L. Castillo Garcia,[13] V. Castillo Gimenez,[161] N. F. Castro,[129a,129e] A. Catinaccio,[36] J. R. Catmore,[124] V. Cavaliere,[29] N. Cavalli,[23b,23a] V. Cavasinni,[73a,73b] E. Celebi,[21a] F. Celli,[125] M. S. Centonze,[69a,69b] K. Cerny,[121] A. S. Cerqueira,[81a] A. Cerri,[145] L. Cerrito,[75a,75b] F. Cerutti,[17a] A. Cervelli,[23b] S. A. Cetin,[21d] Z. Chadi,[35a] D. Chakraborty,[114] M. Chala,[129f] J. Chan,[168] W. S. Chan,[113] W. Y. Chan,[152] J. D. Chapman,[32] B. Chargeishvili,[148b] D. G. Charlton,[20] T. P. Charman,[93] M. Chatterjee,[19] S. Chekanov,[6] S. V. Chekulaev,[155a] G. A. Chelkov,[38,l] A. Chen,[105] B. Chen,[150] B. Chen,[163] C. Chen,[62a] H. Chen,[14c] H. Chen,[29] J. Chen,[62c] J. Chen,[26] S. Chen,[152] S. J. Chen,[14c] X. Chen,[62c] X. Chen,[14b,m] Y. Chen,[62a] C. L. Cheng,[168] H. C. Cheng,[64a] A. Cheplakov,[38] E. Cheremushkina,[48] E. Cherepanova,[113] R. Cherkaoui El Moursli,[35e] E. Cheu,[7] K. Cheung,[65] L. Chevalier,[134] V. Chiarella,[53] G. Chiarelli,[73a] N. Chiedde,[101] G. Chiodini,[69a] A. S. Chisholm,[20] A. Chitan,[27b] Y. H. Chiu,[163] M. V. Chizhov,[38] K. Choi,[11] A. R. Chomont,[74a,74b] Y. Chou,[102] E. Y. S. Chow,[113] T. Chowdhury,[33g] L. D. Christopher,[33g] K. L. Chu,[64a] M. C. Chu,[64a] X. Chu,[14a,14d] J. Chudoba,[130] J. J. Chwastowski,[85] D. Cieri,[109] K. M. Ciesla,[84a] V. Cindro,[92] A. Ciocio,[17a] F. Cirotto,[71a,71b] Z. H. Citron,[167,n] M. Citterio,[70a] D. A. Ciubotaru,[27b] B. M. Ciungu,[154] A. Clark,[56] P. J. Clark,[52] J. M. Clavijo Columbie,[48] S. E. Clawson,[100] C. Clement,[47a,47b] J. Clercx,[48] L. Clissa,[23b,23a] Y. Coadou,[101] M. Cobal,[68a,68c] A. Coccaro,[57b] R. F. Coelho Barrue,[129a] R. Coelho Lopes De Sa,[102] S. Coelli,[70a] H. Cohen,[150] A. E. C. Coimbra,[70a,70b] B. Cole,[41] J. Collot,[60] P. Conde Muiño,[129a,129g] M. P. Connell,[33c] S. H. Connell,[33c] I. A. Connelly,[59] E. I. Conroy,[125] F. Conventi,[71a,o] H. G. Cooke,[20] A. M. Cooper-Sarkar,[125] F. Cormier,[162] L. D. Corpe,[36] M. Corradi,[74a,74b] E. E. Corrigan,[97] F. Corriveau,[103,p] A. Cortes-Gonzalez,[18] M. J. Costa,[161] F. Costanza,[4] D. Costanzo,[138] B. M. Cote,[118] G. Cowan,[94] J. W. Cowley,[32] K. Cranmer,[116] S. Crépé-Renaudin,[60] F. Crescioli,[126] M. Cristinziani,[140] M. Cristoforetti,[77a,77b,q] V. Croft,[157] G. Crosetti,[43b,43a] A. Cueto,[36] T. Cuhadar Donszelmann,[158] H. Cui,[14a,14d] Z. Cui,[7] A. R. Cukierman,[142] W. R. Cunningham,[59] F. Curcio,[43b,43a] P. Czodrowski,[36]

M. M. Czurylo,[63b] M. J. Da Cunha Sargedas De Sousa,[62a] J. V. Da Fonseca Pinto,[81b] C. Da Via,[100] W. Dabrowski,[84a] T. Dado,[49] S. Dahbi,[33g] T. Dai,[105] C. Dallapiccola,[102] M. Dam,[42] G. D'amen,[29] V. D'Amico,[76a,76b] J. Damp,[99] J. R. Dandoy,[127] M. F. Daneri,[30] M. Danninger,[141] V. Dao,[36] G. Darbo,[57b] S. Darmora,[6] S. J. Das,[29] A. Dattagupta,[122] S. D'Auria,[70a,70b] C. David,[155b] T. Davidek,[132] D. R. Davis,[51] B. Davis-Purcell,[34] I. Dawson,[93] K. De,[8] R. De Asmundis,[71a] M. De Beurs,[113] S. De Castro,[23b,23a] N. De Groot,[112] P. de Jong,[113] H. De la Torre,[106] A. De Maria,[14c] A. De Salvo,[74a] U. De Sanctis,[75a,75b] A. De Santo,[145] J. B. De Vivie De Regie,[60] D. V. Dedovich,[38] J. Degens,[113] A. M. Deiana,[44] F. Del Corso,[23b,23a] J. Del Peso,[98] F. Del Rio,[63a] F. Deliot,[134] C. M. Delitzsch,[49] M. Della Pietra,[71a,71b] D. Della Volpe,[56] A. Dell'Acqua,[36] L. Dell'Asta,[70a,70b] M. Delmastro,[4] P. A. Delsart,[60] S. Demers,[170] M. Demichev,[38] S. P. Denisov,[37] L. D'Eramo,[114] D. Derendarz,[85] F. Derue,[126] P. Dervan,[91] K. Desch,[24] K. Dette,[154] C. Deutsch,[24] P. O. Deviveiros,[36] F.A. Di Bello,[74a,74b] A. Di Ciaccio,[75a,75b] L. Di Ciaccio,[4] A. Di Domenico,[74a,74b] C. Di Donato,[71a,71b] A. Di Girolamo,[36] G. Di Gregorio,[73a,73b] A. Di Luca,[77a,77b] B. Di Micco,[76a,76b] R. Di Nardo,[76a,76b] C. Diaconu,[101] F. A. Dias,[113] T. Dias Do Vale,[141] M. A. Diaz,[136a,136b] F.G. Diaz Capriles,[24] M. Didenko,[161] E. B. Diehl,[105] L. Diehl,[54] S. Díez Cornell,[48] C. Diez Pardos,[140] C. Dimitriadi,[24,159] A. Dimitrievska,[17a] W. Ding,[14b] J. Dingfelder,[24] I-M. Dinu,[27b] S. J. Dittmeier,[63b] F. Dittus,[36] F. Djama,[101] T. Djobava,[148b] J. I. Djuvsland,[16] D. Dodsworth,[26] C. Doglioni,[100,97] J. Dolejsi,[132] Z. Dolezal,[132] M. Donadelli,[81c] B. Dong,[62c] J. Donini,[40] A. D'Onofrio,[14c] M. D'Onofrio,[91] J. Dopke,[133] A. Doria,[71a] M. T. Dova,[89] A. T. Doyle,[59] M. A. Draguet,[125] E. Drechsler,[141] E. Dreyer,[167] I. Drivas-koulouris,[10] A. S. Drobac,[157] D. Du,[62a] T.A. du Pree,[113] F. Dubinin,[37] M. Dubovsky,[28a] E. Duchovni,[167] G. Duckeck,[108] O. A. Ducu,[36] D. Duda,[109] A. Dudarev,[36] M. D'uffizi,[100] L. Duflot,[66] M. Dührssen,[36] C. Dülsen,[169] A. E. Dumitriu,[27b] M. Dunford,[63a] S. Dungs,[49] K. Dunne,[47a,47b] A. Duperrin,[101] H. Duran Yildiz,[3a] M. Düren,[58] A. Durglishvili,[148b] B. L. Dwyer,[114] G. I. Dyckes,[17a] M. Dyndal,[84a] S. Dysch,[100] B. S. Dziedzic,[85] Z. O. Earnshaw,[145] B. Eckerova,[28a] M. G. Eggleston,[51] E. Egidio Purcino De Souza,[81b] L. F. Ehrke,[56] G. Eigen,[16] K. Einsweiler,[17a] T. Ekelof,[159] P. A. Ekman,[97] Y. El Ghazali,[35b] H. El Jarrari,[35e,147] A. El Moussaouy,[35a] V. Ellajosyula,[159] M. Ellert,[159] F. Ellinghaus,[169] A. A. Elliot,[93] N. Ellis,[36] J. Elmsheuser,[29] M. Elsing,[36] D. Emeliyanov,[133] A. Emerman,[41] Y. Enari,[152] I. Ene,[17a] S. Epari,[13] J. Erdmann,[49] A. Ereditato,[19] P. A. Erland,[85] M. Errenst,[169] M. Escalier,[66] C. Escobar,[161] E. Etzion,[150] G. Evans,[129a] H. Evans,[67] M. O. Evans,[145] A. Ezhilov,[37] S. Ezzarqtouni,[35a] F. Fabbri,[59] L. Fabbri,[23b,23a] G. Facini,[95] V. Fadeyev,[135] R. M. Fakhrutdinov,[37] S. Falciano,[74a] P. J. Falke,[24] S. Falke,[36] J. Faltova,[132] Y. Fan,[14a] Y. Fang,[14a,14d] G. Fanourakis,[46] M. Fanti,[70a,70b] M. Faraj,[68a,68b] A. Farbin,[8] A. Farilla,[76a] T. Farooque,[106] S. M. Farrington,[52] F. Fassi,[35e] D. Fassouliotis,[9] M. Faucci Giannelli,[75a,75b] W. J. Fawcett,[32] L. Fayard,[66] O. L. Fedin,[37,1] G. Fedotov,[37] M. Feickert,[160] L. Feligioni,[101] A. Fell,[138] D. E. Fellers,[122] C. Feng,[62b] M. Feng,[14b] Z. Feng,[113] M. J. Fenton,[158] A. B. Fenyuk,[37] L. Ferencz,[48] S. W. Ferguson,[45] J.A. Fernandez Pretel,[54] J. Ferrando,[48] A. Ferrari,[159] P. Ferrari,[113] R. Ferrari,[72a] D. Ferrere,[56] C. Ferretti,[105] F. Fiedler,[99] A. Filipčič,[92] E. K. Filmer,[1] F. Filthaut,[112] M. C. N. Fiolhais,[129a,129c,r] L. Fiorini,[161] F. Fischer,[140] W. C. Fisher,[106] T. Fitschen,[20,66] I. Fleck,[140] P. Fleischmann,[105] T. Flick,[169] L. Flores,[127] M. Flores,[33d,33e,33f] L.R. Flores Castillo,[64a] F. M. Follega,[77a,77b] N. Fomin,[16] J. H. Foo,[154] B. C. Forland,[67] A. Formica,[134] A. C. Forti,[100] E. Fortin,[101] A. W. Fortman,[61] M. G. Foti,[17a] L. Fountas,[9] D. Fournier,[66] H. Fox,[90] P. Francavilla,[73a,73b] S. Francescato,[61] M. Franchini,[23b,23a] S. Franchino,[63a] D. Francis,[36] L. Franco,[112] L. Franconi,[19] M. Franklin,[61] G. Frattari,[26] A. C. Freegard,[93] P. M. Freeman,[20] W. S. Freund,[81b] N. Fritzsche,[50] A. Froch,[54] D. Froidevaux,[36] J. A. Frost,[125] Y. Fu,[62a] M. Fujimoto,[117] E. Fullana Torregrosa,[161,i] J. Fuster,[161] A. Gabrielli,[23b,23a] A. Gabrielli,[36] P. Gadow,[48] G. Gagliardi,[57b,57a] L. G. Gagnon,[17a] G. E. Gallardo,[125] E. J. Gallas,[125] B. J. Gallop,[133] R. Gamboa Goni,[93] K. K. Gan,[118] S. Ganguly,[152] J. Gao,[62a] Y. Gao,[52] F.M. Garay Walls,[136a,136b] B. Garcia,[29,g] C. García,[161] J. E. García Navarro,[161] J. A. García Pascual,[14a] M. Garcia-Sciveres,[17a] R. W. Gardner,[39] D. Garg,[79] R. B. Garg,[142] S. Gargiulo,[54] C. A. Garner,[154] V. Garonne,[29] S. J. Gasiorowski,[137] P. Gaspar,[81b] G. Gaudio,[72a] V. Gautam,[13] P. Gauzzi,[74a,74b] I. L. Gavrilenko,[37] A. Gavrilyuk,[37] C. Gay,[162] G. Gaycken,[48] E. N. Gazis,[10] A. A. Geanta,[27b,27e] C. M. Gee,[135] J. Geisen,[97] M. Geisen,[99] C. Gemme,[57b] M. H. Genest,[60] S. Gentile,[74a,74b] S. George,[94] W. F. George,[20] T. Geralis,[46] L. O. Gerlach,[55] P. Gessinger-Befurt,[36] M. Ghasemi Bostanabad,[163] M. Ghneimat,[140] A. Ghosal,[140] A. Ghosh,[158] A. Ghosh,[7] B. Giacobbe,[23b] S. Giagu,[74a,74b] N. Giangiacomi,[154] P. Giannetti,[73a] A. Giannini,[62a] S. M. Gibson,[94] M. Gignac,[135] D. T. Gil,[84b] A. K. Gilbert,[84a] B. J. Gilbert,[41] D. Gillberg,[34] G. Gilles,[113] N. E. K. Gillwald,[48] L. Ginabat,[126] D. M. Gingrich,[2,d] M. P. Giordani,[68a,68c] P. F. Giraud,[134] G. Giugliarelli,[68a,68c] D. Giugni,[70a] F. Giuli,[36] I. Gkialas,[9,s] L. K. Gladilin,[37] C. Glasman,[98] G. R. Gledhill,[122] M. Glisic,[122] I. Gnesi,[43b,t] Y. Go,[29,g] M. Goblirsch-Kolb,[26] D. Godin,[107] S. Goldfarb,[104] T. Golling,[56] M. G. D. Gololo,[33g] D. Golubkov,[37] J. P. Gombas,[106] A. Gomes,[129a,129b] G. Gomes Da Silva,[140] A. J. Gomez Delegido,[161] R. Goncalves Gama,[55] R. Gonçalo,[129a,129c] G. Gonella,[122] L. Gonella,[20] A. Gongadze,[38] F. Gonnella,[20] J. L. Gonski,[41] R. Y. González Andana,[52] S. González de la Hoz,[161] S. Gonzalez Fernandez,[13] R. Gonzalez Lopez,[91] C. Gonzalez Renteria,[17a] R. Gonzalez Suarez,[159] S. Gonzalez-Sevilla,[56] G.R. Gonzalvo Rodriguez,[161] L. Goossens,[36] N. A. Gorasia,[20] P. A. Gorbounov,[37] B. Gorini,[36] E. Gorini,[69a,69b] A. Gorišek,[92] A. T. Goshaw,[51] M. I. Gostkin,[38] C. A. Gottardo,[36] M. Gouighri,[35b,35c] V. Goumarre,[48]

A. G. Goussiou,[137] N. Govender,[33c] C. Goy,[4] I. Grabowska-Bold,[84a] K. Graham,[34] E. Gramstad,[124] S. Grancagnolo,[18] M. Grandi,[145] V. Gratchev,[37,i] P. M. Gravila,[27f,27g] F. G. Gravili,[69a,69b] H. M. Gray,[17a] M. Greco,[69a,69b] C. Grefe,[24] I. M. Gregor,[48] P. Grenier,[142] C. Grieco,[13] A. A. Grillo,[135] K. Grimm,[31,u] S. Grinstein,[13,v] J.-F. Grivaz,[66] E. Gross,[167] J. Grosse-Knetter,[55] C. Grud,[105] A. Grummer,[111] J. C. Grundy,[125] L. Guan,[105] W. Guan,[168] C. Gubbels,[162] J.G.R. Guerrero Rojas,[161] G. Guerrieri,[68a,68b] F. Guescini,[109] R. Gugel,[99] J. A. M. Guhit,[105] A. Guida,[48] T. Guillemin,[4] E. Guilloton,[165,133] S. Guindon,[36] F. Guo,[14a,14d] J. Guo,[62c] L. Guo,[66] Y. Guo,[105] R. Gupta,[48] S. Gurbuz,[24] S. S. Gurdasani,[54] G. Gustavino,[36] M. Guth,[56] P. Gutierrez,[119] L. F. Gutierrez Zagazeta,[127] C. Gutschow,[95] C. Guyot,[134] C. Gwenlan,[125] C. B. Gwilliam,[91] E. S. Haaland,[124] A. Haas,[116] M. Habedank,[48] C. Haber,[17a] H. K. Hadavand,[8] A. Hadef,[99] S. Hadzic,[109] M. Haleem,[164] J. Haley,[120] J. J. Hall,[138] G. D. Hallewell,[101] L. Halser,[19] K. Hamano,[163] H. Hamdaoui,[35e,35f] M. Hamer,[24] G. N. Hamity,[52] J. Han,[62b] K. Han,[62a] L. Han,[14c] L. Han,[62a] S. Han,[17a] Y. F. Han,[154] K. Hanagaki,[82] M. Hance,[135] D. A. Hangal,[41,c] M. D. Hank,[39] R. Hankache,[100] J. B. Hansen,[42] J. D. Hansen,[42] P. H. Hansen,[42] K. Hara,[156] D. Harada,[56] T. Harenberg,[169] S. Harkusha,[37] Y. T. Harris,[125] N. M. Harrison,[118] P. F. Harrison,[165] N. M. Hartman,[142] N. M. Hartmann,[108] Y. Hasegawa,[139] A. Hasib,[52] S. Haug,[19] R. Hauser,[106] M. Havranek,[131] C. M. Hawkes,[20] R. J. Hawkings,[36] S. Hayashida,[110] D. Hayden,[106] C. Hayes,[105] R. L. Hayes,[162] C. P. Hays,[125] J. M. Hays,[93] H. S. Hayward,[91] F. He,[62a] Y. He,[153] Y. He,[126] M. P. Heath,[52] V. Hedberg,[97] A. L. Heggelund,[124] N. D. Hehir,[93] C. Heidegger,[54] K. K. Heidegger,[54] W. D. Heidorn,[80] J. Heilman,[34] S. Heim,[48] T. Heim,[17a] J. G. Heinlein,[127] J. J. Heinrich,[122] L. Heinrich,[109] J. Hejbal,[130] L. Helary,[48] A. Held,[168] S. Hellesund,[124] C. M. Helling,[162] S. Hellman,[47a,47b] C. Helsens,[36] R. C. W. Henderson,[90] L. Henkelmann,[32] A.M. Henriques Correia,[36] H. Herde,[142] Y. Hernández Jiménez,[144] H. Herr,[99] M. G. Herrmann,[108] T. Herrmann,[50] G. Herten,[54] R. Hertenberger,[108] L. Hervas,[36] N. P. Hessey,[155a] H. Hibi,[83] E. Higón-Rodriguez,[161] S. J. Hillier,[20] I. Hinchliffe,[17a] F. Hinterkeuser,[24] M. Hirose,[123] S. Hirose,[156] D. Hirschbuehl,[169] T. G. Hitchings,[100] B. Hiti,[92] J. Hobbs,[144] R. Hobincu,[27e] N. Hod,[167] M. C. Hodgkinson,[138] B. H. Hodkinson,[32] A. Hoecker,[36] J. Hofer,[48] D. Hohn,[54] T. Holm,[24] M. Holzbock,[109] L. B. A. H. Hommels,[32] B. P. Honan,[100] J. Hong,[62c] T. M. Hong,[128] Y. Hong,[55] J. C. Honig,[54] A. Hönle,[109] B. H. Hooberman,[160] W. H. Hopkins,[6] Y. Horii,[110] S. Hou,[147] A. S. Howard,[92] J. Howarth,[59] J. Hoya,[89] M. Hrabovsky,[121] A. Hrynevich,[37] T. Hryn'ova,[4] P. J. Hsu,[65] S.-C. Hsu,[137] Q. Hu,[41,c] Y. F. Hu,[14a,14d,w] D. P. Huang,[95] S. Huang,[64b] X. Huang,[14c] Y. Huang,[62a] Y. Huang,[14a] Z. Huang,[100] Z. Hubacek,[131] M. Huebner,[24] F. Huegging,[24] T. B. Huffman,[125] M. Huhtinen,[36] S. K. Huiberts,[16] R. Hulsken,[103] N. Huseynov,[12,l] J. Huston,[106] J. Huth,[61] R. Hyneman,[142] S. Hyrych,[28a] G. Iacobucci,[56] G. Iakovidis,[29] I. Ibragimov,[140] L. Iconomidou-Fayard,[66] P. Iengo,[71a,71b] R. Iguchi,[152] T. Iizawa,[56] Y. Ikegami,[82] A. Ilg,[19] N. Ilic,[154] H. Imam,[35a] T. Ingebretsen Carlson,[47a,47b] G. Introzzi,[72a,72b] M. Iodice,[76a] V. Ippolito,[74a,74b] M. Ishino,[152] W. Islam,[168] C. Issever,[18,48] S. Istin,[21a,x] H. Ito,[166] J. M. Iturbe Ponce,[64a] R. Iuppa,[77a,77b] A. Ivina,[167] J. M. Izen,[45] V. Izzo,[71a] P. Jacka,[130,131] P. Jackson,[1] R. M. Jacobs,[48] B. P. Jaeger,[141] C. S. Jagfeld,[108] G. Jäkel,[169] K. Jakobs,[54] T. Jakoubek,[167] J. Jamieson,[59] K. W. Janas,[84a] G. Jarlskog,[97] A. E. Jaspan,[91] T. Javůrek,[36] M. Javurkova,[102] F. Jeanneau,[134] L. Jeanty,[122] J. Jejelava,[148a,y] P. Jenni,[54,z] C. E. Jessiman,[34] S. Jézéquel,[4] J. Jia,[144] X. Jia,[61] X. Jia,[14a,14d] Z. Jia,[14c] Y. Jiang,[62a] S. Jiggins,[52] J. Jimenez Pena,[109] S. Jin,[14c] A. Jinaru,[27b] O. Jinnouchi,[153] H. Jivan,[33g] P. Johansson,[138] K. A. Johns,[7] C. A. Johnson,[67] D. M. Jones,[32] E. Jones,[165] P. Jones,[32] R. W. L. Jones,[90] T. J. Jones,[91] J. Jovicevic,[15] X. Ju,[17a] J. J. Junggeburth,[36] A. Juste Rozas,[13,v] S. Kabana,[136e] A. Kaczmarska,[85] M. Kado,[74a,74b] H. Kagan,[118] M. Kagan,[142] A. Kahn,[41] A. Kahn,[127] C. Kahra,[99] T. Kaji,[166] E. Kajomovitz,[149] N. Kakati,[167] C. W. Kalderon,[29] A. Kamenshchikov,[154] N. J. Kang,[135] Y. Kano,[110] D. Kar,[33g] K. Karava,[125] M. J. Kareem,[155b] E. Karentzos,[54] I. Karkanias,[151] S. N. Karpov,[38] Z. M. Karpova,[38] V. Kartvelishvili,[90] A. N. Karyukhin,[37] E. Kasimi,[151] C. Kato,[62d] J. Katzy,[48] S. Kaur,[34] K. Kawade,[139] K. Kawagoe,[88] T. Kawaguchi,[110] T. Kawamoto,[134] G. Kawamura,[55] E. F. Kay,[163] F. I. Kaya,[157] S. Kazakos,[13] V. F. Kazanin,[37] Y. Ke,[144] J. M. Keaveney,[33a] R. Keeler,[163] G. V. Kehris,[61] J. S. Keller,[34] A. S. Kelly,[95] D. Kelsey,[145] J. J. Kempster,[20] J. Kendrick,[20] K. E. Kennedy,[41] O. Kepka,[130] B. P. Kerridge,[165] S. Kersten,[169] B. P. Kerševan,[92] L. Keszeghova,[28a] S. Ketabchi Haghighat,[154] M. Khandoga,[126] A. Khanov,[120] A. G. Kharlamov,[37] T. Kharlamova,[37] E. E. Khoda,[137] T. J. Khoo,[18] G. Khoriauli,[164] J. Khubua,[148b,148c] Y. A. R. Khwaira,[66] M. Kiehn,[36] A. Kilgallon,[122] D. W. Kim,[47a,47b] E. Kim,[153] Y. K. Kim,[39] N. Kimura,[95] A. Kirchhoff,[55] D. Kirchmeier,[50] C. Kirfel,[24] J. Kirk,[133] A. E. Kiryunin,[109] T. Kishimoto,[152] D. P. Kisliuk,[154] C. Kitsaki,[10] O. Kivernyk,[24] M. Klassen,[63a] C. Klein,[34] L. Klein,[164] M. H. Klein,[105] M. Klein,[91] U. Klein,[91] P. Klimek,[36] A. Klimentov,[29] F. Klimpel,[109] T. Klingl,[24] T. Klioutchnikova,[36] F. F. Klitzner,[108] P. Kluit,[113] S. Kluth,[109] E. Kneringer,[78] T. M. Knight,[154] A. Knue,[54] D. Kobayashi,[88] R. Kobayashi,[86] M. Kocian,[142] T. Kodama,[152] P. Kodyš,[132] D. M. Koeck,[145] P. T. Koenig,[24] T. Koffas,[34] N. M. Köhler,[36] M. Kolb,[134] I. Koletsou,[4] T. Komarek,[121] K. Köneke,[54] A. X. Y. Kong,[1] T. Kono,[117] N. Konstantinidis,[95] B. Konya,[97] R. Kopeliansky,[67] S. Koperny,[84a] K. Korcyl,[85] K. Kordas,[151] G. Koren,[150] A. Korn,[95] S. Korn,[55] I. Korolkov,[13] N. Korotkova,[37] B. Kortman,[113] O. Kortner,[109] S. Kortner,[109] W. H. Kostecka,[114] V. V. Kostyukhin,[140] A. Kotsokechagia,[66] A. Kotwal,[51] A. Koulouris,[36] A. Kourkoumeli-Charalampidi,[72a,72b] C. Kourkoumelis,[9] E. Kourlitis,[6] O. Kovanda,[145] R. Kowalewski,[163]

W. Kozanecki,[134] A. S. Kozhin,[37] V. A. Kramarenko,[37] G. Kramberger,[92] P. Kramer,[99] M. W. Krasny,[126] A. Krasznahorkay,[36] J. A. Kremer,[99] T. Kresse,[50] J. Kretzschmar,[91] K. Kreul,[18] P. Krieger,[154] F. Krieter,[108] S. Krishnamurthy,[102] A. Krishnan,[63b] M. Krivos,[132] K. Krizka,[17a] K. Kroeninger,[49] H. Kroha,[109] J. Kroll,[130] J. Kroll,[127] K. S. Krowpman,[106] U. Kruchonak,[38] H. Krüger,[24] N. Krumnack,[80] M. C. Kruse,[51] J. A. Krzysiak,[85] A. Kubota,[153] O. Kuchinskaia,[37] S. Kuday,[3a] D. Kuechler,[48] J. T. Kuechler,[48] S. Kuehn,[36] T. Kuhl,[48] V. Kukhtin,[38] Y. Kulchitsky,[37,l] S. Kuleshov,[136d,136b] M. Kumar,[33g] N. Kumari,[101] M. Kuna,[60] A. Kupco,[130] T. Kupfer,[49] A. Kupich,[37] O. Kuprash,[54] H. Kurashige,[83] L. L. Kurchaninov,[155a] Y. A. Kurochkin,[37] A. Kurova,[37] E. S. Kuwertz,[36] M. Kuze,[153] A. K. Kvam,[102] J. Kvita,[121] T. Kwan,[103] K. W. Kwok,[64a] N. G. Kyriacou,[105] L. A. O. Laatu,[101] C. Lacasta,[161] F. Lacava,[74a,74b] H. Lacker,[18] D. Lacour,[126] N. N. Lad,[95] E. Ladygin,[38] B. Laforge,[126] T. Lagouri,[136e] S. Lai,[55] I. K. Lakomiec,[84a] N. Lalloue,[60] J. E. Lambert,[119] S. Lammers,[67] W. Lampl,[7] C. Lampoudis,[151] A. N. Lancaster,[114] E. Lançon,[29] U. Landgraf,[54] M. P. J. Landon,[93] V. S. Lang,[54] R. J. Langenberg,[102] A. J. Lankford,[158] F. Lanni,[29] K. Lantzsch,[24] A. Lanza,[72a] A. Lapertosa,[57b,57a] J. F. Laporte,[134] T. Lari,[70a] F. Lasagni Manghi,[23b] M. Lassnig,[36] V. Latonova,[130] T. S. Lau,[64a] A. Laudrain,[99] A. Laurier,[34] S. D. Lawlor,[94] Z. Lawrence,[100] M. Lazzaroni,[70a,70b] B. Le,[100] B. Leban,[92] A. Lebedev,[80] M. LeBlanc,[36] T. LeCompte,[6] F. Ledroit-Guillon,[60] A. C. A. Lee,[95] G. R. Lee,[16] L. Lee,[61] S. C. Lee,[147] S. Lee,[47a,47b] T. F. Lee,[91] L. L. Leeuw,[33c] H. P. Lefebvre,[94] M. Lefebvre,[163] C. Leggett,[17a] K. Lehmann,[141] G. Lehmann Miotto,[36] W. A. Leight,[102] A. Leisos,[151,aa] M. A. L. Leite,[81c] C. E. Leitgeb,[48] R. Leitner,[132] K. J. C. Leney,[44] T. Lenz,[24] S. Leone,[73a] C. Leonidopoulos,[52] A. Leopold,[143] C. Leroy,[107] R. Les,[106] C. G. Lester,[32] M. Levchenko,[37] J. Levêque,[4] D. Levin,[105] L. J. Levinson,[167] M. P. Lewicki,[85] D. J. Lewis,[20] B. Li,[14b] B. Li,[62b] C. Li,[62a] C.-Q. Li,[62c,62d] H. Li,[62a] H. Li,[62b] H. Li,[14c] H. Li,[62b] J. Li,[62c] K. Li,[137] L. Li,[62c] M. Li,[14a,14d] Q. Y. Li,[62a] S. Li,[62d,62c,ab] T. Li,[62b] X. Li,[103] Z. Li,[62b] Z. Li,[125] Z. Li,[103] Z. Li,[91] Z. Liang,[14a] M. Liberatore,[48] B. Liberti,[75a] K. Lie,[64c] J. Lieber Marin,[81b] K. Lin,[106] R. A. Linck,[67] R. E. Lindley,[7] J. H. Lindon,[2] A. Linss,[48] E. Lipeles,[127] A. Lipniacka,[16] A. Lister,[162] J. D. Little,[4] B. Liu,[14a] B. X. Liu,[141] D. Liu,[62d,62c] J. B. Liu,[62a] J. K. K. Liu,[32] K. Liu,[62d,62c] M. Liu,[62a] M. Y. Liu,[62a] P. Liu,[14a] Q. Liu,[62d,137,62c] X. Liu,[62a] Y. Liu,[48] Y. Liu,[14c,14d] Y. L. Liu,[105] Y. W. Liu,[62a] M. Livan,[72a,72b] J. Llorente Merino,[141] S. L. Lloyd,[93] E. M. Lobodzinska,[48] P. Loch,[7] S. Loffredo,[75a,75b] T. Lohse,[18] K. Lohwasser,[138] M. Lokajicek,[130] J. D. Long,[160] I. Longarini,[74a,74b] L. Longo,[69a,69b] R. Longo,[160] I. Lopez Paz,[36] A. Lopez Solis,[48] J. Lorenz,[108] N. Lorenzo Martinez,[4] A. M. Lory,[108] A. Lösle,[54] X. Lou,[47a,47b] X. Lou,[14a,14d] A. Lounis,[66] J. Love,[6] P. A. Love,[90] J.J. Lozano Bahilo,[161] G. Lu,[14a,14d] M. Lu,[79] S. Lu,[127] Y. J. Lu,[65] H. J. Lubatti,[137] C. Luci,[74a,74b] F. L. Lucio Alves,[14c] A. Lucotte,[60] F. Luehring,[67] I. Luise,[144] O. Lukianchuk,[66] O. Lundberg,[143] B. Lund-Jensen,[143] N. A. Luongo,[122] M. S. Lutz,[150] D. Lynn,[29] H. Lyons,[91] R. Lysak,[130] E. Lytken,[97] F. Lyu,[14a] V. Lyubushkin,[38] T. Lyubushkina,[38] H. Ma,[29] L. L. Ma,[62b] Y. Ma,[95] D.M. Mac Donell,[163] G. Maccarrone,[53] J. C. MacDonald,[138] R. Madar,[40] W. F. Mader,[50] J. Maeda,[83] T. Maeno,[29] M. Maerker,[50] V. Magerl,[54] J. Magro,[68a,68c] H. Maguire,[138] D. J. Mahon,[41] C. Maidantchik,[81b] A. Maio,[129a,129b,129d] K. Maj,[84a] O. Majersky,[28a] S. Majewski,[122] N. Makovec,[66] V. Maksimovic,[15] B. Malaescu,[126] Pa. Malecki,[85] V. P. Maleev,[37] F. Malek,[60] D. Malito,[43b,43a] U. Mallik,[79] C. Malone,[32] S. Maltezos,[10] S. Malyukov,[38] J. Mamuzic,[13] G. Mancini,[53] G. Manco,[72a,72b] J. P. Mandalia,[93] I. Mandić,[92] L. Manhaes de Andrade Filho,[81a] I. M. Maniatis,[151] M. Manisha,[134] J. Manjarres Ramos,[50] D. C. Mankad,[167] K. H. Mankinen,[97] A. Mann,[108] A. Manousos,[78] B. Mansoulie,[134] S. Manzoni,[36] A. Marantis,[151] G. Marchiori,[5] M. Marcisovsky,[130] L. Marcoccia,[75a,75b] C. Marcon,[70a,70b] M. Marinescu,[20] M. Marjanovic,[119] Z. Marshall,[17a] S. Marti-Garcia,[161] T. A. Martin,[165] V. J. Martin,[52] B. Martin dit Latour,[16] L. Martinelli,[74a,74b] M. Martinez,[13,v] P. Martinez Agullo,[161] V. I. Martinez Outschoorn,[102] P. Martinez Suarez,[13] S. Martin-Haugh,[133] V. S. Martoiu,[27b] A. C. Martyniuk,[95] A. Marzin,[36] S. R. Maschek,[109] L. Masetti,[99] T. Mashimo,[152] J. Masik,[100] A. L. Maslennikov,[37] L. Massa,[23b] P. Massarotti,[71a,71b] P. Mastrandrea,[73a,73b] A. Mastroberardino,[43b,43a] T. Masubuchi,[152] T. Mathisen,[159] A. Matic,[108] N. Matsuzawa,[152] J. Maurer,[27b] B. Maček,[92] D. A. Maximov,[37] R. Mazini,[147] I. Maznas,[151] M. Mazza,[106] S. M. Mazza,[135] C. Mc Ginn,[29,g] J. P. Mc Gowan,[103] S.P. Mc Kee,[105] T. G. McCarthy,[109] W. P. McCormack,[17a] E. F. McDonald,[104] A. E. McDougall,[113] J. A. Mcfayden,[145] G. Mchedlidze,[148b] R. P. Mckenzie,[33g] T. C. Mclachlan,[48] D. J. Mclaughlin,[95] K. D. McLean,[163] S. J. McMahon,[133] P. C. McNamara,[104] R. A. McPherson,[163,p] J. E. Mdhluli,[33g] S. Meehan,[36] T. Megy,[40] S. Mehlhase,[108] A. Mehta,[91] B. Meirose,[45] D. Melini,[149] B.R. Mellado Garcia,[33g] A. H. Melo,[55] F. Meloni,[48] E.D. Mendes Gouveia,[129a] A.M. Mendes Jacques Da Costa,[20] H. Y. Meng,[154] L. Meng,[90] S. Menke,[109] M. Mentink,[36] E. Meoni,[43b,43a] C. Merlassino,[125] L. Merola,[71a,71b] C. Meroni,[70a] G. Merz,[105] O. Meshkov,[37] J. K. R. Meshreki,[140] J. Metcalfe,[6] A. S. Mete,[6] C. Meyer,[67] J.-P. Meyer,[134] M. Michetti,[18] R. P. Middleton,[133] L. Mijović,[52] G. Mikenberg,[167] M. Mikestikova,[130] M. Mikuž,[92] H. Mildner,[138] A. Milic,[154] C. D. Milke,[44] D. W. Miller,[39] L. S. Miller,[34] A. Milov,[167] D. A. Milstead,[47a,47b] T. Min,[14c] A. A. Minaenko,[37] I. A. Minashvili,[148b] L. Mince,[59] A. I. Mincer,[116] B. Mindur,[84a] M. Mineev,[38] Y. Minegishi,[152] Y. Mino,[86] L. M. Mir,[13] M. Miralles Lopez,[161] M. Mironova,[125] T. Mitani,[166] A. Mitra,[165] V. A. Mitsou,[161] O. Miu,[154] P. S. Miyagawa,[93] Y. Miyazaki,[88] A. Mizukami,[82] J. U. Mjörnmark,[97] T. Mkrtchyan,[63a] M. Mlynarikova,[114] T. Moa,[47a,47b]

S. Mobius,[55] K. Mochizuki,[107] P. Moder,[48] P. Mogg,[108] A. F. Mohammed,[14a,14d] S. Mohapatra,[41] G. Mokgatitswane,[33g] B. Mondal,[140] S. Mondal,[131] K. Mönig,[48] E. Monnier,[101] L. Monsonis Romero,[161] J. Montejo Berlingen,[36] M. Montella,[118] F. Monticelli,[89] N. Morange,[66] A. L. Moreira De Carvalho,[129a] M. Moreno Llácer,[161] C. Moreno Martinez,[13] P. Morettini,[57b] S. Morgenstern,[165] M. Morii,[61] M. Morinaga,[152] V. Morisbak,[124] A. K. Morley,[36] F. Morodei,[74a,74b] L. Morvaj,[36] P. Moschovakos,[36] B. Moser,[36] M. Mosidze,[148b] T. Moskalets,[54] P. Moskvitina,[112] J. Moss,[31,ac] E. J. W. Moyse,[102] S. Muanza,[101] J. Mueller,[128] D. Muenstermann,[90] R. Müller,[19] G. A. Mullier,[97] J. J. Mullin,[127] D. P. Mungo,[70a,70b] J. L. Munoz Martinez,[13] D. Munoz Perez,[161] F. J. Munoz Sanchez,[100] M. Murin,[100] W. J. Murray,[165,133] A. Murrone,[70a,70b] J. M. Muse,[119] M. Muškinja,[17a] C. Mwewa,[29] A. G. Myagkov,[37,1] A. J. Myers,[8] A. A. Myers,[128] G. Myers,[67] M. Myska,[131] B. P. Nachman,[17a] O. Nackenhorst,[49] A. Nag,[50] K. Nagai,[125] K. Nagano,[82] J. L. Nagle,[29,g] E. Nagy,[101] A. M. Nairz,[36] Y. Nakahama,[82] K. Nakamura,[82] H. Nanjo,[123] R. Narayan,[44] E. A. Narayanan,[111] I. Naryshkin,[37] M. Naseri,[34] C. Nass,[24] G. Navarro,[22a] J. Navarro-Gonzalez,[161] R. Nayak,[150] P. Y. Nechaeva,[37] F. Nechansky,[48] T. J. Neep,[20] A. Negri,[72a,72b] M. Negrini,[23b] C. Nellist,[112] C. Nelson,[103] K. Nelson,[105] S. Nemecek,[130] M. Nessi,[36,ad] M. S. Neubauer,[160] F. Neuhaus,[99] J. Neundorf,[48] R. Newhouse,[162] P. R. Newman,[20] C. W. Ng,[128] Y. S. Ng,[18] Y. W. Y. Ng,[158] B. Ngair,[35e] H. D. N. Nguyen,[107] R. B. Nickerson,[125] R. Nicolaidou,[134] J. Nielsen,[135] M. Niemeyer,[55] N. Nikiforou,[36] V. Nikolaenko,[37,1] I. Nikolic-Audit,[126] K. Nikolopoulos,[20] P. Nilsson,[29] H. R. Nindhito,[56] A. Nisati,[74a] N. Nishu,[2] R. Nisius,[109] J.-E. Nitschke,[50] E. K. Nkadimeng,[33g] S. J. Noacco Rosende,[89] T. Nobe,[152] D. L. Noel,[32] Y. Noguchi,[86] T. Nommensen,[146] M. A. Nomura,[29] M. B. Norfolk,[138] R. R. B. Norisam,[95] B. J. Norman,[34] J. Novak,[92] T. Novak,[48] O. Novgorodova,[50] L. Novotny,[131] R. Novotny,[111] L. Nozka,[121] K. Ntekas,[158] E. Nurse,[95] F. G. Oakham,[34,d] J. Ocariz,[126] A. Ochi,[83] I. Ochoa,[129a] S. Oerdek,[159] A. Ogrodnik,[84a] A. Oh,[100] C. C. Ohm,[143] H. Oide,[153] R. Oishi,[152] M. L. Ojeda,[48] Y. Okazaki,[86] M. W. O'Keefe,[91] Y. Okumura,[152] A. Olariu,[27b] L.F. Oleiro Seabra,[129a] S. A. Olivares Pino,[136e] D. Oliveira Damazio,[29] D. Oliveira Goncalves,[81a] J. L. Oliver,[158] M. J. R. Olsson,[158] A. Olszewski,[85] J. Olszowska,[85,i] Ö.O. Öncel,[54] D. C. O'Neil,[141] A. P. O'Neill,[19] A. Onofre,[129a,129e] P. U. E. Onyisi,[11] M. J. Oreglia,[39] G. E. Orellana,[89] D. Orestano,[76a,76b] N. Orlando,[13] R. S. Orr,[154] V. O'Shea,[59] R. Ospanov,[62a] G. Otero y Garzon,[30] H. Otono,[88] P. S. Ott,[63a] G. J. Ottino,[17a] M. Ouchrif,[35d] J. Ouellette,[29,g] F. Ould-Saada,[124] M. Owen,[59] R. E. Owen,[133] K. Y. Oyulmaz,[21a] V. E. Ozcan,[21a] N. Ozturk,[8] S. Ozturk,[21d] J. Pacalt,[121] H. A. Pacey,[32] K. Pachal,[51] A. Pacheco Pages,[13] C. Padilla Aranda,[13] G. Padovano,[74a,74b] S. Pagan Griso,[17a] G. Palacino,[67] A. Palazzo,[69a,69b] S. Palazzo,[52] S. Palestini,[36] M. Palka,[84b] J. Pan,[170] T. Pan,[64a] D. K. Panchal,[11] C. E. Pandini,[113] J.G. Panduro Vazquez,[94] H. Pang,[14b] P. Pani,[48] G. Panizzo,[68a,68c] L. Paolozzi,[56] C. Papadatos,[107] S. Parajuli,[44] A. Paramonov,[6] C. Paraskevopoulos,[10] D. Paredes Hernandez,[64b] T. H. Park,[154] M. A. Parker,[32] F. Parodi,[57b,57a] E. W. Parrish,[114] V. A. Parrish,[52] J. A. Parsons,[41] U. Parzefall,[54] B. Pascual Dias,[107] L. Pascual Dominguez,[150] V. R. Pascuzzi,[17a] F. Pasquali,[113] E. Pasqualucci,[74a] S. Passaggio,[57b] F. Pastore,[94] P. Pasuwan,[47a,47b] J. R. Pater,[100] J. Patton,[91] T. Pauly,[36] J. Pearkes,[142] M. Pedersen,[124] R. Pedro,[129a] S. V. Peleganchuk,[37] O. Penc,[36] C. Peng,[64b] H. Peng,[62a] K. E. Penski,[108] M. Penzin,[37] B. S. Peralva,[81d,81d] A. P. Pereira Peixoto,[60] L. Pereira Sanchez,[47a,47b] D. V. Perepelitsa,[29,g] E. Perez Codina,[155a] M. Perganti,[10] L. Perini,[70a,70b,i] H. Pernegger,[36] S. Perrella,[36] A. Perrevoort,[112] O. Perrin,[40] K. Peters,[48] R. F. Y. Peters,[100] B. A. Petersen,[36] T. C. Petersen,[42] E. Petit,[101] V. Petousis,[131] C. Petridou,[151] A. Petrukhin,[140] M. Pettee,[17a] N. E. Pettersson,[36] A. Petukhov,[37] K. Petukhova,[132] A. Peyaud,[134] R. Pezoa,[136f] L. Pezzotti,[36] G. Pezzullo,[170] T. Pham,[104] P. W. Phillips,[133] M. W. Phipps,[160] G. Piacquadio,[144] E. Pianori,[17a] F. Piazza,[70a,70b] R. Piegaia,[30] D. Pietreanu,[27b] A. D. Pilkington,[100] M. Pinamonti,[68a,68c] J. L. Pinfold,[2] B.C. Pinheiro Pereira,[129a] C. Pitman Donaldson,[95] D. A. Pizzi,[34] L. Pizzimento,[75a,75b] A. Pizzini,[113] M.-A. Pleier,[29] V. Plesanovs,[54] V. Pleskot,[132] E. Plotnikova,[38] G. Poddar,[4] R. Poettgen,[97] L. Poggioli,[126] I. Pogrebnyak,[106] D. Pohl,[24] I. Pokharel,[55] S. Polacek,[132] G. Polesello,[72a] A. Poley,[141,155a] R. Polifka,[131] A. Polini,[23b] C. S. Pollard,[125] Z. B. Pollock,[118] V. Polychronakos,[29] D. Ponomarenko,[37] L. Pontecorvo,[36] S. Popa,[27a] G. A. Popeneciu,[27d] D. M. Portillo Quintero,[155a] S. Pospisil,[131] P. Postolache,[27c] K. Potamianos,[125] I. N. Potrap,[38] C. J. Potter,[32] H. Potti,[1] T. Poulsen,[48] J. Poveda,[161] G. Pownall,[48] M.E. Pozo Astigarraga,[36] A. Prades Ibanez,[161] M. M. Prapa,[46] D. Price,[100] M. Primavera,[69a] M.A. Principe Martin,[98] M. L. Proffitt,[137] N. Proklova,[37] K. Prokofiev,[64c] G. Proto,[75a,75b] S. Protopopescu,[29] J. Proudfoot,[6] M. Przybycien,[84a] J. E. Puddefoot,[138] D. Pudzha,[37] P. Puzo,[66] D. Pyatiizbyantseva,[37] J. Qian,[105] Y. Qin,[100] T. Qiu,[93] A. Quadt,[55] M. Queitsch-Maitland,[100] G. Rabanal Bolanos,[61] D. Rafanoharana,[54] F. Ragusa,[70a,70b] J. L. Rainbolt,[39] J. A. Raine,[56] S. Rajagopalan,[29] E. Ramakoti,[37] K. Ran,[48,14d] V. Raskina,[126] D. F. Rassloff,[63a] S. Rave,[99] B. Ravina,[59] I. Ravinovich,[167] M. Raymond,[36] A. L. Read,[124] N. P. Readioff,[138] D. M. Rebuzzi,[72a,72b] G. Redlinger,[29] K. Reeves,[45] J. A. Reidelsturz,[169] D. Reikher,[150] A. Reiss,[99] A. Rej,[140] C. Rembser,[36] A. Renardi,[48] M. Renda,[27b] M. B. Rendel,[109] A. G. Rennie,[59] S. Resconi,[70a] M. Ressegotti,[57b,57a] E. D. Resseguie,[17a] S. Rettie,[95] B. Reynolds,[118] E. Reynolds,[17a] M. Rezaei Estabragh,[169] O. L. Rezanova,[37] P. Reznicek,[132] E. Ricci,[77a,77b] R. Richter,[109] S. Richter,[47a,47b] E. Richter-Was,[84b] M. Ridel,[126] P. Rieck,[116] P. Riedler,[36] M. Rijssenbeek,[144] A. Rimoldi,[72a,72b] M. Rimoldi,[48] L. Rinaldi,[23b,23a] T. T. Rinn,[29]

M. P. Rinnagel,[108] G. Ripellino,[143] I. Riu,[13] P. Rivadeneira,[48] J. C. Rivera Vergara,[163] F. Rizatdinova,[120] E. Rizvi,[93] C. Rizzi,[56] B. A. Roberts,[165] B. R. Roberts,[17a] S. H. Robertson,[103,p] M. Robin,[48] D. Robinson,[32] C. M. Robles Gajardo,[136f] M. Robles Manzano,[99] A. Robson,[59] A. Rocchi,[75a,75b] C. Roda,[73a,73b] S. Rodriguez Bosca,[63a] Y. Rodriguez Garcia,[22a] A. Rodriguez Rodriguez,[54] A. M. Rodríguez Vera,[155b] S. Roe,[36] J. T. Roemer,[158] A. R. Roepe-Gier,[119] J. Roggel,[169] O. Røhne,[124] R. A. Rojas,[163] B. Roland,[54] C. P. A. Roland,[67] J. Roloff,[29] A. Romaniouk,[37] E. Romano,[72a,72b] M. Romano,[23b] A.C. Romero Hernandez,[160] N. Rompotis,[91] L. Roos,[126] S. Rosati,[74a] B. J. Rosser,[39] E. Rossi,[4] E. Rossi,[71a,71b] L. P. Rossi,[57b] L. Rossini,[48] R. Rosten,[118] M. Rotaru,[27b] B. Rottler,[54] D. Rousseau,[66] D. Rousso,[32] G. Rovelli,[72a,72b] A. Roy,[160] A. Rozanov,[101] Y. Rozen,[149] X. Ruan,[33g] A. Rubio Jimenez,[161] A. J. Ruby,[91] V. H. Ruelas Rivera,[18] T. A. Ruggeri,[1] F. Rühr,[54] A. Ruiz-Martinez,[161] A. Rummler,[36] Z. Rurikova,[54] N. A. Rusakovich,[38] H. L. Russell,[163] J. P. Rutherfoord,[7] E. M. Rüttinger,[138] K. Rybacki,[90] M. Rybar,[132] E. B. Rye,[124] A. Ryzhov,[37] J. A. Sabater Iglesias,[56] P. Sabatini,[161] L. Sabetta,[74a,74b] H. F.-W. Sadrozinski,[135] F. Safai Tehrani,[74a] B. Safarzadeh Samani,[145] M. Safdari,[142] S. Saha,[103] M. Sahinsoy,[109] M. Saimpert,[134] M. Saito,[152] T. Saito,[152] D. Salamani,[36] G. Salamanna,[76a,76b] A. Salnikov,[142] J. Salt,[161] A. Salvador Salas,[13] D. Salvatore,[43b,43a] F. Salvatore,[145] A. Salzburger,[36] D. Sammel,[54] D. Sampsonidis,[151] D. Sampsonidou,[62d,62c] J. Sánchez,[161] A. Sanchez Pineda,[4] V. Sanchez Sebastian,[161] H. Sandaker,[124] C. O. Sander,[48] J. A. Sandesara,[102] M. Sandhoff,[169] C. Sandoval,[22b] D. P. C. Sankey,[133] A. Sansoni,[53] L. Santi,[74a,74b] C. Santoni,[40] H. Santos,[129a,129b] S. N. Santpur,[17a] A. Santra,[167] K. A. Saoucha,[138] J. G. Saraiva,[129a,129d] J. Sardain,[7] O. Sasaki,[82] K. Sato,[156] C. Sauer,[63b] F. Sauerburger,[54] E. Sauvan,[4] P. Savard,[154,d] R. Sawada,[152] C. Sawyer,[133] L. Sawyer,[96] I. Sayago Galvan,[161] C. Sbarra,[23b] A. Sbrizzi,[23b,23a] T. Scanlon,[95] J. Schaarschmidt,[137] P. Schacht,[109] D. Schaefer,[39] U. Schäfer,[99] A. C. Schaffer,[66] D. Schaile,[108] R. D. Schamberger,[144] E. Schanet,[108] C. Scharf,[18] V. A. Schegelsky,[37] D. Scheirich,[132] F. Schenck,[18] M. Schernau,[158] C. Scheulen,[55] C. Schiavi,[57b,57a] Z. M. Schillaci,[26] E. J. Schioppa,[69a,69b] M. Schioppa,[43b,43a] B. Schlag,[99] K. E. Schleicher,[54] S. Schlenker,[36] K. Schmieden,[99] C. Schmitt,[99] S. Schmitt,[48] L. Schoeffel,[134] A. Schoening,[63b] P. G. Scholer,[54] E. Schopf,[125] M. Schott,[99] J. Schovancova,[36] S. Schramm,[56] F. Schroeder,[169] H.-C. Schultz-Coulon,[63a] M. Schumacher,[54] B. A. Schumm,[135] Ph. Schune,[134] A. Schwartzman,[142] T. A. Schwarz,[105] Ph. Schwemling,[134] R. Schwienhorst,[106] A. Sciandra,[135] G. Sciolla,[26] F. Scuri,[73a] F. Scutti,[104] C. D. Sebastiani,[91] K. Sedlaczek,[49] P. Seema,[18] S. C. Seidel,[111] A. Seiden,[135] B. D. Seidlitz,[41] T. Seiss,[39] C. Seitz,[48] J. M. Seixas,[81b] G. Sekhniaidze,[71a] S. J. Sekula,[44] L. Selem,[4] N. Semprini-Cesari,[23b,23a] S. Sen,[51] D. Sengupta,[56] V. Senthilkumar,[161] L. Serin,[66] L. Serkin,[68a,68b] M. Sessa,[76a,76b] H. Severini,[119] S. Sevova,[142] F. Sforza,[57b,57a] A. Sfyrla,[56] E. Shabalina,[55] R. Shaheen,[143] J. D. Shahinian,[127] N. W. Shaikh,[47a,47b] D. Shaked Renous,[167] L. Y. Shan,[14a] M. Shapiro,[17a] A. Sharma,[36] A. S. Sharma,[162] P. Sharma,[79] S. Sharma,[48] P. B. Shatalov,[37] K. Shaw,[145] S. M. Shaw,[100] Q. Shen,[62c] P. Sherwood,[95] L. Shi,[95] C. O. Shimmin,[170] Y. Shimogama,[166] J. D. Shinner,[94] I. P. J. Shipsey,[125] S. Shirabe,[60] M. Shiyakova,[38] J. Shlomi,[167] M. J. Shochet,[39] J. Shojaii,[104] D. R. Shope,[143] S. Shrestha,[118,ae] E. M. Shrif,[33g] M. J. Shroff,[163] P. Sicho,[130] A. M. Sickles,[160] E. Sideras Haddad,[33g] O. Sidiropoulou,[36] A. Sidoti,[23b] F. Siegert,[50] Dj. Sijacki,[15] R. Sikora,[84a] F. Sili,[89] J. M. Silva,[20] M.V. Silva Oliveira,[36] S. B. Silverstein,[47a] S. Simion,[66] R. Simoniello,[36] E. L. Simpson,[59] N. D. Simpson,[97] S. Simsek,[21d] S. Sindhu,[55] P. Sinervo,[154] V. Sinetckii,[37] S. Singh,[141] S. Singh,[154] S. Sinha,[48] S. Sinha,[33g] M. Sioli,[23b,23a] I. Siral,[122] S. Yu. Sivoklokov,[37,i] J. Sjölin,[47a,47b] A. Skaf,[55] E. Skorda,[97] P. Skubic,[119] M. Slawinska,[85] V. Smakhtin,[167] B. H. Smart,[133] J. Smiesko,[132] S.Yu. Smirnov,[37] Y. Smirnov,[37] L. N. Smirnova,[37,l] O. Smirnova,[97] A. C. Smith,[41] E. A. Smith,[39] H. A. Smith,[125] J. L. Smith,[91] R. Smith,[142] M. Smizanska,[90] K. Smolek,[131] A. Smykiewicz,[85] A. A. Snesarev,[37] H. L. Snoek,[113] S. Snyder,[29] R. Sobie,[163,p] A. Soffer,[150] C. A. Solans Sanchez,[36] E. Yu. Soldatov,[37] U. Soldevila,[161] A. A. Solodkov,[37] S. Solomon,[54] A. Soloshenko,[38] K. Solovieva,[54] O. V. Solovyanov,[37] V. Solovyev,[37] P. Sommer,[36] A. Sonay,[13] W. Y. Song,[155b] A. Sopczak,[131] A. L. Sopio,[95] F. Sopkova,[28b] V. Sothilingam,[63a] S. Sottocornola,[72a,72b] R. Soualah,[115c] Z. Soumaimi,[35e] D. South,[48] S. Spagnolo,[69a,69b] M. Spalla,[109] F. Spanò,[94] D. Sperlich,[54] G. Spigo,[36] M. Spina,[145] S. Spinali,[90] D. P. Spiteri,[59] M. Spousta,[132] E. J. Staats,[34] A. Stabile,[70a,70b] R. Stamen,[63a] M. Stamenkovic,[113] A. Stampekis,[20] M. Standke,[24] E. Stanecka,[85] B. Stanislaus,[17a] M. M. Stanitzki,[48] M. Stankaityte,[125] B. Stapf,[48] E. A. Starchenko,[37] G. H. Stark,[135] J. Stark,[101] D. M. Starko,[155b] P. Staroba,[130] P. Starovoitov,[63a] S. Stärz,[103] R. Staszewski,[85] G. Stavropoulos,[46] J. Steentoft,[159] P. Steinberg,[29] A. L. Steinhebel,[122] B. Stelzer,[141,155a] H. J. Stelzer,[128] O. Stelzer-Chilton,[155a] H. Stenzel,[58] T. J. Stevenson,[145] G. A. Stewart,[36] M. C. Stockton,[36] G. Stoicea,[27b] M. Stolarski,[129a] S. Stonjek,[109] A. Straessner,[50] J. Strandberg,[143] S. Strandberg,[47a,47b] M. Strauss,[119] T. Strebler,[101] P. Strizenec,[28b] R. Ströhmer,[164] D. M. Strom,[122] L. R. Strom,[48] R. Stroynowski,[44] A. Strubig,[47a,47b] S. A. Stucci,[29] B. Stugu,[16] J. Stupak,[119] N. A. Styles,[48] D. Su,[142] S. Su,[62a] W. Su,[62d,137,62c] X. Su,[62a,66] K. Sugizaki,[152] V. V. Sulin,[37] M. J. Sullivan,[91] D. M. S. Sultan,[77a,77b] L. Sultanaliyeva,[37] S. Sultansoy,[3b] T. Sumida,[86] S. Sun,[105] S. Sun,[168] O. Sunneborn Gudnadottir,[159] M. R. Sutton,[145] M. Svatos,[130] M. Swiatlowski,[155a] T. Swirski,[164] I. Sykora,[28a] M. Sykora,[132] T. Sykora,[132] D. Ta,[99] K. Tackmann,[48,af] A. Taffard,[158] R. Tafirout,[155a] J. S. Tafoya Vargas,[66] R. H. M. Taibah,[126] R. Takashima,[87] K. Takeda,[83] E. P. Takeva,[52] Y. Takubo,[82] M. Talby,[101] A. A. Talyshev,[37]

K. C. Tam,[64b] N. M. Tamir,[150] A. Tanaka,[152] J. Tanaka,[152] R. Tanaka,[66] M. Tanasini,[57b,57a] J. Tang,[62c] Z. Tao,[162] S. Tapia Araya,[80] S. Tapprogge,[99] A. Tarek Abouelfadl Mohamed,[106] S. Tarem,[149] K. Tariq,[62b] G. Tarna,[27b] G. F. Tartarelli,[70a] P. Tas,[132] M. Tasevsky,[130] E. Tassi,[43b,43a] A. C. Tate,[160] G. Tateno,[152] Y. Tayalati,[35e] G. N. Taylor,[104] W. Taylor,[155b] H. Teagle,[91] A. S. Tee,[168] R. Teixeira De Lima,[142] P. Teixeira-Dias,[94] J. J. Teoh,[154] K. Terashi,[152] J. Terron,[98] S. Terzo,[13] M. Testa,[53] R. J. Teuscher,[154,p] A. Thaler,[78] O. Theiner,[56] N. Themistokleous,[52] T. Theveneaux-Pelzer,[18] O. Thielmann,[169] D. W. Thomas,[94] J. P. Thomas,[20] E. A. Thompson,[48] P. D. Thompson,[20] E. Thomson,[127] E. J. Thorpe,[93] Y. Tian,[55] V. Tikhomirov,[37,1] Yu. A. Tikhonov,[37] S. Timoshenko,[37] E. X. L. Ting,[1] P. Tipton,[170] S. Tisserant,[101] S. H. Tlou,[33g] A. Tnourji,[40] K. Todome,[23b,23a] S. Todorova-Nova,[132] S. Todt,[50] M. Togawa,[82] J. Tojo,[88] S. Tokár,[28a] K. Tokushuku,[82] R. Tombs,[32] M. Tomoto,[82,110] L. Tompkins,[142] K. W. Topolnicki,[84b] P. Tornambe,[102] E. Torrence,[122] H. Torres,[50] E. Torró Pastor,[161] M. Toscani,[30] C. Tosciri,[39] D. R. Tovey,[138] A. Traeet,[16] I. S. Trandafir,[27b] T. Trefzger,[164] A. Tricoli,[29] I. M. Trigger,[155a] S. Trincaz-Duvoid,[126] D. A. Trischuk,[162] B. Trocmé,[60] A. Trofymov,[66] C. Troncon,[70a] L. Truong,[33c] M. Trzebinski,[85] A. Trzupek,[85] F. Tsai,[144] M. Tsai,[105] A. Tsiamis,[151] P. V. Tsiareshka,[37] S. Tsigaridas,[155a] A. Tsirigotis,[151,aa] V. Tsiskaridze,[144] E. G. Tskhadadze,[148a] M. Tsopoulou,[151] Y. Tsujikawa,[86] I. I. Tsukerman,[37] V. Tsulaia,[17a] S. Tsuno,[82] O. Tsur,[149] D. Tsybychev,[144] Y. Tu,[64b] A. Tudorache,[27b] V. Tudorache,[27b] A. N. Tuna,[36] S. Turchikhin,[38] I. Turk Cakir,[3a] R. Turra,[70a] T. Turtuvshin,[38] P. M. Tuts,[41] S. Tzamarias,[151] P. Tzanis,[10] E. Tzovara,[99] K. Uchida,[152] F. Ukegawa,[156] P. A. Ulloa Poblete,[136c] G. Unal,[36] M. Unal,[11] A. Undrus,[29] G. Unel,[158] K. Uno,[152] J. Urban,[28b] P. Urquijo,[104] G. Usai,[8] R. Ushioda,[153] M. Usman,[107] Z. Uysal,[21b] V. Vacek,[131] B. Vachon,[103] K. O. H. Vadla,[124] T. Vafeiadis,[36] C. Valderanis,[108] E. Valdes Santurio,[47a,47b] M. Valente,[155a] S. Valentinetti,[23b,23a] A. Valero,[161] A. Vallier,[101] J.A. Valls Ferrer,[161] T. R. Van Daalen,[137] P. Van Gemmeren,[6] M. Van Rijnbach,[124,36] S. Van Stroud,[95] I. Van Vulpen,[113] M. Vanadia,[75a,75b] W. Vandelli,[36] M. Vandenbroucke,[134] E. R. Vandewall,[120] D. Vannicola,[150] L. Vannoli,[57b,57a] R. Vari,[74a] E. W. Varnes,[7] C. Varni,[17a] T. Varol,[147] D. Varouchas,[66] L. Varriale,[161] K. E. Varvell,[146] M. E. Vasile,[27b] L. Vaslin,[40] G. A. Vasquez,[163] F. Vazeille,[40] T. Vazquez Schroeder,[36] J. Veatch,[31] V. Vecchio,[100] M. J. Veen,[113] I. Veliscek,[125] L. M. Veloce,[154] F. Veloso,[129a,129c] S. Veneziano,[74a] A. Ventura,[69a,69b] A. Verbytskyi,[109] M. Verducci,[73a,73b] C. Vergis,[24] M. Verissimo De Araujo,[81b] W. Verkerke,[113] J. C. Vermeulen,[113] C. Vernieri,[142] P. J. Verschuuren,[94] M. Vessella,[102] M. L. Vesterbacka,[116] M. C. Vetterli,[141,d] A. Vgenopoulos,[151] N. Viaux Maira,[136f] T. Vickey,[138] O. E. Vickey Boeriu,[138] G. H. A. Viehhauser,[125] L. Vigani,[63b] M. Villa,[23b,23a] M. Villaplana Perez,[161] E. M. Villhauer,[52] E. Vilucchi,[53] M. G. Vincter,[34] G. S. Virdee,[20] A. Vishwakarma,[52] C. Vittori,[23b,23a] I. Vivarelli,[145] V. Vladimirov,[165] E. Voevodina,[109] F. Vogel,[108] P. Vokac,[131] J. Von Ahnen,[48] E. Von Toerne,[24] B. Vormwald,[36] V. Vorobel,[132] K. Vorobev,[37] M. Vos,[161] J. H. Vossebeld,[91] M. Vozak,[113] L. Vozdecky,[93] N. Vranjes,[15] M. Vranjes Milosavljevic,[15] M. Vreeswijk,[113] R. Vuillermet,[36] O. Vujinovic,[99] I. Vukotic,[39] S. Wada,[156] C. Wagner,[102] W. Wagner,[169] S. Wahdan,[169] H. Wahlberg,[89] R. Wakasa,[156] M. Wakida,[110] V. M. Walbrecht,[109] J. Walder,[133] R. Walker,[108] W. Walkowiak,[140] A. M. Wang,[61] A. Z. Wang,[168] C. Wang,[62a] C. Wang,[62c] H. Wang,[17a] J. Wang,[64a] P. Wang,[44] R.-J. Wang,[99] R. Wang,[61] R. Wang,[6] S. M. Wang,[147] S. Wang,[62b] T. Wang,[62a] W. T. Wang,[79] W. X. Wang,[62a] X. Wang,[14c] X. Wang,[160] X. Wang,[62c] Y. Wang,[62d] Y. Wang,[14c] Z. Wang,[105] Z. Wang,[62d,51,62c] Z. Wang,[105] A. Warburton,[103] R. J. Ward,[20] N. Warrack,[59] A. T. Watson,[20] M. F. Watson,[20] G. Watts,[137] B. M. Waugh,[95] A. F. Webb,[11] C. Weber,[29] M. S. Weber,[19] S. A. Weber,[34] S. M. Weber,[63a] C. Wei,[62a] Y. Wei,[125] A. R. Weidberg,[125] J. Weingarten,[49] M. Weirich,[99] C. Weiser,[54] C. J. Wells,[48] T. Wenaus,[29] B. Wendland,[49] T. Wengler,[36] N. S. Wenke,[109] N. Wermes,[24] M. Wessels,[63a] K. Whalen,[122] A. M. Wharton,[90] A. S. White,[61] A. White,[8] M. J. White,[1] D. Whiteson,[158] L. Wickremasinghe,[123] W. Wiedenmann,[168] C. Wiel,[50] M. Wielers,[133] N. Wieseotte,[99] C. Wiglesworth,[42] L. A. M. Wiik-Fuchs,[54] D. J. Wilbern,[119] H. G. Wilkens,[36] D. M. Williams,[41] H. H. Williams,[127] S. Williams,[32] S. Willocq,[102] P. J. Windischhofer,[125] F. Winklmeier,[122] B. T. Winter,[54] M. Wittgen,[142] M. Wobisch,[96] A. Wolf,[99] R. Wölker,[125] J. Wollrath,[158] M. W. Wolter,[85] H. Wolters,[129a,129c] V. W. S. Wong,[162] A. F. Wongel,[48] S. D. Worm,[48] B. K. Wosiek,[85] K. W. Woźniak,[85] K. Wraight,[59] J. Wu,[14a,14d] M. Wu,[64a] S. L. Wu,[168] X. Wu,[56] Y. Wu,[62a] Z. Wu,[134,62a] J. Wuerzinger,[125] T. R. Wyatt,[100] B. M. Wynne,[52] S. Xella,[42] L. Xia,[14c] M. Xia,[14b] J. Xiang,[64c] X. Xiao,[105] M. Xie,[62a] X. Xie,[62a] J. Xiong,[17a] I. Xiotidis,[145] D. Xu,[14a] H. Xu,[62a] H. Xu,[62a] L. Xu,[62a] R. Xu,[127] T. Xu,[105] W. Xu,[105] Y. Xu,[14b] Z. Xu,[62b] Z. Xu,[142] B. Yabsley,[146] S. Yacoob,[33a] N. Yamaguchi,[88] Y. Yamaguchi,[153] H. Yamauchi,[156] T. Yamazaki,[17a] Y. Yamazaki,[83] J. Yan,[62c] S. Yan,[125] Z. Yan,[25] H. J. Yang,[62c,62d] H. T. Yang,[17a] S. Yang,[62a] T. Yang,[64c] X. Yang,[62a] X. Yang,[14a] Y. Yang,[44] Z. Yang,[62a,105] W.-M. Yao,[17a] Y. C. Yap,[48] H. Ye,[14c] J. Ye,[44] S. Ye,[29] X. Ye,[62a] Y. Yeh,[95] I. Yeletskikh,[38] M. R. Yexley,[90] P. Yin,[41] K. Yorita,[166] C. J. S. Young,[54] C. Young,[142] M. Yuan,[105] R. Yuan,[62b,ag] L. Yue,[95] X. Yue,[63a] M. Zaazoua,[35e] B. Zabinski,[85] E. Zaid,[52] T. Zakareishvili,[148b] N. Zakharchuk,[34] S. Zambito,[56] J. A. Zamora Saa,[136d] J. Zang,[152] D. Zanzi,[54] O. Zaplatilek,[131] S. V. Zeißner,[49] C. Zeitnitz,[169] J. C. Zeng,[160] D. T. Zenger, Jr,[26] O. Zenin,[37] T. Ženiš,[28a] S. Zenz,[93] S. Zerradi,[35a] D. Zerwas,[66] B. Zhang,[14c] D. F. Zhang,[138] G. Zhang,[14b] J. Zhang,[6] K. Zhang,[14a,14d] L. Zhang,[14c] P. Zhang,[14a,14d] R. Zhang,[168] S. Zhang,[105] T. Zhang,[152] X. Zhang,[62c] X. Zhang,[62b] Z. Zhang,[17a] Z. Zhang,[66] H. Zhao,[137] P. Zhao,[51]

T. Zhao,[62b] Y. Zhao,[135] Z. Zhao,[62a] A. Zhemchugov,[38] Z. Zheng,[142] D. Zhong,[160] B. Zhou,[105] C. Zhou,[168] H. Zhou,[7] N. Zhou,[62c] Y. Zhou,[7] C. G. Zhu,[62b] C. Zhu,[14a,14d] H. L. Zhu,[62a] H. Zhu,[14a] J. Zhu,[105] Y. Zhu,[62c] Y. Zhu,[62a] X. Zhuang,[14a] K. Zhukov,[37] V. Zhulanov,[37] N. I. Zimine,[38] J. Zinsser,[63b] M. Ziolkowski,[140] L. Živković,[15] A. Zoccoli,[23b,23a] K. Zoch,[56] T. G. Zorbas,[138] O. Zormpa,[46] W. Zou,[41] and L. Zwalinski[36]

(ATLAS Collaboration)

[1]*Department of Physics, University of Adelaide, Adelaide, Australia*
[2]*Department of Physics, University of Alberta, Edmonton AB, Canada*
[3a]*Department of Physics, Ankara University, Ankara,Türkiye*
[3b]*Division of Physics, TOBB University of Economics and Technology, Ankara, Türkiye*
[4]*LAPP, Univ. Savoie Mont Blanc, CNRS/IN2P3, Annecy, France*
[5]*APC, Université Paris Cité, CNRS/IN2P3, Paris, France*
[6]*High Energy Physics Division, Argonne National Laboratory, Argonne, Illinois, USA*
[7]*Department of Physics, University of Arizona, Tucson, Arizona, USA*
[8]*Department of Physics, University of Texas at Arlington, Arlington, Texas, USA*
[9]*Physics Department, National and Kapodistrian University of Athens, Athens, Greece*
[10]*Physics Department, National Technical University of Athens, Zografou, Greece*
[11]*Department of Physics, University of Texas at Austin, Austin, Texas, USA*
[12]*Institute of Physics, Azerbaijan Academy of Sciences, Baku, Azerbaijan*
[13]*Institut de Física d'Altes Energies (IFAE), Barcelona Institute of Science and Technology, Barcelona, Spain*
[14a]*Institute of High Energy Physics, Chinese Academy of Sciences, Beijing, China*
[14b]*Physics Department, Tsinghua University, Beijing, China*
[14c]*Department of Physics, Nanjing University, Nanjing, China*
[14d]*University of Chinese Academy of Science (UCAS), Beijing, China*
[15]*Institute of Physics, University of Belgrade, Belgrade, Serbia*
[16]*Department for Physics and Technology, University of Bergen, Bergen, Norway*
[17a]*Physics Division, Lawrence Berkeley National Laboratory, Berkeley, California, USA*
[17b]*University of California, Berkeley, California, USA*
[18]*Institut für Physik, Humboldt Universität zu Berlin, Berlin, Germany*
[19]*Albert Einstein Center for Fundamental Physics and Laboratory for High Energy Physics, University of Bern, Bern, Switzerland*
[20]*School of Physics and Astronomy, University of Birmingham, Birmingham, United Kingdom*
[21a]*Department of Physics, Bogazici University, Istanbul, Türkiye*
[21b]*Department of Physics Engineering, Gaziantep University, Gaziantep, Türkiye*
[21c]*Department of Physics, Istanbul University, Istanbul, Türkiye*
[21d]*Istinye University, Sariyer, Istanbul, Türkiye*
[22a]*Facultad de Ciencias y Centro de Investigaciónes, Universidad Antonio Nariño, Bogotá, Colombia*
[22b]*Departamento de Física, Universidad Nacional de Colombia, Bogotá, Colombia*
[23a]*Dipartimento di Fisica e Astronomia A. Righi, Università di Bologna, Bologna, Italy*
[23b]*INFN Sezione di Bologna, Italy*
[24]*Physikalisches Institut, Universität Bonn, Bonn, Germany*
[25]*Department of Physics, Boston University, Boston, Massachusetts, USA*
[26]*Department of Physics, Brandeis University, Waltham, Massachusetts, USA*
[27a]*Transilvania University of Brasov, Brasov, Romania*
[27b]*Horia Hulubei National Institute of Physics and Nuclear Engineering, Bucharest, Romania*
[27c]*Department of Physics, Alexandru Ioan Cuza University of Iasi, Iasi, Romania*
[27d]*National Institute for Research and Development of Isotopic and Molecular Technologies, Physics Department, Cluj-Napoca, Romania*
[27e]*University Politehnica Bucharest, Bucharest, Romania*
[27f]*West University in Timisoara, Timisoara, Romania*
[27g]*Faculty of Physics, University of Bucharest, Bucharest, Romania*
[28a]*Faculty of Mathematics, Physics and Informatics, Comenius University, Bratislava, Slovak Republic*
[28b]*Department of Subnuclear Physics, Institute of Experimental Physics of the Slovak Academy of Sciences, Kosice, Slovak Republic*
[29]*Physics Department, Brookhaven National Laboratory, Upton, New York, USA*
[30]*Universidad de Buenos Aires, Facultad de Ciencias Exactas y Naturales, Departamento de Física, y CONICET, Instituto de Física de Buenos Aires (IFIBA), Buenos Aires, Argentina*
[31]*California State University, California, USA*
[32]*Cavendish Laboratory, University of Cambridge, Cambridge, United Kingdom*
[33a]*Department of Physics, University of Cape Town, Cape Town, South Africa*

[33b]*iThemba Labs, Western Cape, South Africa*
[33c]*Department of Mechanical Engineering Science, University of Johannesburg, Johannesburg, South Africa*
[33d]*National Institute of Physics, University of the Philippines Diliman (Philippines), South Africa*
[33e]*University of South Africa, Department of Physics, Pretoria, South Africa*
[33f]*University of Zululand, KwaDlangezwa, South Africa*
[33g]*School of Physics, University of the Witwatersrand, Johannesburg, South Africa*
[34]*Department of Physics, Carleton University, Ottawa ON, Canada*
[35a]*Faculté des Sciences Ain Chock, Réseau Universitaire de Physique des Hautes Energies—Université Hassan II, Casablanca, Morocco*
[35b]*Faculté des Sciences, Université Ibn-Tofail, Kénitra, Morocco*
[35c]*Faculté des Sciences Semlalia, Université Cadi Ayyad, LPHEA-Marrakech, Morocco*
[35d]*LPMR, Faculté des Sciences, Université Mohamed Premier, Oujda, Morocco*
[35e]*Faculté des sciences, Université Mohammed V, Rabat, Morocco*
[35f]*Institute of Applied Physics, Mohammed VI Polytechnic University, Ben Guerir, Morocco*
[36]*CERN, Geneva, Switzerland*
[37]*Affiliated with an institute covered by a cooperation agreement with CERN*
[38]*Affiliated with an international laboratory covered by a cooperation agreement with CERN*
[39]*Enrico Fermi Institute, University of Chicago, Chicago, Illinois, USA*
[40]*LPC, Université Clermont Auvergne, CNRS/IN2P3, Clermont-Ferrand, France*
[41]*Nevis Laboratory, Columbia University, Irvington, New York, USA*
[42]*Niels Bohr Institute, University of Copenhagen, Copenhagen, Denmark*
[43a]*Dipartimento di Fisica, Università della Calabria, Rende, Italy*
[43b]*INFN Gruppo Collegato di Cosenza, Laboratori Nazionali di Frascati, Italy*
[44]*Physics Department, Southern Methodist University, Dallas, Texas, USA*
[45]*Physics Department, University of Texas at Dallas, Richardson, Texas, USA*
[46]*National Centre for Scientific Research "Demokritos", Agia Paraskevi, Greece*
[47a]*Department of Physics, Stockholm University, Sweden*
[47b]*Oskar Klein Centre, Stockholm, Sweden*
[48]*Deutsches Elektronen-Synchrotron DESY, Hamburg and Zeuthen, Germany*
[49]*Fakultät Physik, Technische Universität Dortmund, Dortmund, Germany*
[50]*Institut für Kern- und Teilchenphysik, Technische Universität Dresden, Dresden, Germany*
[51]*Department of Physics, Duke University, Durham, North Carolina, USA*
[52]*SUPA—School of Physics and Astronomy, University of Edinburgh, Edinburgh, United Kingdom*
[53]*INFN e Laboratori Nazionali di Frascati, Frascati, Italy*
[54]*Physikalisches Institut, Albert-Ludwigs-Universität Freiburg, Freiburg, Germany*
[55]*II. Physikalisches Institut, Georg-August-Universität Göttingen, Göttingen, Germany*
[56]*Département de Physique Nucléaire et Corpusculaire, Université de Genève, Genève, Switzerland*
[57a]*Dipartimento di Fisica, Università di Genova, Genova, Italy*
[57b]*INFN Sezione di Genova, Italy*
[58]*II. Physikalisches Institut, Justus-Liebig-Universität Giessen, Giessen, Germany*
[59]*SUPA—School of Physics and Astronomy, University of Glasgow, Glasgow, United Kingdom*
[60]*LPSC, Université Grenoble Alpes, CNRS/IN2P3, Grenoble INP, Grenoble, France*
[61]*Laboratory for Particle Physics and Cosmology, Harvard University, Cambridge, Massachusetts, USA*
[62a]*Department of Modern Physics and State Key Laboratory of Particle Detection and Electronics, University of Science and Technology of China, Hefei, China*
[62b]*Institute of Frontier and Interdisciplinary Science and Key Laboratory of Particle Physics and Particle Irradiation (MOE), Shandong University, Qingdao, China*
[62c]*School of Physics and Astronomy, Shanghai Jiao Tong University, Key Laboratory for Particle Astrophysics and Cosmology (MOE), SKLPPC, Shanghai, China*
[62d]*Tsung-Dao Lee Institute, Shanghai, China*
[63a]*Kirchhoff-Institut für Physik, Ruprecht-Karls-Universität Heidelberg, Heidelberg, Germany*
[63b]*Physikalisches Institut, Ruprecht-Karls-Universität Heidelberg, Heidelberg, Germany*
[64a]*Department of Physics, Chinese University of Hong Kong, Shatin, N.T., Hong Kong, China*
[64b]*Department of Physics, University of Hong Kong, Hong Kong, China*
[64c]*Department of Physics and Institute for Advanced Study, Hong Kong University of Science and Technology, Clear Water Bay, Kowloon, Hong Kong, China*
[65]*Department of Physics, National Tsing Hua University, Hsinchu, Taiwan*
[66]*IJCLab, Université Paris-Saclay, CNRS/IN2P3, 91405, Orsay, France*
[67]*Department of Physics, Indiana University, Bloomington, Indiana, USA*
[68a]*INFN Gruppo Collegato di Udine, Sezione di Trieste, Udine, Italy*

[68b]*ICTP, Trieste, Italy*
[68c]*Dipartimento Politecnico di Ingegneria e Architettura, Università di Udine, Udine, Italy*
[69a]*INFN Sezione di Lecce, Italy*
[69b]*Dipartimento di Matematica e Fisica, Università del Salento, Lecce, Italy*
[70a]*INFN Sezione di Milano, Italy*
[70b]*Dipartimento di Fisica, Università di Milano, Milano, Italy*
[71a]*INFN Sezione di Napoli, Italy*
[71b]*Dipartimento di Fisica, Università di Napoli, Napoli, Italy*
[72a]*INFN Sezione di Pavia, Italy*
[72b]*Dipartimento di Fisica, Università di Pavia, Pavia, Italy*
[73a]*INFN Sezione di Pisa, Italy*
[73b]*Dipartimento di Fisica E. Fermi, Università di Pisa, Pisa, Italy*
[74a]*INFN Sezione di Roma, Italy*
[74b]*Dipartimento di Fisica, Sapienza Università di Roma, Roma, Italy*
[75a]*INFN Sezione di Roma Tor Vergata, Italy*
[75b]*Dipartimento di Fisica, Università di Roma Tor Vergata, Roma, Italy*
[76a]*INFN Sezione di Roma Tre, Italy*
[76b]*Dipartimento di Matematica e Fisica, Università Roma Tre, Roma, Italy*
[77a]*INFN-TIFPA, Italy*
[77b]*Università degli Studi di Trento, Trento, Italy*
[78]*Universität Innsbruck, Department of Astro and Particle Physics, Innsbruck, Austria*
[79]*University of Iowa, Iowa City, Iowa, USA*
[80]*Department of Physics and Astronomy, Iowa State University, Ames, Iowa, USA*
[81a]*Departamento de Engenharia Elétrica, Universidade Federal de Juiz de Fora (UFJF), Juiz de Fora, Brazil*
[81b]*Universidade Federal do Rio De Janeiro COPPE/EE/IF, Rio de Janeiro, Brazil*
[81c]*Instituto de Física, Universidade de São Paulo, São Paulo, Brazil*
[81d]*Rio de Janeiro State University, Rio de Janeiro, Brazil*
[82]*KEK, High Energy Accelerator Research Organization, Tsukuba, Japan*
[83]*Graduate School of Science, Kobe University, Kobe, Japan*
[84a]*AGH University of Science and Technology, Faculty of Physics and Applied Computer Science, Krakow, Poland*
[84b]*Marian Smoluchowski Institute of Physics, Jagiellonian University, Krakow, Poland*
[85]*Institute of Nuclear Physics Polish Academy of Sciences, Krakow, Poland*
[86]*Faculty of Science, Kyoto University, Kyoto, Japan*
[87]*Kyoto University of Education, Kyoto, Japan*
[88]*Research Center for Advanced Particle Physics and Department of Physics, Kyushu University, Fukuoka, Japan*
[89]*Instituto de Física La Plata, Universidad Nacional de La Plata and CONICET, La Plata, Argentina*
[90]*Physics Department, Lancaster University, Lancaster, United Kingdom*
[91]*Oliver Lodge Laboratory, University of Liverpool, Liverpool, United Kingdom*
[92]*Department of Experimental Particle Physics, Jožef Stefan Institute and Department of Physics, University of Ljubljana, Ljubljana, Slovenia*
[93]*School of Physics and Astronomy, Queen Mary University of London, London, United Kingdom*
[94]*Department of Physics, Royal Holloway University of London, Egham, United Kingdom*
[95]*Department of Physics and Astronomy, University College London, London, United Kingdom*
[96]*Louisiana Tech University, Ruston, Louisiana, USA*
[97]*Fysiska institutionen, Lunds universitet, Lund, Sweden*
[98]*Departamento de Física Teorica C-15 and CIAFF, Universidad Autónoma de Madrid, Madrid, Spain*
[99]*Institut für Physik, Universität Mainz, Mainz, Germany*
[100]*School of Physics and Astronomy, University of Manchester, Manchester, United Kingdom*
[101]*CPPM, Aix-Marseille Université, CNRS/IN2P3, Marseille, France*
[102]*Department of Physics, University of Massachusetts, Amherst, Massachusetts, USA*
[103]*Department of Physics, McGill University, Montreal QC, Canada*
[104]*School of Physics, University of Melbourne, Victoria, Australia*
[105]*Department of Physics, University of Michigan, Ann Arbor, Michigan, USA*
[106]*Department of Physics and Astronomy, Michigan State University, East Lansing, Michigan, USA*
[107]*Group of Particle Physics, University of Montreal, Montreal QC, Canada*
[108]*Fakultät für Physik, Ludwig-Maximilians-Universität München, München, Germany*
[109]*Max-Planck-Institut für Physik (Werner-Heisenberg-Institut), München, Germany*
[110]*Graduate School of Science and Kobayashi-Maskawa Institute, Nagoya University, Nagoya, Japan*
[111]*Department of Physics and Astronomy, University of New Mexico, Albuquerque, New Mexico, USA*
[112]*Institute for Mathematics, Astrophysics and Particle Physics, Radboud University/Nikhef, Nijmegen, Netherlands*

[113]*Nikhef National Institute for Subatomic Physics and University of Amsterdam, Amsterdam, Netherlands*
[114]*Department of Physics, Northern Illinois University, DeKalb, Illinois, USA*
[115a]*New York University Abu Dhabi, Abu Dhabi, United Arab Emirates*
[115b]*United Arab Emirates University, Al Ain, United Arab Emirates*
[115c]*University of Sharjah, Sharjah, United Arab Emirates*
[116]*Department of Physics, New York University, New York, New York, USA*
[117]*Ochanomizu University, Otsuka, Bunkyo-ku, Tokyo, Japan*
[118]*Ohio State University, Columbus, Ohio, USA*
[119]*Homer L. Dodge Department of Physics and Astronomy, University of Oklahoma, Norman, Oklahoma, USA*
[120]*Department of Physics, Oklahoma State University, Stillwater, Oklahoma, USA*
[121]*Palacký University, Joint Laboratory of Optics, Olomouc, Czech Republic*
[122]*Institute for Fundamental Science, University of Oregon, Eugene, Oregon, USA*
[123]*Graduate School of Science, Osaka University, Osaka, Japan*
[124]*Department of Physics, University of Oslo, Oslo, Norway*
[125]*Department of Physics, Oxford University, Oxford, United Kingdom*
[126]*LPNHE, Sorbonne Université, Université Paris Cité, CNRS/IN2P3, Paris, France*
[127]*Department of Physics, University of Pennsylvania, Philadelphia, Pennsylvania, USA*
[128]*Department of Physics and Astronomy, University of Pittsburgh, Pittsburgh, Pennsylvania, USA*
[129a]*Laboratório de Instrumentação e Física Experimental de Partículas—LIP, Lisboa, Portugal*
[129b]*Departamento de Física, Faculdade de Ciências, Universidade de Lisboa, Lisboa, Portugal*
[129c]*Departamento de Física, Universidade de Coimbra, Coimbra, Portugal*
[129d]*Centro de Física Nuclear da Universidade de Lisboa, Lisboa, Portugal*
[129e]*Departamento de Física, Universidade do Minho, Braga, Portugal*
[129f]*Departamento de Física Teórica y del Cosmos, Universidad de Granada, Granada (Spain), Portugal*
[129g]*Instituto Superior Técnico, Universidade de Lisboa, Lisboa, Portugal*
[130]*Institute of Physics of the Czech Academy of Sciences, Prague, Czech Republic*
[131]*Czech Technical University in Prague, Prague, Czech Republic*
[132]*Charles University, Faculty of Mathematics and Physics, Prague, Czech Republic*
[133]*Particle Physics Department, Rutherford Appleton Laboratory, Didcot, United Kingdom*
[134]*IRFU, CEA, Université Paris-Saclay, Gif-sur-Yvette, France*
[135]*Santa Cruz Institute for Particle Physics, University of California Santa Cruz, Santa Cruz, California, USA*
[136a]*Departamento de Física, Pontificia Universidad Católica de Chile, Santiago, Chile*
[136b]*Millennium Institute for Subatomic physics at high energy frontier (SAPHIR), Santiago, Chile*
[136c]*Instituto de Investigación Multidisciplinario en Ciencia y Tecnología, y Departamento de Física, Universidad de La Serena, Chile*
[136d]*Universidad Andres Bello, Department of Physics, Santiago, Chile*
[136e]*Instituto de Alta Investigación, Universidad de Tarapacá, Arica, Chile*
[136f]*Departamento de Física, Universidad Técnica Federico Santa María, Valparaíso, Chile*
[137]*Department of Physics, University of Washington, Seattle, Washington, USA*
[138]*Department of Physics and Astronomy, University of Sheffield, Sheffield, United Kingdom*
[139]*Department of Physics, Shinshu University, Nagano, Japan*
[140]*Department Physik, Universität Siegen, Siegen, Germany*
[141]*Department of Physics, Simon Fraser University, Burnaby BC, Canada*
[142]*SLAC National Accelerator Laboratory, Stanford, California, USA*
[143]*Department of Physics, Royal Institute of Technology, Stockholm, Sweden*
[144]*Departments of Physics and Astronomy, Stony Brook University, Stony Brook, New York, USA*
[145]*Department of Physics and Astronomy, University of Sussex, Brighton, United Kingdom*
[146]*School of Physics, University of Sydney, Sydney, Australia*
[147]*Institute of Physics, Academia Sinica, Taipei, Taiwan*
[148a]*E. Andronikashvili Institute of Physics, Iv. Javakhishvili Tbilisi State University, Tbilisi, Georgia*
[148b]*High Energy Physics Institute, Tbilisi State University, Tbilisi, Georgia*
[148c]*University of Georgia, Tbilisi, Georgia*
[149]*Department of Physics, Technion, Israel Institute of Technology, Haifa, Israel*
[150]*Raymond and Beverly Sackler School of Physics and Astronomy, Tel Aviv University, Tel Aviv, Israel*
[151]*Department of Physics, Aristotle University of Thessaloniki, Thessaloniki, Greece*
[152]*International Center for Elementary Particle Physics and Department of Physics, University of Tokyo, Tokyo, Japan*
[153]*Department of Physics, Tokyo Institute of Technology, Tokyo, Japan*
[154]*Department of Physics, University of Toronto, Toronto ON, Canada*
[155a]*TRIUMF, Vancouver BC, Canada*
[155b]*Department of Physics and Astronomy, York University, Toronto ON, Canada*

[156]*Division of Physics and Tomonaga Center for the History of the Universe, Faculty of Pure and Applied Sciences, University of Tsukuba, Tsukuba, Japan*
[157]*Department of Physics and Astronomy, Tufts University, Medford, Massachusetts, USA*
[158]*Department of Physics and Astronomy, University of California Irvine, Irvine, California, USA*
[159]*Department of Physics and Astronomy, University of Uppsala, Uppsala, Sweden*
[160]*Department of Physics, University of Illinois, Urbana, Illinois, USA*
[161]*Instituto de Física Corpuscular (IFIC), Centro Mixto Universidad de Valencia—CSIC, Valencia, Spain*
[162]*Department of Physics, University of British Columbia, Vancouver BC, Canada*
[163]*Department of Physics and Astronomy, University of Victoria, Victoria BC, Canada*
[164]*Fakultät für Physik und Astronomie, Julius-Maximilians-Universität Würzburg, Würzburg, Germany*
[165]*Department of Physics, University of Warwick, Coventry, United Kingdom*
[166]*Waseda University, Tokyo, Japan*
[167]*Department of Particle Physics and Astrophysics, Weizmann Institute of Science, Rehovot, Israel*
[168]*Department of Physics, University of Wisconsin, Madison, Wisconsin, USA*
[169]*Fakultät für Mathematik und Naturwissenschaften, Fachgruppe Physik, Bergische Universität Wuppertal, Wuppertal, Germany*
[170]*Department of Physics, Yale University, New Haven, Connecticut, USA*

[a]Also at Department of Physics, King's College London, London, United Kingdom.
[b]Also at Institute of Physics, Azerbaijan Academy of Sciences, Baku, Azerbaijan.
[c]Also at Lawrence Livermore National Laboratory, Livermore, California, USA.
[d]Also at TRIUMF, Vancouver BC, Canada.
[e]Also at Department of Physics, University of Thessaly, Greece.
[f]Also at Department of Physics, University of Fribourg, Fribourg, Switzerland.
[g]Also at University of Colorado Boulder, Department of Physics, Colorado, USA.
[h]Also at Department of Physics and Astronomy, University of Louisville, Louisville, Kentucky, USA.
[i]Deceased.
[j]Also at Department of Physics, Westmont College, Santa Barbara, California, USA.
[k]Also at Departament de Fisica de la Universitat Autonoma de Barcelona, Barcelona, Spain.
[l]Also Affiliated with an institute covered by a cooperation agreement with CERN.
[m]Also at The Collaborative Innovation Center of Quantum Matter (CICQM), Beijing, China.
[n]Also at Department of Physics, Ben Gurion University of the Negev, Beer Sheva, Israel.
[o]Also at Università di Napoli Parthenope, Napoli, Italy.
[p]Also at Institute of Particle Physics (IPP), Canada.
[q]Also at Bruno Kessler Foundation, Trento, Italy.
[r]Also at Borough of Manhattan Community College, City University of New York, New York, New York, USA.
[s]Also at Department of Financial and Management Engineering, University of the Aegean, Chios, Greece.
[t]Also at Centro Studi e Ricerche Enrico Fermi, Italy.
[u]Also at Department of Physics, California State University, East Bay, California, USA.
[v]Also at Institucio Catalana de Recerca i Estudis Avancats, ICREA, Barcelona, Spain.
[w]Also at University of Chinese Academy of Sciences (UCAS), Beijing, China.
[x]Also at Yeditepe University, Physics Department, Istanbul, Türkiye.
[y]Also at Institute of Theoretical Physics, Ilia State University, Tbilisi, Georgia.
[z]Also at CERN, Geneva, Switzerland.
[aa]Also at Hellenic Open University, Patras, Greece.
[ab]Also at Center for High Energy Physics, Peking University, China.
[ac]Also at Department of Physics, California State University, Sacramento, California, USA.
[ad]Also at Département de Physique Nucléaire et Corpusculaire, Université de Genève, Genève, Switzerland.
[ae]Also at Washington College, Maryland, USA.
[af]Also at Institut für Experimentalphysik, Universität Hamburg, Hamburg, Germany.
[ag]Also at Department of Physics and Astronomy, Michigan State University, East Lansing, Michigan, USA.